Durham University

Durham E-Theses

Synthesis and characterisation of branched polymers

Dodds, Jonathan M.

How to cite:

Dodds, Jonathan M. (2009) *Synthesis and characterisation of branched polymers*, Durham theses, Durham University. Available at Durham E-Theses Online: http://etheses.dur.ac.uk/2125/

Use policy

The full-text may be used and/or reproduced, and given to third parties in any format or medium, without prior permission or charge, for personal research or study, educational, or not-for-profit purposes provided that:

- a full bibliographic reference is made to the original source
- a link is made to the metadata record in Durham E-Theses
- the full-text is not changed in any way

The full-text must not be sold in any format or medium without the formal permission of the copyright holders.

Please consult the full Durham E-Theses policy for further details.

Academic Support Office, The Palatine Centre, Durham University, Stockton Road, Durham, DH1 3LE
e-mail: e-theses.admin@durham.ac.uk Tel: +44 0191 334 6107
http://etheses.dur.ac.uk

Synthesis and Characterisation of Branched Polymers.

Submitted in Fulfillment for the Degree of PhD.
University of Durham.
April 2009.

Jonathan M. Dodds

The copyright of this thesis rests with the author or the university to which it was submitted. No quotation from it, or information derived from it may be published without the prior written consent of the author or university, and any information derived from it should be acknowledged.

2 3 JUN 2009

This copy has been supplied for the purpose of research or private study on the understanding that it is copyright material and that no quotation from the thesis may be published without proper acknowledgement.

Synthesis and Characterisation of Branched Polymers.

Jonathan M. Dodds

ABSTRACT: HyperMacs and HyperBlocks are polymers with highly branched architectures. The building blocks for these materials, AB_2 macromonomers, are synthesized by living anionic polymerization and are well-defined in terms of molecular weight and polydispersity. The nature of the coupling reaction used to generate the highly branched HyperMacs results in branched polymers with a distribution of molecular weights and architectures.

Previously a strategy for the synthesis of polystyrene HyperMacs has been reported in which the extent of reaction was limited by an unknown factor. In this thesis the modifications made to the synthetic strategy are reported for the production of more highly branched polystyrene HyperMacs or 'super' HyperMacs. Other variations along this theme include the addition of a B_3 core creating core HyperMacs.

Modifications to the improved HyperMac synthesis enabled the construction of polybutadiene AB_2 macromonomers, resulting in polybutadiene HyperMacs; as well as triblock copolymer AB_2 macromonomers constructed from polystyrene and polyisoprene forming block copolymer HyperMacs termed HyperBlocks.

Characterisation of the materials above involved techniques including rheology, thermal analysis including differential scanning caliorimetry, (DSC), and dynamic mechanical analysis, (DMA), x-ray scattering (small angle x-ray scattering, SAXS) and transition electron microscopy, (TEM).

Melt rheology showed polystyrene HyperMacs to be thermorheologically simple and HyperMacs showed little evidence for relaxation by reptation. Their rheological behaviour agreed well with the Cayley tree model for hierarchical relaxation in tube models of branched polymers.

HyperBlocks showed phase separated morphologies with two distinct glass transition temperatures for their constituents. However the highly branched architecture of HyperBlocks disrupts long-range order seen in the macromonomers, as observed by SAXS and TEM.

Acknowledgements.

I would like to thank my parents and twin James for the encouragement and support they have provided me throughout this course of study.

Particular thanks go to PhD supervisors Lian R. Hutchings and Nigel Clarke for their faith, guidance and supervision over the past few years.

Scientifically I would like to thank the following people for their help and collaboration throughout this degree: Tim Gough, Solomon M. Kimani, Edoardo de Luca, Judith A. Elder, Stephen A. Collins, Stephanie Henderson, Mathieu Dylikowski, Junjie Wu, Emily Smith, Christine Richardson, David Rees, Daniel J. Read, Isobel Grillo, Jimmy Mays, Don Baird, Christopher McGrady, Douglas Carswell, Alan Kenwright, Christine Heffernan, academic and non-academic staff in the Department of Chemistry University of Durham, members of Microscale Polymer Processing Consortium (μPP2) and EPSRC for funding.

Special thanks to Caroline Zeyfert, Ross Carnachan, Gregory Hunt, Will Bergius, David W. Johnson, Barry Dean, Alison Parry, Seb Spain, Jonathan Fay, Matt Gibson and Noodle for putting up with me over the past few years.

Contents.

1. *Introduction.*

1.1 What is a Polymer? – Definitions and History.[1]

A polymer (macromolecule) is a material composed of many molecules termed monomers linked together, usually by covalent bonds. The process of linking monomers to one another to form a chain is a polymerization reaction. The building up of molecules into long chains gives rise to the unique properties of polymers.

Polymers are ubiquitous in nature, from biological materials such as collagen, to the DNA making up our genetic fingerprint. The wide range of polymers available today, both synthetic and naturally occurring polymers, is extraordinary. This text concentrates on a relatively narrow area of polymer science, but it is hopefully a small jigsaw piece in the giant puzzle of the polymer world.

Polymer manufacturing has been a rapidly expanding area for many decades, initially with the extraction and modification of natural rubber for specific applications; however as demand exceeded economic natural production and the desire for new materials increased, completely synthetic routes evolved. One of the earliest manufacturing processes was the vulcanisation of natural rubber by Charles Goodyear,[2] where sulphur was used for the vulcanisation of Indian rubber to improve its physical properties for use in the fledgling automotive industry.

One of the first truly synthetic polymers, known as Bakelite, soon entered the marketplace. Formed from phenol formaldehyde resin (thermosetting), this was the first material used for the construction of a wide range of commercial materials, including tooth brush bristles and wire insulation.[3] It is a notable inclusion here as this is one of the first industrial applications of polymers in a commercial sense, laying the foundations for the polymer industry today. Bakelite production gradually declined due to cheaper non thermosetting alternatives such as polystyrene which were easier to prepare on larger scales with more versatile applications (thermosoftening), resulting in the more common use of polymers that we see today.

1.1.1 Classification According to Structure.

Polymers can be divided into three categories; linear, branched and networks. Since the discovery of synthetic polymers, studies have been undertaken to understand the

correlation between the molecular architectures and the physical properties of a polymer.

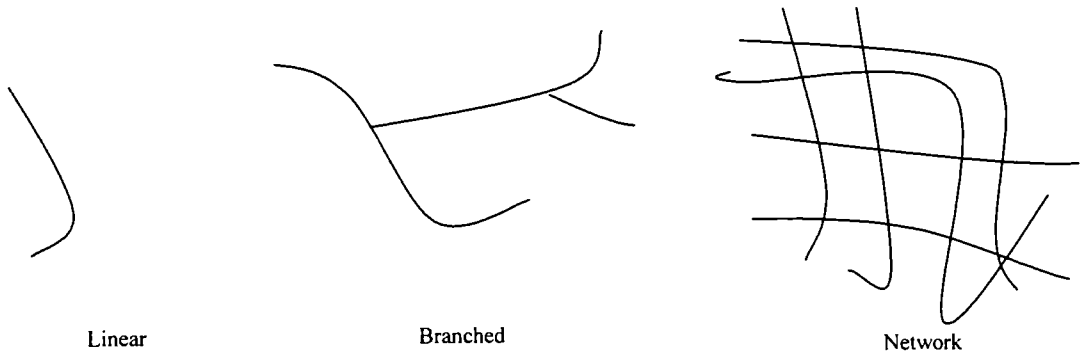

Figure 1.1 Cartoon images of linear, branched and network polymers.

Linear polymers are macromolecules with two chain ends. This may be simply drawn as a line and are conceptually the simplest type of polymers.

Branched polymers are linear polymers with branches that are introduced to the linear backbone at locations called branch points. Introducing branching into linear polymers increases the number of chain ends compared to linear polymers.

Network polymers are essentially one giant molecule, where each polymer chain is connected to each other by a series of branch points. True networks are insoluble in all solvents, but may swell in compatible solvents.

1.1.2 Classification According to Properties.

Polymers may also be classified according to their properties - thermosets, thermoplastics and elastomers.

Thermosets are polymer networks where the properties are influenced by the high degree of crosslinking, as described for networks in the previous section, these tend to be insoluble and difficult to process. A good example of this type of material is Bakealite.

Thermoplastics or plastics melt when heat is applied, these structures may be linear or branched and importantly can be injection moulded and extruded. These have a T_g (glass transition temperature) where the material starts to become ductile under heating, before melting (T_m) at a higher temperature. This type of polymer forms the majority of commercially produced materials in industry due to its versatility over the other polymer types.

Elastomers are rubbery networks constructed from crosslinked polymers that can be stretched and recover to their original size once the applied stress is removed. This property exists due to the low crosslinking density of the materials, allowing the recovery of the original material dimensions.

1.1.2.1 Molecular Weight Terminology.

Previously we've seen above how polymers may be classified according to structure/properties and later mechanisms, but how does one keep track of the size of polymers? The answer is using average terms related to the molecular weight distribution of the materials, namely number average molecular weight (M_n), weight average molecular weight (M_w) and polydispersity index (PDI). These describe the distribution of polymer chain lengths in a material. The following definitions apply to macromolecules in discrete fractions, such as *i* discrete fractions containing N_i molecules of M_i molecular mass. This allows polymers to be compared to one another and these terms are used throughout this text.

Definitions of the three parameters above are as follows:

- M_n is the sum of the products of the molar mass of each fraction multiplied by the mole fraction,

  $$\overline{M}_n = \sum X_i M_i$$

  where X_i is the mole fraction of molecules of molar mass M_i. i.e.

  $$\overline{M}_n = \sum {N_i M_i} \Big/ \sum N_i$$

  or the arithmetic mean of the molar mass.

- M_w is the sum of the products of the molar mass of each fraction multiplied by its weight fraction.

  $$\overline{M}_w = \sum w_i M_i$$

  where w_i is defined as the mass of molecules present:

  $$w_i = {N_i M_i} \Big/ \sum N_i M_i$$

- The polydispersity radio, or PDI:

  $$PDI = \overline{M}_w \Big/ \overline{M}_n$$

This is a guide to the width of the molar mass distribution of a polymer. A low polydispersity indicates a narrow distribution; however the standard deviation of this is reported by Rane and Choi[4] as being a more accurate guide to molecular weight distribution. A theoretical PDI = 1.00 indicates a monodisperse polymer chain, where all the polymers are the same length.

1.1.3 Classification According to Mechanism.

Polymerisation reactions generally fall under two general mechanisms; step-growth and chain-growth polymerisations.

1.1.3.1 Step Growth Polymerisation.

This mechanism involves the growth of a polymer in a step-wise fashion, where any two molecular species can come together and react, e.g. a monomer may add to a trimer, or two dimers combine to form a tetramer and so on and so forth to build up molecular weight. Typically a polymerisation using this method consumes the monomer relatively rapidly, forming larger species that then polymerise to create material of higher molecular weight. Typical step growth polymerisations involve the formation of materials such as polyethylene (PET) from ethylene glycol and terephthalic acid.

1.1.3.2 Chain Growth Polymerisation.

Chain growth polymerisation occurs where only the monomer adds to a reactive growing chain end, potentially leading to a much more controlled polymer growth. In this case the monomer is consumed steadily throughout the reaction. The predictable chain growth allows the potential for the formation of complex architectures, which is of relevance later in this text. Figure 1.2 describes a conceptual radical chain growth polymerisation reaction involving initiation, propagation and the two termination reactions of re-combination and disproportion.

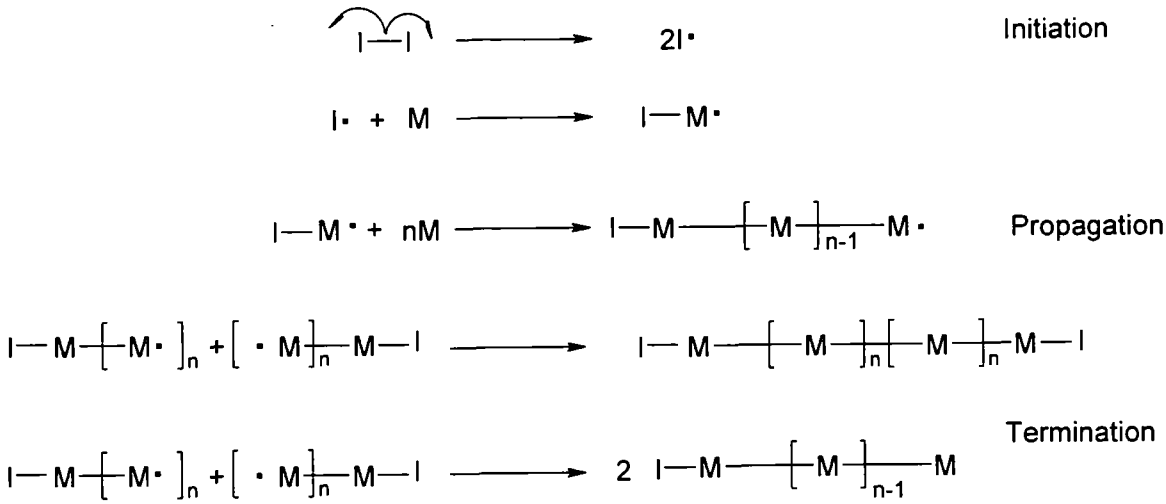

Figure 1.2 Conceptual polymerization reaction. Initiation, propagation and termination.

1.2 Controlled/ Living Polymerisation.

The term 'living polymerisation' was introduced by Szwarc et al. [5] to define a synthetic strategy for polymerisation which proceeds in the absence of termination or chain transfer reactions.

Controlled/living polymerisations may be achieved using a number of techniques, described in later sections, however a set of defining criteria associated with living polymerisations is described below:

- Polymerisation continues until the monomer supply has been consumed; addition of further monomer would restart growth of the polymer.
- The number average molecular weight (M_n) is a linear function of conversion. This may be monitored by the consumption of monomer during the polymerisation.
- The number of polymer molecules (active centres) is constant.
- The molecular weight of the polymer can be controlled by the stoichiometry of the reaction.
- Narrow molecular weight distribution polymers are produced.
- Block copolymers can be prepared by sequential monomer addition.
- Chain-end functionalisation can be achieved quantitatively, as controlled termination of a living polymer site can result in specific chain end functionalisation.

Apart from the basic thermal radical initiation of polymer materials in bulk, solution or emulsion polymerisations, various controlled mechanisms exist for the production of well defined materials. Living polymerisation, specifically anionic polymerisation is discussed in detail later in this text, however to put this into context, various other controlled polymerisation reactions are known and discussed. Most of these are based on controlled/living radical polymerisation, described below.

1.2.1 Controlled Free Radical.

Free-radical polymerisation is possibly one of the simplest methods for the formation of polymers. Free radicals are highly reactive unpaired electrons that react as active sites for the polymerisation of monomers - reactions proceed via a chain growth mechanism. Initiation requires a source of radicals; typically an azo or peroxide based initiator. Indeed a vast amount of industrially produced polymers are manufactured using this method, yielding materials cheaply with relatively high polydispersities. Lowering the polydispersity of materials made using this method requires stabilization of the radical species, sufficient enough for controlled polymerisation, but reactive enough for the polymerisation to occur.

Various techniques described in the following sections show how control can be achieved.[6]

Controlled radical polymerisations proceed on the basis of establishing a dynamic equilibrium between propagating radical and dormant species. Radicals are trapped in two possible ways, in a deactivation/activation cycle shown in Figure 1.3, or a reversible transfer mechanism shown in Figure 1.4

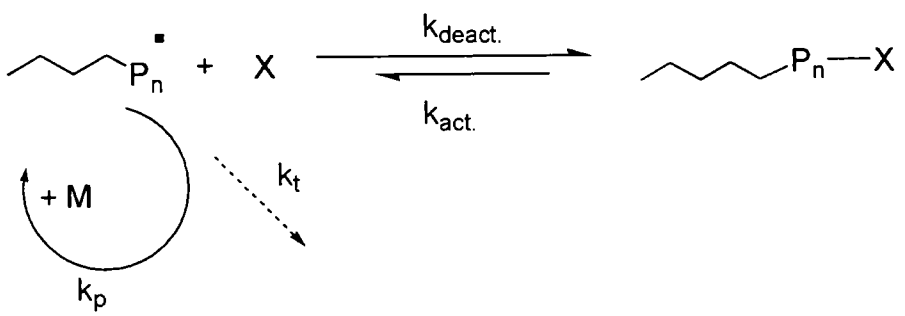

Figure 1.3 Generic deactivation/activation controlled free radical reaction.[6]

Deactivation/Activation is shown in Figure 1.3, where a self regulating reaction provides control over the reactive centre. Radicals at the propagation site are trapped by X, which may be reactivated. In this scheme, radicals react with the species X (they may propagate and terminate separately), thereby inhibiting termination with each other. This introduces the control over the polymerisation reaction as the 1st order propagation reaction competes against the second order termination reaction. Deactivated species are regenerated via a number of ways, described below. Reactions following this process require a stoichiometric amount of mediating species, as they are end capped with this functional group.

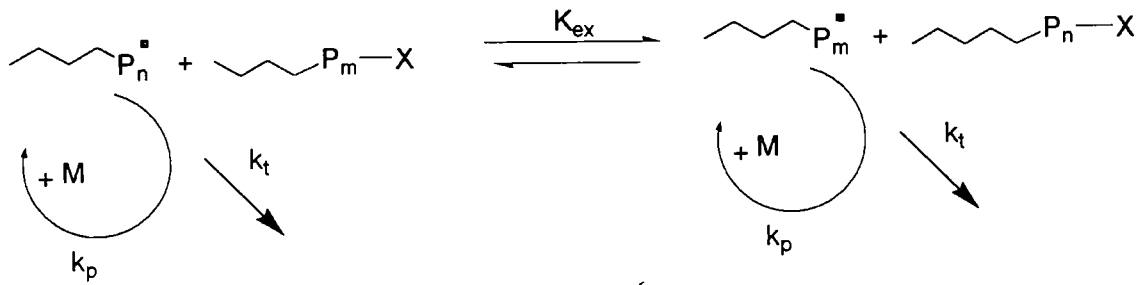

Figure 1.4 Reversible transfer of radical species.[6]

Degenerative transfer, as shown in Figure 1.4 is slightly different to the reaction in Figure1.3. In this case a relatively small amount of initiator is used compared to the chain transfer agent X, as the transfer agent plays the roll of the deactivating species. Reactive radical species can be deactivated, and reactivated by the transfer agent, creating control over the polymerisation reaction.

In all cases of controlled free radical polymerisation, the selectivity and control of the reaction relies on the ability of the growing species of the polymer chain to react with only a few monomer units before deactivation. The kinetics of the reaction required for this control is the interplay between k_p (propagation rate constant) the kinetics of the deactivation mechanism and k_t (termination rate constant).

1.2.1.1 ATRP.

ATRP (atom transfer radical polymerisation) is a transition metal mediated controlled radical polymerisation reactions that proceed via a reverse transfer reaction involving an alkyl halide (Figure 1.3)[6]. Polymerisations have been successfully achieved using many transition metals, with varied solvents and monomers, the best results are achieved

using the copper halides. Tuning catalyst parameters is achieved by the addition of various ligands (typically 2,2- bipyridine (bpyn)) which associate with the transition metal centre for more control over the reactions. Significantly, polymerisation temperatures are lower than that of nitroxide mediated polymerisations (NMP), and Cu based centers handily have a wide scope of monomers including acrylates and styrenes. Disadvantages are that the system is more oxygen sensitive than nitroxide mediated polymerisation techniques, and the polymers have residual Cu present. This is difficult to remove; inherently making polymers constructed using this technique unsuitable for medical applications.

1.2.1.2 RAFT.

RAFT (reverse-addition fragmentation chain transfer polymerisation) is a controlled /living polymerisation technique which uses dithioesters as transfer agents. This technique uses a mechanism described in Figure 1.4, as the trapped radicals fragment to generate different carbon and sulfur compounds. The exchange reactions are relatively fast, which controls the polymerisation. Figure 1.5 shows the mechanism of a typical RAFT polymerisation.[7] Initially the RAFT agent reacts with a propagating radical (P_n•) created from a thermal initiator and monomer. Fragmentation results in the formation of a new radical R• which can act as an initiator generating a new propagating radical P_m•. Again equilibrium occurs resulting in controlled chain growth, creating the living characteristics of the polymerisation.

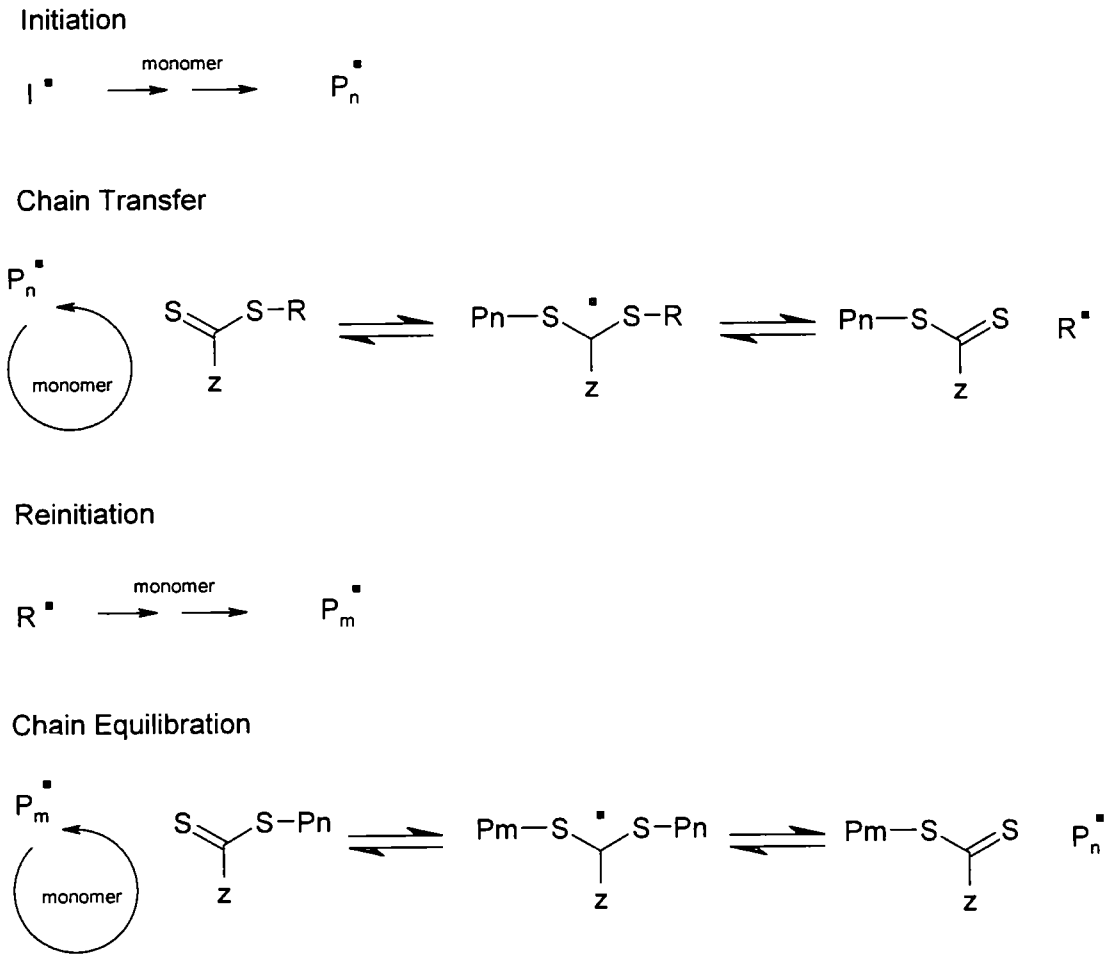

Figure 1.5 Generic RAFT polymerization mechanism.

RAFT agents are specifically chosen for a wide variety of particular monomers, as shown by the variable Z group in Figure 1.5. Polymerisations are relatively tolerant to moisture, but not oxygen; even aqueous RAFT has been reported.[8]

Disadvantages of RAFT polymerisations include the synthesis of specific pure RAFT agents, in some cases requiring long synthetic strategies. Also the reactions have relatively long (apart from aqueous solutions) polymerisation times in comparison to other controlled living techniques. The presence of sulfur at the polymer chain end post polymerisation allows the potential for the formation of well-defined block copolymers, but also creates some problems – sulphur smells strongly and imparts a pink colouration into the polymers.

1.2.1.3 NMP.

Nitroxide mediated polymerisation (NMP), is based on the mechanism shown in Figure 1.3 above, where an air stable nitroxide radical such as 2,2,6,6-tetramethylpiperidine 1-oxyl (TEMPO based derivatives – Figure 1.6) is used as the deactivating species in the reaction.

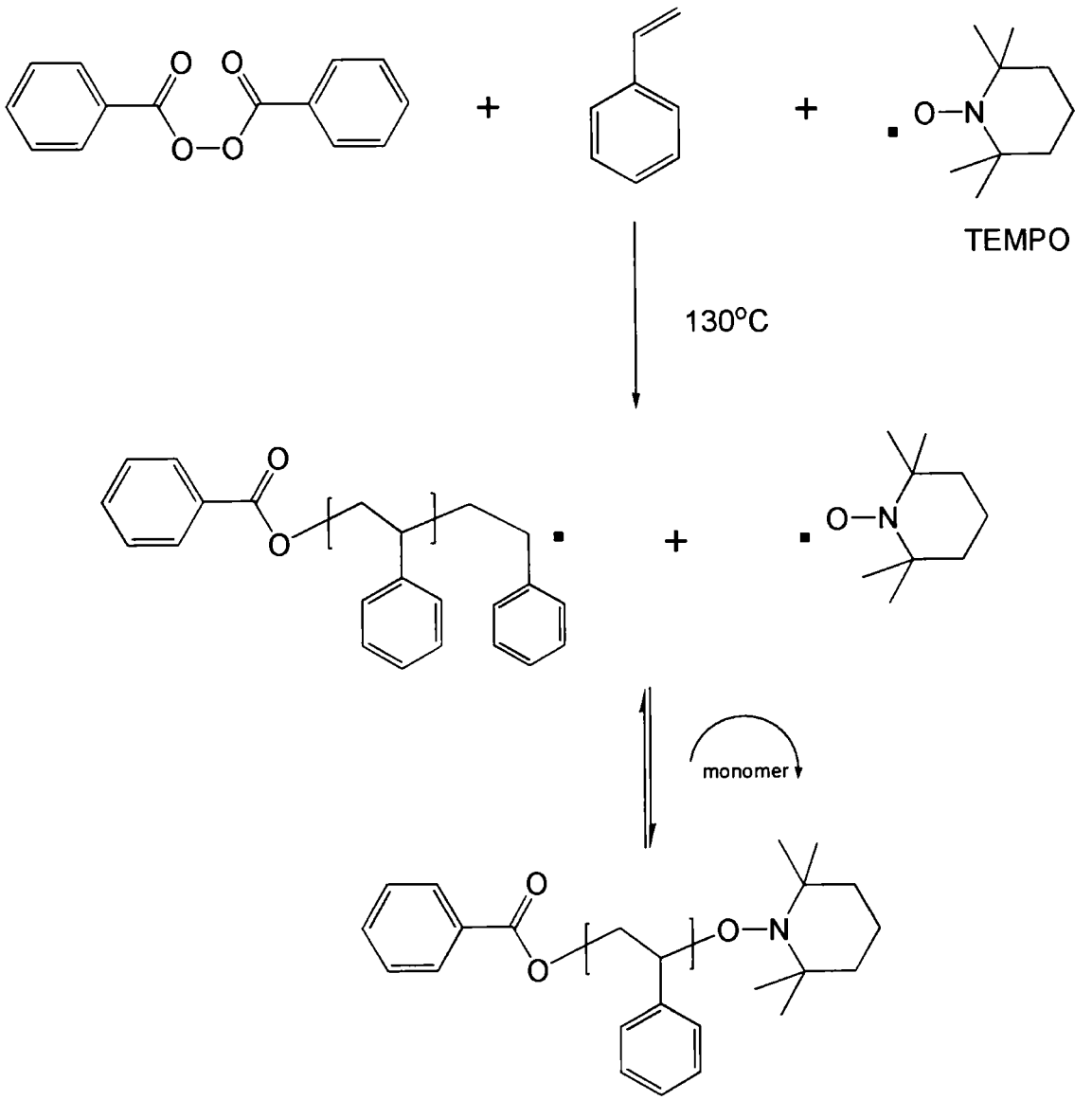

Figure 1.6 TEMPO (2,2,6,6-Tetramethylpiperidine 1-oxyl) mediated styrene polymerisation.[9]

TEMPO is suitable for the controlled polymerisation of styrene (PDI ~ 1.2), however the regeneration step is relatively slow, and fails to retain control when used to polymerise other common monomers, such as acrylates. Modified TEMPO derivatives may control polymerisation of other monomers, but tend to be specialized to certain

reactions. The narrow availability of monomers and the relatively high temperatures required (ca. 130°C) for this type of polymerisation mean that more versatile controlled radical techniques are generally used. However for specific applications where traces of transition metals or sulfur are forbidden, such as biomedical applications, this provides a useful route to controlled polymerisation.

1.2.2 ROMP.

Ring-opening metathesis polymerisation (ROMP)[10] is a polymerisation that involves the formation of polymer from unsaturated cyclic and bicyclic monomers. Not a radical mechanism, but producing materials in a controlled way, the reaction is based on olefin metathesis, involving a metal-mediated carbon-carbon double bond exchange. The mechanism can be described as a chain growth polymerisation reaction, with the unique property that the monomer double bonds are incorporated into the polymer backbone, shown in Figure 1.7.

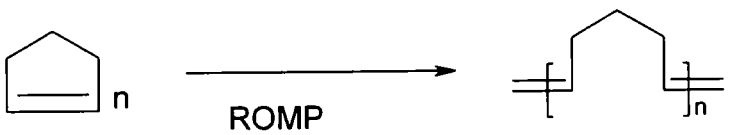

Figure 1.7 ROMP polymerisation showing the alkene incorporation into the polymer backbone.

Reactions are reversible in relation to the metathesis transition step, controllable to some extent by changing the catalyst ligands. Despite this, polymers are synthesised using this technique as the entropy of removing the ring strain by going from monomer to polymer is enough of a driving force for the reaction to proceed. The common use of highly strained monomers such as norbornene provides a route to controlled polymerisation using this technique. Propagating centres exist as either metallacyclobutane or metal alkylidine structures depending on reaction conditions.

Polymerisation occurs with minimal amounts of chain transfer or termination, and terminating reagents can be used for end capping; i.e., this follows the rules defined for the production of a controlled living polymer.

The first ROMP catalysts were based on Ti salts described by Ziegler and Natta[11], which were air and moisture sensitive and difficult to handle. Polymers constructed with these complexes were relatively uncontrolled, however improvements have been made.

Innovative catalysts based on Mo or W metal centers were described by Schrock[12], advancing this technique with a wider range of monomers including esters and amides, making this polymerisation type more universally applicable.

The latest and most commonly used catalysts, developed by Grubbs[13] are based on Ru complexes are relatively universal, and tolerant to most functionalities including water, (apart from oxygen) and produce relatively well-defined materials.

1.2.3 Ionic Polymerisation.

Ionic polymerization occurs via an active chain end which bears an ionic charge, either positive (cationic) or negative (anionic). Monomers suitable for polymerization by each of these mechanisms must be able to stabilize the charge for polymerisation to proceed.

1.2.3.1 Cationic Polymerisation.

Cationic polymerisation is a chain growth polymerisation with a positively charged propagation centre, in some cases exhibiting the seven defining properties of living polymerization (section 1.2.3.2). Typical initiators include Lewis acids such as BF_3 (boron triflouride), $SnCl_4$ (tin tetrachloride) or $AlCl_3$ (aluminium chloride) for the initiation (with small amounts of water) of various vinyl monomers with electron-donating side groups. This group is required as this type of substituent stabilises the propagating charge on the living chain end, as shown in figure 1.8.

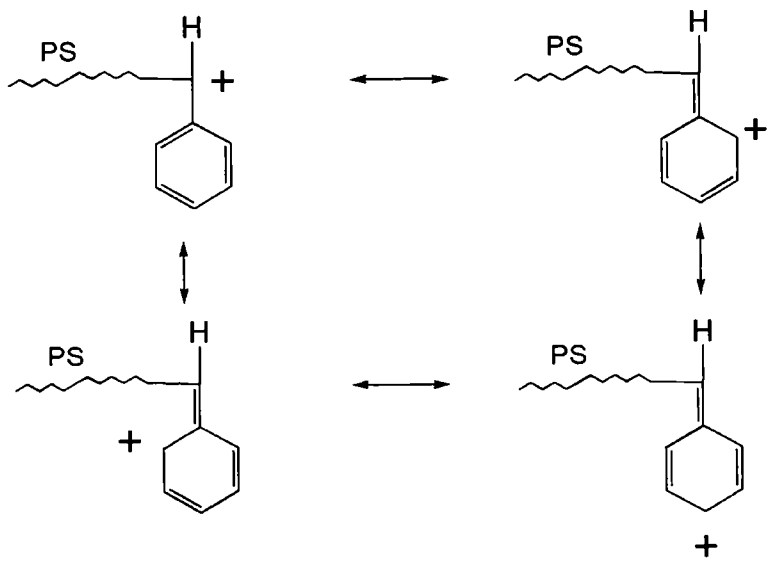

Figure 1.8 Stabilization of polystyrene cation, making the monomer suitable for living cationic polymerisation.

Cationic polymerisation has a fast propagation step requiring polymerisations to be carried out at low temperatures (-70°C). This minimises side reactions such as chain transfer and back-biting reactions which can result in decreased control.

Monomers with strongly electron donating groups that may not be polymerised by an anionic mechanism, maybe polymerisable via cationic polymerisation. An important example of this is the cationic polymerisation of isobutylene,[14] the only synthetic route to this commercial material due to the monomer reactivity.

1.2.3.2 Anionic Polymerisation.

Anionic polymerisation provides probably the best route for the construction of well-defined polymers. Molecular weight, molecular weight distribution and chain end functionality can all be controlled with this method. High vacuum techniques, or inert atmospheres are required to minimise impurities to maintain the production of homogeneous polymers which can lead to unique polymer architectures.

Certain anionic polymerisation may be described as living; the two main classes of monomers which may be used with this type of polymerisation are vinyl type monomers, such as styrene (Table 1.1) and cyclic monomers, such as lactones[15]. Vinyl monomers have functionality provided by one or more double bonds, while cyclic monomers ring open with the attack of nucleophiles; both producing living chain ends. Importantly the monomer reactivity, stability of the propagating carbanionic species and that of the initiator contribute towards the ability of a monomer to undergo anionic polymerisation.

Vinyl	Cyclic
Styrene and derivatives	Epoxides
Vinylpyridines	Sulphides
Dienes	Lactones/Lactides
Alkyl Acrylates and Methacrylates	Carbonates
Acrylonitriles	Lactams
Vinyl Ketones	Siloxanes
Nitroethylenes	

Table 1.1 Typical monomers used in anionic polymerisation.[15]

Alkyl lithium initiators are most commonly used as initiators in anionic polymerisation (Figure 1.9) as they are efficient, available commercially and relatively easily prepared. Reactivity of the initiators can be changed by varying the alkyl group and the solvent in which the initiator is used. A typical anionic polymerisation reaction of styrene is shown in Figure 1.9 demonstrating initiation, propagation and termination, where s-BuLi is used as the simplest initiator.

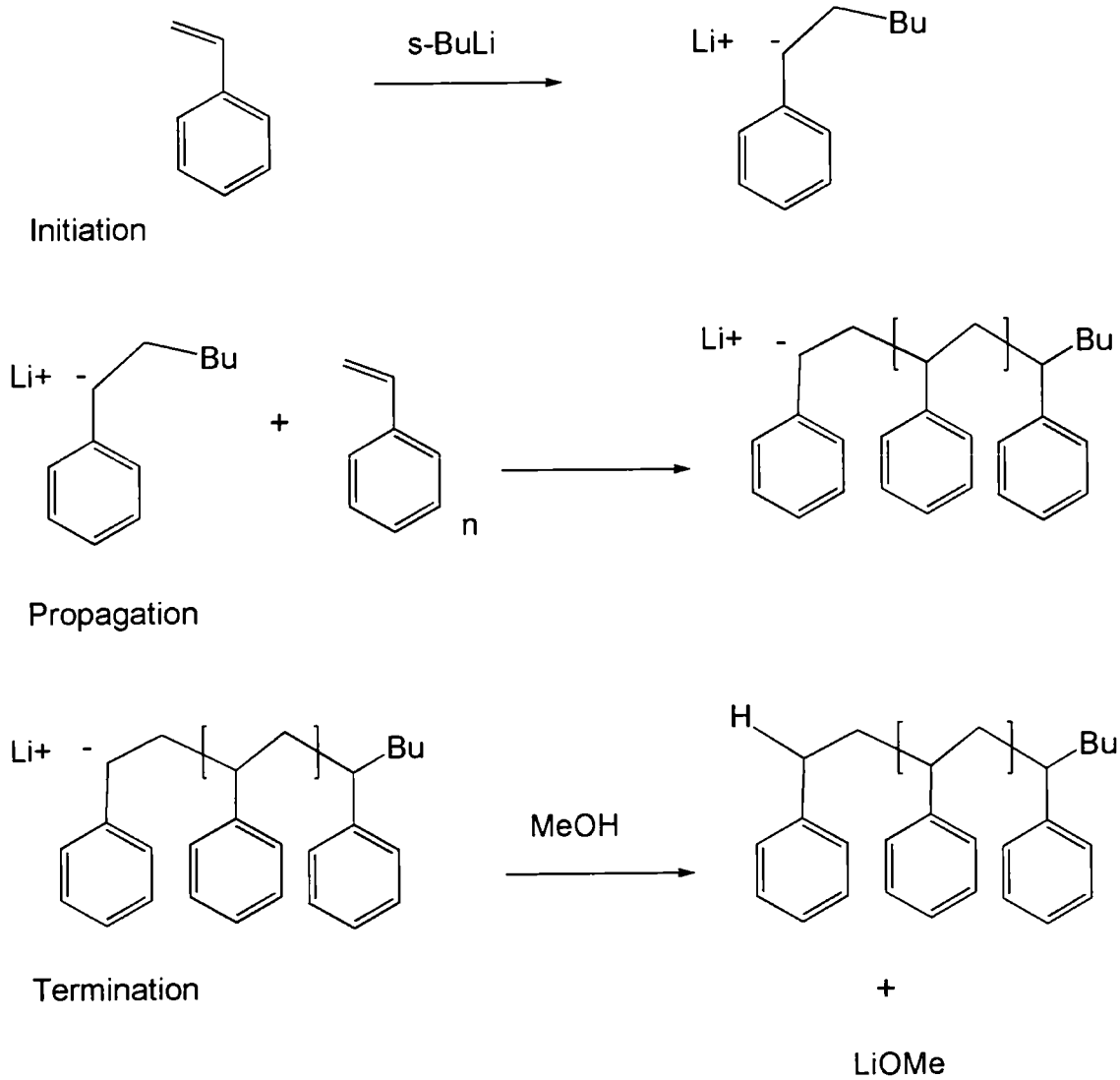

Figure 1.9 Initiation, propagation and termination. (In terms of anionic polymerisation of styrene with an alkyl lithium initiator forming polystyrene.)

Functionalisation of polymer chain ends can be achieved in a variety of ways, for example the addition of end capping agents, crosslinkers or use of functional initiators[15]. One of most reliable end functionalisation reactions is the addition of 1,1 – diphenylethylene (DPE) derivatives to the living chain end. Qualitative end capping is

achieved as the vinyl group of the DPE group is reactive, but the steric bulk of the phenyl groups prevent homopolymerisation, resulting in the introduction of a single DPE unit. End functionalisation using DPE derivatives is reviewed by Hirao[16] who describes the versatile use of this vinyl derivative.

Ethylene oxide can be used for the preparation of hydroxyl end functionalised polymers. This reaction is reported as being almost quantitive and is one of the most simplistic end functionalisation reactions used in anionic polymerisation.[15]

Hadjichristidis et al.[17, 18] introduces a review of linking chemistry and anionic polymerisation, containing sections on DPE derivatives and other non-living linking reactions including the use of carbon dioxide and chlorosilanes.

A defining criteria for living polymerisation is the formation of controlled block copolymers. Anionic polymerisation is particularly suitable for block copolymer synthesis however; three important factors need to be considered for the formation of these materials[15]:

- The second block monomer has to be compatible with the first, i.e. the first must be able to initiate the polymerisation of the second polymer block.
- The crossover reaction from monomer A to monomer B requires the second monomer initiation to be faster than the propagation of the second monomer. Without this criteria block copolymers are formed, but the control over polydispersity usually associated with anionic polymerisation would be lost.
- High purity second monomer must be used, as any impurities will cause living chain ends to be terminated, reducing the number of chain ends and creating low molecular weight impurities. Impurities are also a concern with end functionalisation reactions, as any present prevent quantitative polymer functionalisation.

1.2.3.2.1 Commerical Applications of Anionic Polymerisation.

High vacuum techniques and laborious solvent and monomer purification paints a picture of a very academic route for polymer synthesis. However, commercial applications of anionically synthesised polymers under the Kraton®, and Firestone brands have wide ranging industrial applications.[15] Kraton polymers are thermoplastic elastomers (TPEs) based predominantly on block copolymers of polystyrene, polyisoprene and polybutadiene.

Block copolymers forming thermoplastic elastomers (TPEs) generally combine a glassy type polymer with a diene, forming materials with the strength associated with the glassy polymer and the soft rubbery properties of the rubber diene. They have many commercial uses, including bitumen modification, adhesives, packaging and act as alternatives to natural rubber.

Other commercial uses of anionic polymerisation include the synthesis of telomers; liquid hydrocarbon polymers.[15] Typically constructed from butadiene or isoprene using metallic based initiators, these materials have applications as surface coatings, sealants and adhesion promoters due to their comparatively low viscosity. More akin to resins than elastomers, the unsaturation signifies the ability to co-cure and, with additional functionality such as maleinisation even become water soluble.

1.3 Branched Polymers for Structure Property Correlation Studies.

Architecture plays a significant role in how materials behave under various conditions at varying length scales, and this is no different in the polymeric world. Polymer properties and processing depend heavily on composition, molecular weight, polydispersity, as well as many other variables, one of the most significant being architecture.

The processing of linear polymers and the underlying physics has been investigated for many years.[19] An ongoing challenge for polymer chemists, physicists and engineers is to understand how branching affects polymer processing. Many industrially produced branched polymers inherently have a wide polydispersity, as well as randomly branched architectures, making accurate modeling and prediction of polymer properties very difficult. A tried and tested approach is to produce well-defined model polymer materials to develop models and theories with the aim that these theories can be applied to less well-defined industrial materials. Over the years ever more complex branched structures have been studied.

1.3.1 Star Branched Polymers.

The presence of one branch point in a polymer results in simplest branched polymer, the star. Synthesis of model star branched polymers generally occurs by two synthetic routes, the arm first and core first approach. One of the earliest reports by Gervasi and Gosnell[20] describes four and six arm polystyrene stars constructed using the arm first

approach. Living monodisperse polystyrene chains were coupled to multifunctional core molecules. Worsfold[21] and Meunier et al.[22] used chlorosilane coupling agents – a method that has been used frequently since. Construction of branched polymers using this approach is preferred for the synthesis of model stars, as it allows accurate characterisation of the arm, before adding the branch point. Numerous examples of the assembly of stars with chlorosilane coupling are reported for a wide ranging number of arms including 4 and up to 128 arms by Hadjichristidis et al.[17, 18, 23, 24]

The core first approach involves the growth of arms from a multi functional core, and offers less control over the structure. One of the distinct disadvantages of the core first approach is the inability to characterize the molecular weight of the arms independently. Hirao et al. [25] report regular, well-defined star-branched polymers. Stars with up to 33 arms were prepared, showing the characteristic viscosity properties of highly branched structures.

Another type of star branched polymer is the mikto arm stars in which the star is comprised of 'arms' of different polymers. The first example was reported by Hadjichristidis[26] was a 3 arm star shown in Figure 1.10 consisting of an arm each of polyisoprene, polystyrene and polybutadiene.

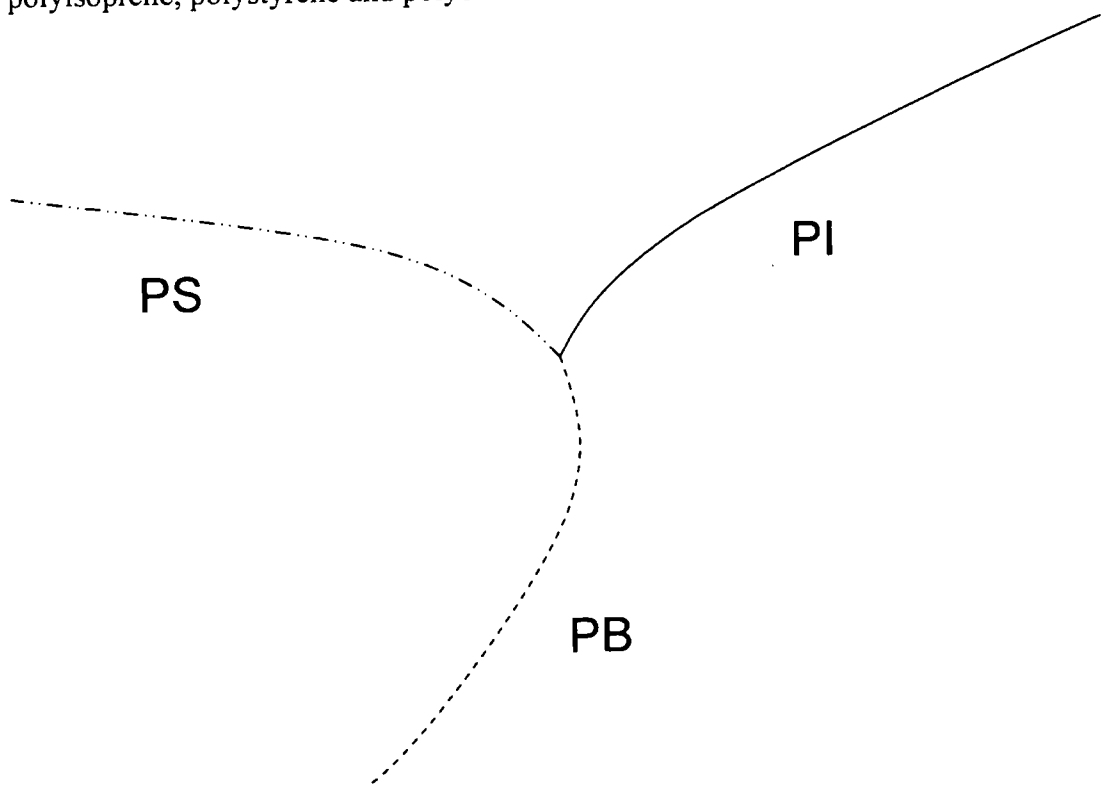

Figure 1.10 Miktoarm star copolymer constructed from polystyrene, polyisoprene and polybutadiene.[26]

The synthesis relies on chlorosilane coupling reactions with sequential polymer addition. After fractionation, well-defined stars with polydispersity of around 1.03 were reported, demonstrating a technique for the assembly of variable arm compositions.

A recent review focusing on dendritic star type branched materials formed using anionic polymerisation is described by Hirao et al.[27], here branched materials formed primarily using iterative methodology are described from stars up to larger dendrimer structures. Coupling reactions include chlorosilane and diphenylethylene (DPE) based chemistry, highlighting the unique benefits of this chemistry for the production of novel branched materials.

Stars are still an area of interest due to their simple, yet non-linear architectures. Clarke et al.[28] report the diffusion behavior and viscosity of a series of 4-armed polystyrene stars for confirming star behavior predicted by the tube model. Qian et al.[29] looked at the surface tension of symmetric star polymer melts and found that addition of branch points alter the relationship between molecular weight and surface tension.

1.3.2 H Shaped Polymers.

The next level of complexity of branched architecture arises from the introduction of a 2nd branch point. Conceptually this creates two stars coupled to each other, or an H-shaped polymer. This architecture increases the complexity of branching of the star polymer and importantly from a modeling perspective introduces arms and backbones. This is a valuable addition, as these potentially introduce sequential relaxation regimes within the polymer rheology.

Roovers et al.[30] first described the synthesis of polystyrene H shaped polymers, using anionic polymerisation and chlorosilane coupling agents. These well defined polymers were designed for structure-property correlation studies and the rheological properties have been reported[31].

Construction of similar branched polymers made from polyisoprene which have more polymer entanglements was achieved using a difunctional initiator and chlorosilane coupling and was reported by Young et al.[32] (Figure 1.11). This group reports many advances in synthesis, modeling and characterisation of H-shaped polymers, relying on the synthesis of model architectures for the validation of complex polymer dynamics.[33,34, 35, 36]

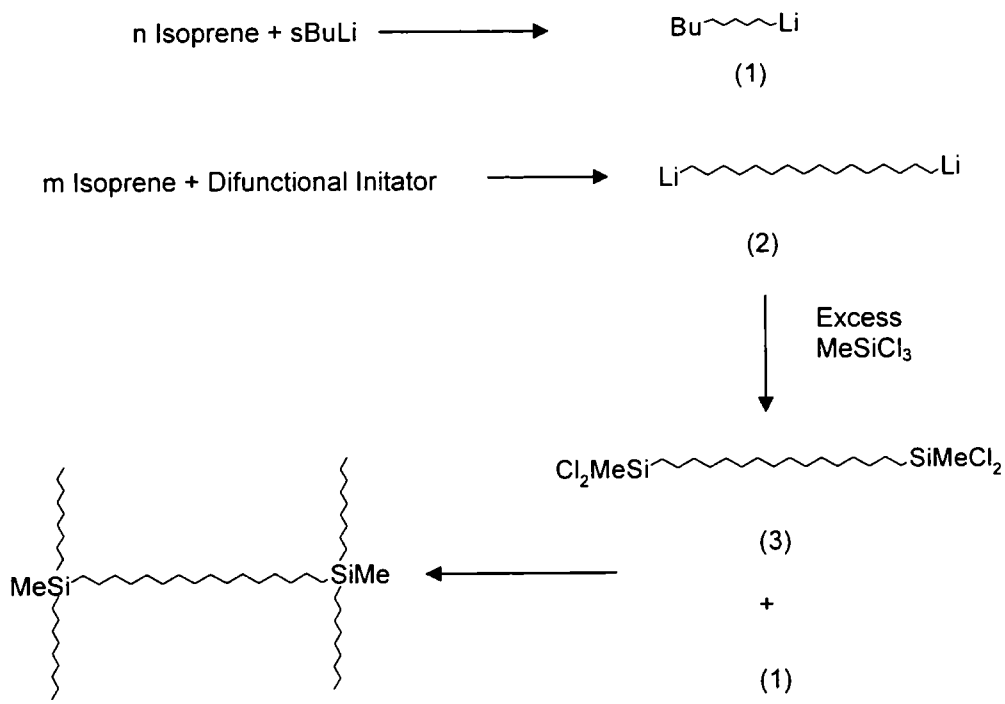

Figure 1.11 Formation of H-shaped polyisoprene using a difunctional initator and chlorosilane coupling.[32]

Figure 1.11 shows the assembly of an H-shaped polymer. The backbone of polyisoprene (2), is end-capped with methyltrichlorosilane (3) and then arms are coupled to this functionality, forming the H (4). This synthetic route allows the characterisation independently of backbone and arms during the reactions, critical for the production of model materials for structure-property correlation studies.

Super H-shaped polymers start to bridge the gap between a small number of branch points and an increasing number of polymer chain arms, as the six polyisoprene arms are coupled with a polystyrene cross-bar are reported by Hadjichristidis et al.[37] Increasing the number of arms develops the structures towards highly branched materials, with small incremental steps of complexity. Addition of more arms to two branch points leads to novel architectures in many respects; increasing the number of branch points with a linear backbone results in a comb.

1.3.3 Comb Polymers.

Additional branch points along a linear backbone results in a comb branched polymer. Comb branched polymers are constructed via a number of routes including grafting from and grafting onto. As previously discussed for the construction of stars, a

convergent approach is preferred as this provides accurate characterisation of all constituent parts.

Model polystyrene combs are described by Roovers et al.[30, 38] where the branching in the structure is described as modifying the solution properties and glass-transition temperature of the macromolecules attributed to the increase in the number of chain ends.

Well-defined tri and tetra branched comb structures are described by Mays and Hadjichristidis [39] and were constructed with polystyrene backbones and polysioprene arms. Polydispersites are reported to be 1.08 for the complete structures, relying on the favoured chlorosilane coupling to produce model block copolymer materials.

Construction of materials using macromonomers will be covered in later sections, as this is the route in the direction of HyperMacs.

1.3.4 Dendritically Branched Polymers.

Increasing the number of branch points and complexity of branching to give hierarchical branching creates seemingly complex architectures with varying structures. These highly branched dendritic structures provide challenges for both theoreticians and experimentalists at all levels.

1.3.4.1 Dendrimers.

Dendrimers are well-defined highly branched polymers. The structures were conceived as early as the 1950s[40] however it wasn't until the synthesis of Starburst® Dendrimers by Tomalia[41,42,43] and 'Arborol' structures independently by Newkome,[44](in the 1980s) that this type of macromolecule was realised.

There are two synthetic strategies for making dendrimers, the convergent and divergent approaches. The benefits of the two strategies are summarised well by Young[45] in Figure 1.12 Construction of similar molecular architectures is described and the benefits of each growth are compared and contrasted.

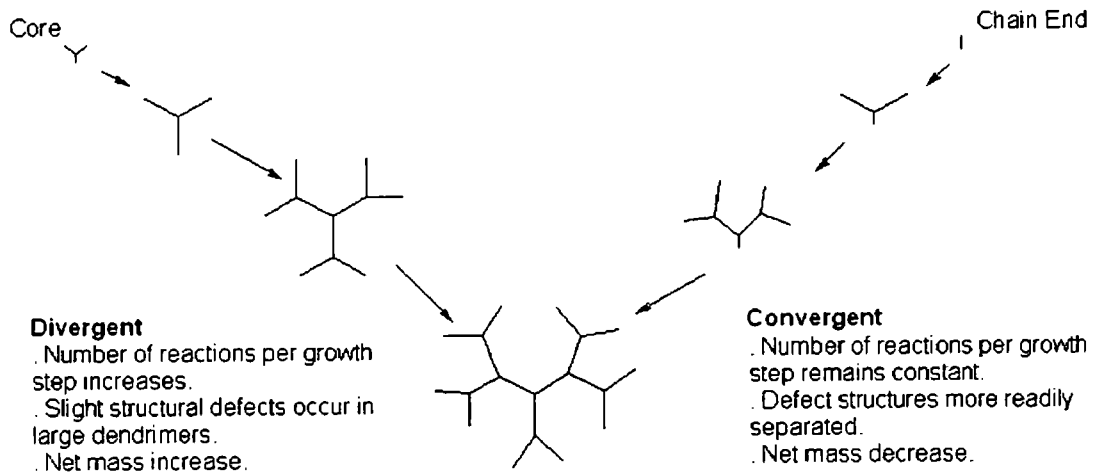

Figure 1.12 Dendrimer growth by divergent and convergent methods.[45]

Early work by Tomalia and Newkome followed the divergent strategy using polyamidoamine[46] materials, but this approach is limited in its success by complex purification steps and incomplete reactions, particularly for the higher generation dendrimers. This resulted in impure heterogeneous materials. The problems associated with the early syntheses were overcome, in some respects, with the convergent synthetic strategy developed by Hawker and Fréchet [47, 48]. They proposed a dendrimer assembly almost in reverse to the previous method, where the molecules were built up from the periphery, rather than the core. The final reaction to produce the dendrimer structure involved the coupling of the dendritic wedges to a multifunctional core (Figure 1.13).

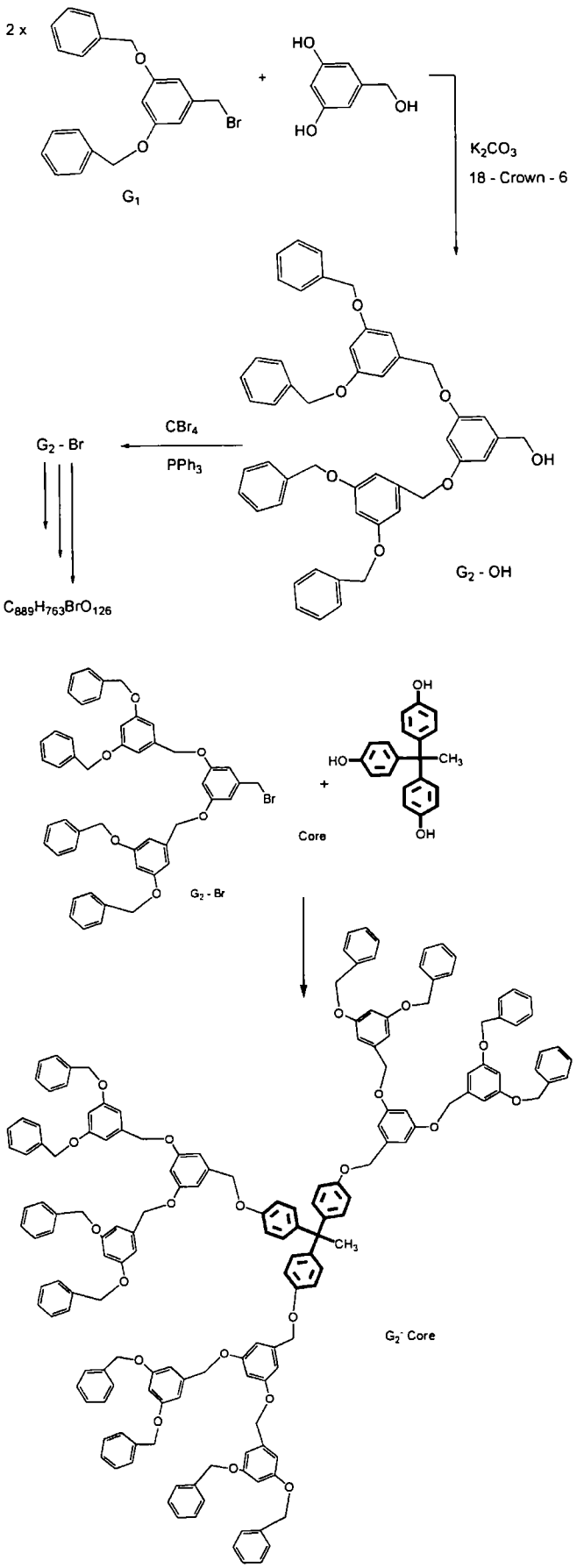

Figure 1.13 Convergent synthesis of dendritic macromolecules.[48]

Although both strategies have their virtues, the convergent approach generally gives more homogeneous structures and is often the preferred method.

1.3.4.2 Hyperbranched Polymers.

Hyperbranched polymers may be described as having dendrimer like architectures with a non-uniform branching structure.[49] These materials consist of a highly random structure and the synthetic techniques are more facile, often in 'one-pot' reactions[34]. The concept of coupling AB_2 molecules into structures with polydispersity ratios between 1.0 and ~5.0 was first discussed by Flory[40, 50], who described the theory behind the molecular weight distribution associated with reaction of the AB_2 monomers, where A selectively reacts with B from another molecule. An example of a hyperbranched coupling reaction of AB_2 monomer is shown in Figure 1.14.

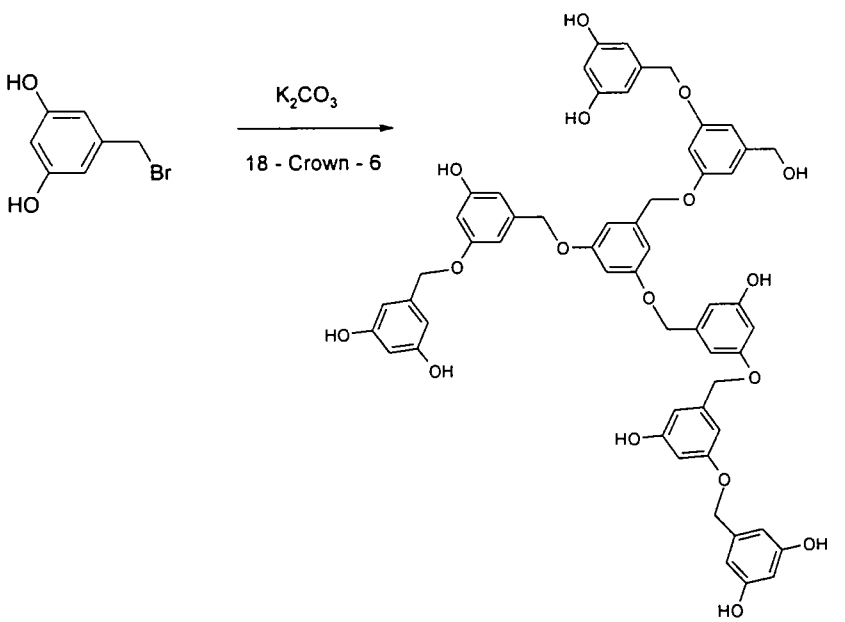

Figure 1.14 Representation of the construction of a hyperbranched polymer from an AB_2 macromonomer.[51]

Hyperbranched polymers offer an economical alternative to dendrimers as a result of the fewer synthetic steps required and the ability to produce large quantities of randomly branched materials.

An excellent review on the general chemistry of hyperbranched polymers is given by Young[45]. A more specific review concentrating on polyester based hyperbranched materials is described by Voit[52] (15 years after discovery), this outlines current research and the progress of commercialization of these types of materials.

1.4 Long Chain Dendritically Branched Polymers.

Combining an increasing number of branch points, hierarchical branching and increasing polymer molecular weight between branch points, results in highly branched materials with high overall molecular weight; the next generation of long chain branched polymers.

When considering long chain hierarchical/dendritically branched polymers we can divide the various materials that have been prepared into two categories, well defined and less well-defined.

1.4.1 Well-Defined Long Chain Branched Polymers.

A number of workers have produced a variety of branched polymers which may be described as long chain branched analogues of dendrimers. These polymers have been called Cayley Trees, dendritically star branched polymers and DendriMacs.[53] They have much in common with dendrimers having very well defined branches, a high degree of structural homogeneity and require time consuming syntheses.

The first reported dendrigraft synthesis appears in the literature as Comb-Burst® polymers by Tomalia et al.[54] A similar synthesis by Gauthier and Möller[55] is reported around the same time period with the synthesis of arborescent dendrigraft polystyrene in a divergent methodology using living polymerisation. This 'one-pot' synthetic procedure evolved from the chemistry performed by Tomalia[54], both examples use divergent syntheses from which polymer chains were grafted to create the macromolecules.

Synthesis of dendrimer-like star polymers is reported by Hedrick and Trollsås,[56] where the divergent synthetic approach is used with aliphatic polyesters to form well-controlled dendrimer-6-arm star materials, confirmed by NMR.

Gnanou and Angot[57] prepared a series of PEO/PS block copolymers with anionic polymerisation of ethylene oxide and ATRP of styrene, for the assembly of a range of branched architectures. This included three and four armed stars, building up to full dendritic materials. These polymers were fully characterized; showing cleavage of the PS blocks synthesised by ATRP from the PEO segments produced well-controlled linear polystyrene, indicative of good control over synthesis of the second block.

Later, the group of Gauthier report the synthesis of material with an arborescent polystyrene architecture[58] using acetylene groups for the introduction of branching.

Generations of branches were introduced sequentially, and are reported to be almost quantitative with the introduction of a few units of isoprene on each chain to increase the efficacy of the end capping reaction of the polystyrene. Polydispersity values of materials were reported as being low – around 1.09, indicating good control over the architecture.

Similar chemistry is used for the construction of randomly branched materials, by the same group, with the formation of polystyrene-poly-2-vinylpyridine block copolymers for the formation of unimolecular micelles.[59]

Dendrigrafts constructed from PEO are reported by Feng et al.[60] and highlight the biomedical applications of this type of material with the water solubility of relatively large molecular weight structures with these branched structures.

Synthesis of well-defined materials has also been reported by Hirao et al.[61] Anionic polymerisation is used to craft PMMA dendrimer like polymers with up to 29 arms using an iterative divergent approach, with benzyl bromide as a coupling agent. Later work with increased branching is reported by the same group[62] where up to seven generations of PMMA, with very low polydispersities (1.03) are created. In agreement with most of the literature, the intrinsic viscosity (η) and g' ($g' = [\eta]_{star}/[\eta]_{linear}$) values decreased with increasing generations - the overall molecular weight reported to be over 10^6 $gmol^{-1}$ for the higher generations of these materials.

Gnanou et al.[63] report the synthesis of well-defined polystyrene branched structures using ATRP. Structures with up to 32 arms were constructed using the core first approach, with iterative bromination reactions creating initiators for ATRP. The limitations of ATRP meant polydispersities were not as low as expected for materials produced by anionic polymerisation.

Bernard et al.[64] report amphiphilic grafts of PS-PEO; the control over these structures is not as great as previous dendrigraft structures[60] due to the 'grafting from' route technique being used for the construction of these novel architectures. The literature reports that the structures, due to their hydrophobic core and hydrophilic shells, have reasonable aqueous solubility with lower polystyrene content and show great potential for delivering hydrophobic molecules in an aqueous medium.

Regularly branched dendritic structures or DendriMacs (Cayley Trees), analogues to dendrimers, are reported by Hutchings et al. where polystyrene[53] and polybutadiene[65] AB_2 macronomomers are coupled in a convergent methodology to produce well defined branched structures. This type of structure can be considered as

being the next generation of dendrimer architectures using linear chains as building blocks rather than monomers. The highly branched materials from this synthesis are particularly important for structure property correlation studies. Synthesis produces well-defined materials but on a relatively small scale due to the associated purification steps required to produce polymers with low polydispersities.

Branched polybutadienes with structures similar to DendriMacs described above are described by Hadjichristitidis et al. [66] based on DPE/chlorosilane chemistry. Polydispersities for this material are around 1.10, suggesting good, but not perfect, control over the architectures of these branched structures for structure-property correlation studies. This follows work on a very similar synthetic strategy using polyisoprene and polystyrene[67] where a macromonomer approach is used to selectively combine polystyrene and polyisoprene into arms of controlled branched materials.

The wide variety of branched polymer architectures available to the synthetic chemist is varied, summarised in a review article by Hadjichristidis et al.[68] The macromonomer strategy for the construction of complex macromolecular structures using DPE, chlorosilanes and VBC (vinylbenzyl chloride) linking chemistry is reviewed. The routes described for constructing branched polymers other than anionic polymerisation including ATRP and ROMP is also suitable for the macromonomer approach of construction.

1.4.2 Less Well-Defined Long Chain Branched Polymers.

The second class of long chain dendritically branched polymers are much less well defined in their structure but have the considerable advantage of ease of synthesis.

Puskas et al.[69] report the synthesis of arboresent and hyperbranched materials using cationic polymerisation with inimers based on polyisobutylenes. Characterisation confirms the increase in branching, with molecular weights of around 10^5 $gmol^{-1}$ and polydispersity reported to be as low as 1.2, suggesting reasonably well defined materials. Adaptations are made to this chemistry for the formation of polyisobutylene-polystyrene branch block copolymers[70] where the materials are reported to have up to 1800% elongation before break and phase separated morphologies. The synthesis is portrayed as being relatively easily for scale up, useful for characterisation.

At least three groups have made hyperbranched polymers using AB_2 monomers that introduce a short linear spacer unit between branch points; Hawker[51] synthesised

hyperbranched polyesters from monomers containing up to 5 units of ethylene glycol, while Feast[71] similarly prepared hyperbranched polyesters with short linear $(CH_2)_x$ units between branch points where x = 2-4.

Frey et al.[72] report branched and functionalised polybutadiene involving AB_n macromonomers. This approach involves the quantitative end capping of mainly 1,2 polybutadiene with chloromethylsilane, and then a hydrosilation coupling reaction for the formation of branched materials in a one-pot procedure.

A more effective approach has been reported by Knauss et al.[73,74,75] who utilises a coupling agent in convergent living anionic polymerisation, to produce polymers with dendritic branching in a one pot reaction where living polystyryl chain ends (Figure 1.15) are used to produce successive generations of branching.

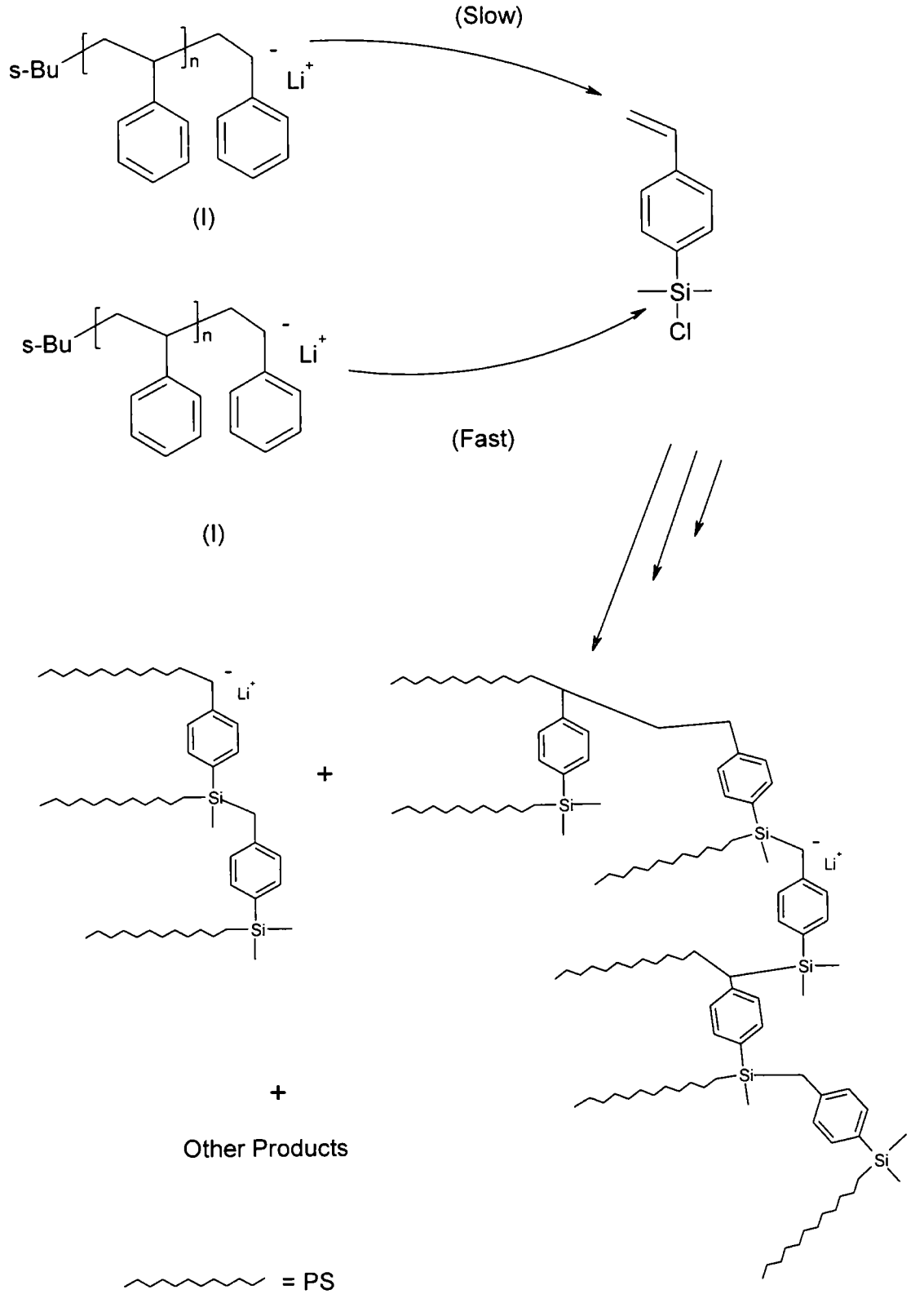

Figure 1.15 Knauss polystyrene synthetic strategy[73]. Initial addition of chlorosilane cross-linker to living PS chain ends results in a selection of numerous branched architectures.

The upper scheme in the diagram shows that the reactivity of the living polystyrene (I) with the coupling agent in a S_N2 type reaction, occurs via two competing reactions. Stoichiometric amounts of coupling agent are added to the reaction, with the vinyl bond less reactive than the chlorosilane. Functionalisation of the polystyrene chains is achieved whilst maintaining the reactivity of the living chain end via the incorporated vinyl group. The polymer is reported not to undergo crosslinking in this convergent route, allowing star shaped polymers to be formed in a one-pot approach. The lower section of Figure 1.15 illustrates possible coupled structures from this reaction; indeed many other examples will be present. Notably, syntheses of this kind have limited control over the polymers forming the hyperbranched type structures, creating randomly branched materials. The Knauss papers [73,74,75] report solution viscosity similar to the dendrigrafts of Gauthier[59], with low values compared to linear polystyrenes. Clearly these polymers are highly branched, but have random polymer chains between branch points.

Hutchings et al.[76] describe the synthesis of polystyrene HyperMacs. Synthesis involves living anionic polymerisation of styrene with a functionalized protected initiator, which is then end-capped with a functional DPE derivative. The protected macromonomer is deprotected and chlorine functionality created from the aliphatic alcohol of the functionalised initiator. A modified Williamson ether coupling is then used for the construction of randomly branched polystyrene in a one-pot reaction. Synthetically this was successful in producing branched materials; however the overall extent of reaction was somewhat disappointing. This was attributed to impurities generated from the decomposition of dimethylformamide (DMF) used in the final coupling reaction, which removed the halide groups from the macromonomers, retarding the extent of the reaction.

The current thesis continues this work, describing the improved synthesis and characterisation of a series of new long-chain branched materials.

1.5 Rheology

1.5 Introduction.

Rheology is the science of the flow and deformation of materials. Bingham coined the phrase that 'Rheology is the study of deformation and flow of matter' in 1929 [73], however the foundations of the science are deeply seated in physics being associated with the terms elasticity and viscosity. The importance of this area cannot be underestimated as rheology is about us everywhere, but in context here, particularly important in polymer processing.

1.5.1 Viscoelasticity.

An introduction to viscoelasticity is given in accounts by Larson[19] and Rohn[78], where the origins of viscoelastic behaviour are derived from Hooke's and Newton's Laws. This created models such as the spring and dashpot model[79] that combines the solid and liquid behaviour from the two classical models into a system that has solid and liquid like behaviour.

In simple deformations, the shear stress, σ (N/m^2), is given by the shear force applied to the sample per unit area of the surface, $\sigma = \frac{F}{A}$

Deformation of the solid is measured by the shear strain, γ, (dimensionless) which is given by the displacement per unit length normal to the shear plates, $\gamma = \frac{\Delta}{H}$, where H is the displacement length.

The deformation rate is specified by the shear rate derivative with respect to time;

$\dot{\gamma} = \frac{d\Delta}{dt} \Big/ H$, which is the change of shear strain with time. Units $\dot{\gamma}$. = (s^{-1})

The shear viscosity may then be defined as $\eta = \sigma / \gamma$.

Classical models for stress-strain relationships include the models for a pure elastic response as, in Hookean spring, and a purely viscous response as, a Newtonian liquid. For the former;

$\sigma(t) = G\gamma(t)$

whilst for the latter;

$$\sigma = \eta\gamma(t)$$

where G is the shear modulus associated with the solid and η, the shear viscosity for the liquid component. These models apply well in a classical sense, but are too simple to be used individually to model a viscoelastic material.

In viscoelastic materials the loading time of the substance is critical, the material is solid like for rapid loading, but liquid like for slow loading. For a Hookean solid, when shear strain γ_0 is applied, the stress would be constant for a classical solid. For a liquid, the stress would be zero as the strain rate is zero. Viscoelastic materials would show a stress value that decreases with time until it reaches an equilibrium value for that particular material, either solid or liquid. A small strain applied to the material may result in a linear response, termed the shear stress relaxation modulus;

$$G(t) = \frac{\sigma(t)}{\gamma_0}$$

In a creep experiment for a viscoelastic material the strain rate decreases with time until it reaches a rate at which it is constant. Removal of the stress results in a creep recovery period, as the material recoils and reaches equilibrium at a smaller strain than when the force was removed. Small shear stresses cause the strain to be a simple deformation in a linear fashion. The ratio of the shear strain to shear stress in a creep measurement is termed the shear creep compliance;

$$J(t) = \frac{\gamma(t)}{\sigma_0}$$

The terms G(t) and J(t) are interrelated through the Boltzmann superposition principle. Using these values, the steady-state viscosity at zero shear rate, η_0, and steady-state recoverable shear compliance, J_e^0, can be introduced which play an important role in the flow properties of materials.

$$J_e^{\,0} = \frac{\gamma_r}{\sigma_0}$$

The product of η_0 and J_e^0 can be shown to be approximately the average relaxation time, τ_0, which is a measure of the time needed for a given material to reach a state of equilibrium,

$$\tau_0 = \eta_0 J_e^{\,0}$$

The relaxation time can be used to roughly determine if a substance is solid, liquid or viscoelastic on the timescale of the experiment and has implications involving non-linear viscoelastic behaviour.

1.5.2 Storage and Loss Moduli.[19, 78]

Methods for determining the dynamics of viscoelastic systems include small-amplitude oscillatory shearing. Rheometers performing this type of experiment usually use cone and plate or parallel plate geometry where the cone or top plate is rotated with an angular velocity that oscillates sinusoidally. The in-phase and the out-of-phase components of the shear stress are measured as a function of frequency, ω (rad s^{-1}). Hence if the strain is,

$$\gamma(t) = \gamma_0 \sin \omega t$$

then the response is given by,

$$\frac{\sigma(t)}{\gamma_0} = G'(\omega)\sin \omega t + G''(\omega)\cos \omega t$$

G' is termed the dynamic storage modulus and G'' the dynamic loss modulus, γ_0 is the strain amplitude and is normally kept low (< 1) to ensure that linear response for the material is achieved, ensuring that valid relaxation times are recorded in equilibrium. The response is of a sinusoidal nature due to the origin of the stress applied to the system. The storage modulus represents the storage of elastic energy; the loss term comes from the dissipation of the energy due to the viscosity of the material. The ratio of the loss to the storage modulus (G''/G') is termed the loss tangent (tan δ) and is high (>1) for liquid like materials and low (< 1) for solid like materials. Figure 1.16. shows the typical G' and G'' mastercurve for a polymer melt dynamic experiment. A mastercurve shows the liquid and solid type behaviour for a particular material.

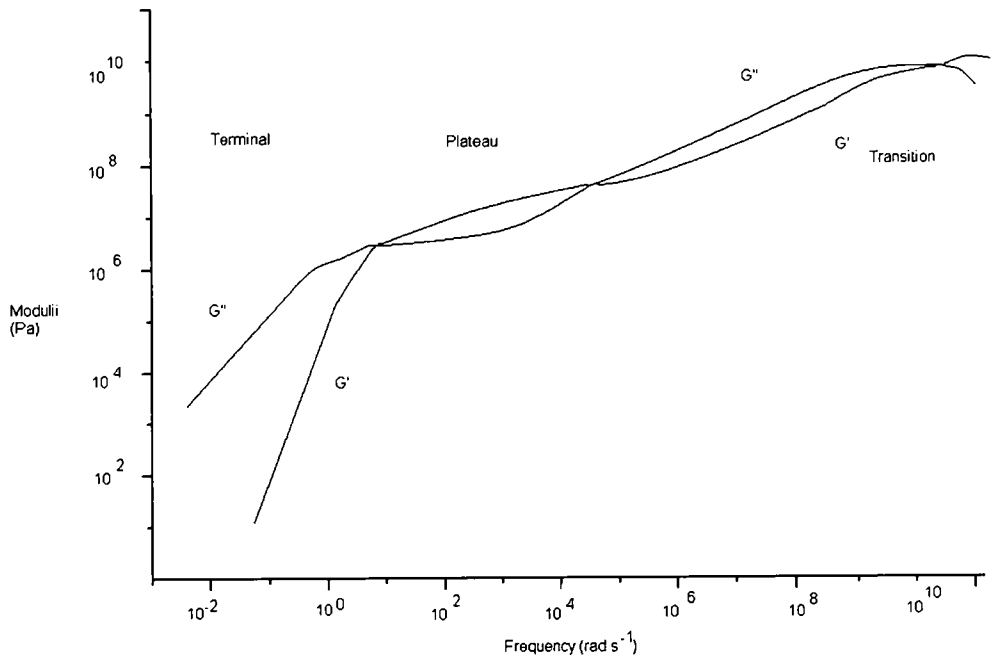

Figure 1.16 Dynamic moduli as a function of frequency (mastercurve) for a typical high molecular weight polymer melt.[19]

The lower frequencies shown in Figure 1.16, where G'' is larger than G', indicate where the viscous (liquid-like) properties of the melt are observed. Increasing the frequency causes G'' and G' to cross and the response from the material enters the plateau region. The plateau region is where factors such as chain entanglement and other complex mechanisms occur, here G' is larger than G''. At higher frequencies G'' crosses G' as the diagram enters the transition zone, where the solid glassy like response to the strain is observed.

In the plateau region where the liquid like behaviour becomes more solid like in appearance (viscoelastic region), the moduli crossover can be used as a reference point. This is because ω_c corresponds to approximately the value of the inverse of the characteristic relaxation time τ, hence $\tau \sim \omega_c^{-1}$, which can be a useful guide to the properties in a material. At the $G' = G''$ crossover the characteristic modulus, G, may be defined, as the modulus at the crossover point.

The zero shear viscosity can then be estimated from the data, by multiplying the relaxation time, τ, and the characteristic modulus, G:

$$\eta_0 \approx G\tau$$

1.6 Polymer Rheology.

Polymer fluids exhibit interesting rheology, which is particularly important in the manufacturing industry. The simple mechanical rheology models, such as the spring and dashpot model[80], are however not particularly successful at modeling viscoelastic regions in polymeric materials due to the number of variables. Therefore a series of molecular models have evolved for these complex systems.

1.6.1 Rouse Model.

Techniques for modeling molecular type polymer systems include the Elastic Dumb-bell Model that developed into the Rouse Model[80]. This model takes into account theory developed in the elastic dumbbell model and applies the model to a number of connected beads and springs, as described by Larson[81]. The Rouse Model is the first type of molecular model that resulted in a non-trivial distribution for polymer relaxation times. It is based on the change in entropy of the polymer chain from a non-random conformation during deformation, then after deformation, where the structure has a tendency to diffuse back to the most random orientations. The dependence of G', G'' and G(t) are successfully modeled by this system when taking into account the relaxation times shown in the spectra. This model gives an accurate description of the time and frequency dependence of the viscoelastic materials in a dilute solution where hydrodynamic interactions are not present. It also works well for polymer melts when the molecular weight is below the entanglement molecular weight as it treats relaxation in an ideal sense, with no reptation or constraint release.

1.6.2 Reptation Theory.

This theory improves the Rouse model to compensate for polymer entanglements at higher molecular weights in polymer melts. The theory behind this model by de Gennes[82] (1991 Nobel Prize for physics), is that for a long polymer chain, the only way for the chain to move through the network of the other chains is through the 'gaps' in the lattice type structure. A good analogy is to imagine a large container filled with snakes. A way for a single reptile to move between two points on either side of the container is to create an imaginary tube between the bodies of neighboring reptiles. By wiggling through this tube, the snake is able to move between points without involving

other snakes in the container. It is in this fashion that we imagine polymer reptation to occur.

For a polymer chain to relax, in terms of reptation, the only way is for it to move along its own contour path. Figure 1.17 shows an imaginary tube through which a chain may reptate:

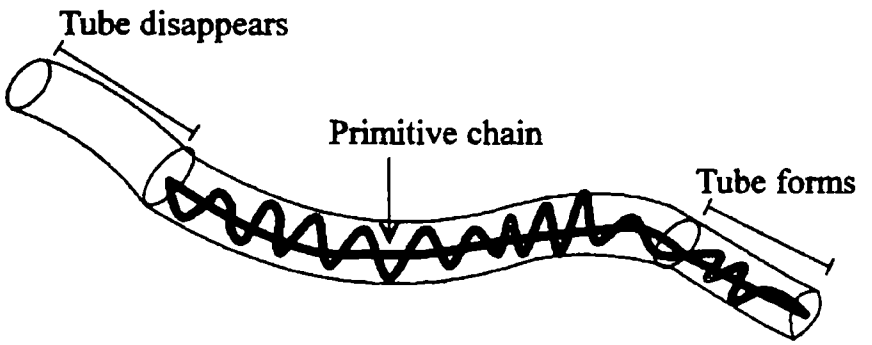

Figure 1.17 Polymer chain reptating through an imaginary tube.[82]

At the high frequency end of the spectrum the Rouse model applies equally as well to these polymer systems, however above the entanglement molecular weight the reptation model is best suited to modeling the relaxation spectra. It is important to realise this proposed mechanism is only one of the more likely relaxation mechanisms for linear materials, as the architecture of the materials is important as branched materials such as stars[83], are less likely to move in this way due to architectural constraints.

1.6.3 Non-Reptative Mechanisms.

Reptation is the proposed relaxation route for the majority of polymers, however as stated for branched materials, and materials of moderate molecular weight/wide polydispersity this relaxation method seems not to fit as well may be possible. A number of modifications or additions to the relaxation methods, such as primitive path fluctuations (breathing modes) or constraint release[19] can be applied at various limits, where reptation fails. Other modifications to the reptation tube model include increasing the tube diameter under certain circumstances to account for certain deviations from the theory and experimental rheology.

Primitive path fluctuations or breathing modes are add-on modifications to the tube model where a polymer is tethered at one end and the polymer breathes to relax. This is

applicable in branched materials, as arm retraction is thermodynamically unfavourable. Pictures speak much more than words in the case of relaxation mechanisms, therefore Figure 1.18 indicates this type of movement.

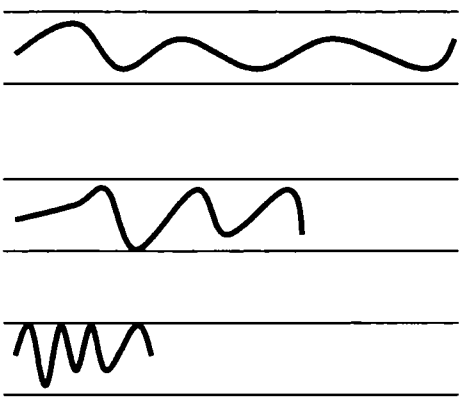

Figure 1.18 The length of the tube for reptation decreases with 'compression' of the chain during this type of fluctuation.

Cartoons shown in the lower of Figure 1.18, indicate that the compression of the polymer chain reduces the size of the tube in which reptation is occurring, relieving the stress associated with that portion of the tube. The concept, although relatively simple is mathematically explained in more depth in theories by Milner and McLeish[83] where the underlying physics of these processes is described in a little more depth.

Constraint release also falls under the non-reptative umbrella, and differs from primitive path fluctuations, as the title suggests by, involving the removal of the barriers forming the tube walls, making it easier for the polymer to relax. A simplistic viewpoint here is the removal of pieces of Velcro stuck together. Imagine the polymer chain in a tube being a single hook and the constraints other hooks. Separating the materials by removing the hooks (removing constraints) allows the polymer to relax in the tube akin to an unstuck piece of Velcro. A cartoon diagram is also a good way to describe this relaxation mechanism.

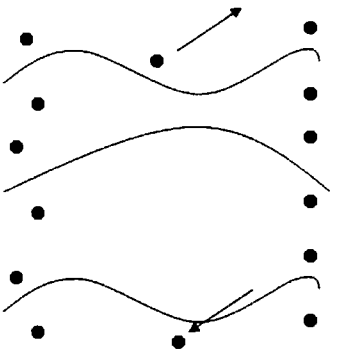

Figure 1.19 Polymer chains constrained by black dots and the movement of constraints allowing relaxation by non-reptative mechanisms[19].

Figure 1.19 shows that the removal of polymer chain constraints allows non-reptative relaxation to occur in one chain. Further refinement to relaxation spectra are needed in this sense for the formation of very accurate mastercurves, along with the addition of small adaptations to existing theories for true experimental data fitting.

These two briefly discussed non-reptative mechanisms are likely to occur in systems where the conditions for reptation are unfavourable. However potentially in the majority of cases, many relaxation mechanisms exist and contribute to relaxation spectra.

1.6.4 Constitutive Equations.

Relatively basic rheology models such as the Rouse and Zimm, introduce simplifications into the materials that they model. The ultimate aim of this type of predictive tool is to enable the prediction of the flow properties of a variety of polydisperse materials for industrial applications. Small additions to the theories developed enable star type branched materials to be modelled using add-ons to existing theories, accounting for particular relaxation modes present in materials under certain circumstances. These include the addition of constraint release and contour length fluctuations to models for relaxation in star polymers where reptation is unlikely to occur due to the architectural branch points.

The Doi and Edwards[84] theory combines the previous equations for reptation entanglements and linear viscoelasticity, into a constitutive equation that creates a model for entanglements and nonlinear response from large deformations. Reptation is considered the only method of relaxation in the model, so the theoretical prediction is

still removed from the data fits. Improvements to this model include those by Milner and McLeish[83] who included Rouse influenced relaxation parameters for star polymers to produce better fitting for the $G''(\omega)$ term. This produced a model that is reported to show good match between experimental and theoretical data.

Slight improvements to all of these models result in reasonably accurate data fit between theoretical and experimental data, highlighting the power that some of these models have for predicting bulk polymer properties. Each of the models seem to mainly evolve from other models, the iterative process means that over time the models are likely to be refined to real systems.

1.6.5 Temperature Dependence – Time Temperature Superposition.

The plot of the moduli show in Figure 1.16 is not normally available from one experiment on a typical rheometer, due to the magnitude of the frequency range. Modern instruments typically measure in the frequency range of 0.01-500.00 rad s^{-1} which means that to produce a master curve, as shown in Figure 1.16, the temperature at which the experiments are conducted needs to be varied to shift the frequency range being probed. Essentially this allows the log G' and log G'' against log frequency plots to be shifted along the frequency axis and superimposed onto one another, forming a master curve. This is applicable to most polymer melts or solutions where there are no phase transitions or other temperature dependent structural changes[85, 86], such materials are termed thermorheologically simple. A shift factor a_t is introduced as the scaling factor between the data curves to be fitted along the log frequency axis. Small shift corrections may be needed along the log moduli axis for the different curve data sets, however the frequency mainly shifts due to the affect of temperature on the polymer chains in the melt. The shift in the frequency values corresponds to the changing ratio of the friction coefficient with temperature. The log moduli data requires limited shifting because this depends on the relationship between G, T and the chain density. As the chain density decreases with temperature, the change in temperature that would require shifting of the curves for the superposition is 'mopped up' by the density change, so the data requires negligible shifting along the log moduli axis.

The shift factor a_t dependence on temperature can be used for the data to fit the WLF (Williams-Landel-Ferry) equation[86] shown below:

$$\log(a_t) = -C_0(T - T_{ref})/(C_1 + T - T_{ref})$$

Where C_0 and C_1 are experimentally determined parameters.

Using a data curve from a reference temperature, such as T_{ref} = 150°C, curves maybe shifted to sufficiently match the required reference curve. This relationship is extremely useful as it allows data sets to be manipulated to provide data about temperatures and frequencies that would be otherwise impossible to obtain.

1.6.6 Rheology of Branched Polymers.

The last several years have seen very rapid and exciting growth in the understanding of entangled polymers physics in both equilibrium and under strain. [87, 88] Furthermore the characterisation of long-chain branched polymer rheology has been an area of active research in both academia and industry. The understanding of the structure-rheology link revealed that the presence of long-chain branching in polymers has a significant impact on the properties of materials in the melt.[89] Consequently, the properties of long-chain branched polymers and similar derivatives attracted significant studies, aiming for a better understanding of the effect of architecture, on melt rheology.

Rheological properties of the Knauss hyperbranched polystyrene [73, 74, 75] are described by Dorgan et al.[90] using dynamic experiments with parallel plate geometry. The data shows that the dendrigraft structure had low melt viscosities and high melt elasticities. It is reported that macromomomers with M_w approaching 100 000 $gmol^{-1}$ show little chain entanglements, indicating the potential for this architecture to be used as viscosity modifiers. Relaxation times fitted neither Rouse or Power Law distributions, but a combination of the two, indicating complex fluid behaviour as well as the limitations in the models previously stated, which may consider only one particular method of relaxation. Figure 1.20 shows the master curve of a highly branched polystyrene derivative with little chain entanglement evidenced by the lack of an obvious plateau region.

Wanger et al.[91] report that Molecular Stress Function Theory (MSF Theory) can be applied to a series of branched polystyrene melts, with reasonable success. MSF Theory is adapted from the Doi-Edwards constitutive equations, which takes into account more than one method of entanglement relaxation (not only reptation) and allows variation in tube diameter in commercial polydisperse materials. In this example it is being applied to analyse rheology data of comb branched PS, with reasonable success.

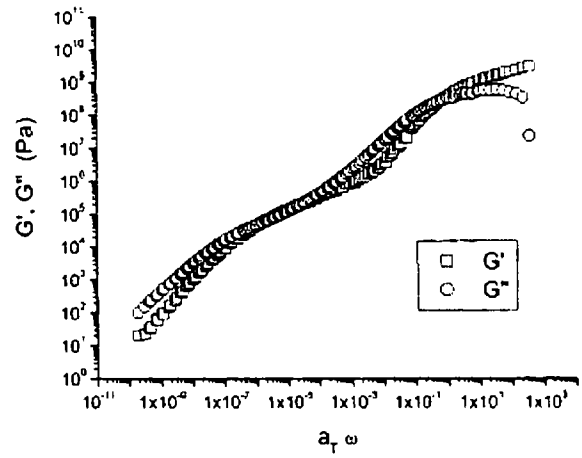

Figure.1.20 Master curve plot of moduli vs. frequency from a 1300 Kgmol^{-1} dendritically branched polystyrene chains. [90] (G' represents the storage modulus, G'' the loss modulus.) Reproduced with permission from Macromolecules 2003, 36, 380. Copyright 2003 American Chemical Society.

The rheology data published for the branched polystyrene systems[90, 91] indicate the correlation between the branching in the macromolecular structures and rheological data. The influence on architecture on the rheological response in materials is of particular interest due to the different relaxation processes that occur compared to the traditional linear structures. Early models of polymer melts, such as the theories developed by Doi and Edwards[84], considered linear polymers which under certain flow conditions were able to model more complex branched materials, such as H shaped polymers. McLeish[92] describes the molecular rheology of H-polymers that also have more complex architecture than linear structures. The main constraint on the flow of the molecule is the branch points between the polymer chains, which may in some cases be considered as two 3 armed stars, for which the flow properties are relatively well understood, as described below. The model is mainly based on Rouse type theories with additional constraints, notably however, reptation is not the main relaxation process due to the linking of the polymer branch points and the constraints on the entanglements.

Star polymers seem to be the most logical step towards the deviation from modeling linear polymers as a star polymer is essentially a linear polymer with a single branch point.[83] Hirao et al.[25] reported chain-end-functionalised polystyrene with butadiene linkers forming star branched polymers. These well-defined star-branched polymers with up to 33 arms showed a characteristic decrease in g' indicative of a higher degree of branching when compared with linear polystyrene of the same molecular weight.

Considering a second branch point, H type polymers where the entanglement network defines a 'tube' in which the molecule may be thought to reptate, but as with the H shaped polymers, the branch points in the star structure probably prevent reptation being the main relaxation process. An alternative mechanism for the relaxation of a branched system is that the arm of the star may retract on itself, however this is considered thermodynamically unfavorable. Other mechanisms such as contour length fluctuation and constraint release[93] exist for the alternative relaxation of this material in the melt.

Addition of many random branch points results in arborescent type polymers which are reported by Hempenius et al.[94] who studied the viscoelastic behaviour of these materials with increasing generations (increased levels of hierarchical branching). The results showed that branched polystyrene architectures have low zero-shear viscosities compared to linear polystyrene of the same molecular weight. Low molecular weight samples ($<1.56 \times 10^5$ $gmol^{-1}$) showed no evidence of entanglement, whereas those of high molecular weight ($>6.8 \times 10^7$ $gmol^{-1}$) showed a plateau region - indicative of chain entanglement.

Relaxation processes present in branched polymers are described by McLeish[95] where the tube model by de Gennes[82] is modified for regularly branched tree molecules (Cayley Trees – Figure 1.21). The dominant features of the melt properties of this type of material are the branching of the material and the mechanism for which the arms of the branched material relax. Clearly the reptation mechanism for arm relaxation cannot occur in the same in an entangled linear polymer as it does for the branched structure, and other mechanisms such as constraint release[96] can account for chain relaxation. The hierarchical branching shown with the different generations numbered 1 to 3 in the figure should be seen in the rheological response in terms of seniority and priority, where different relaxation processes are seen with each generation. The outer segments relax first, then at longer timescales the inner, which may be observed in the relaxation response.

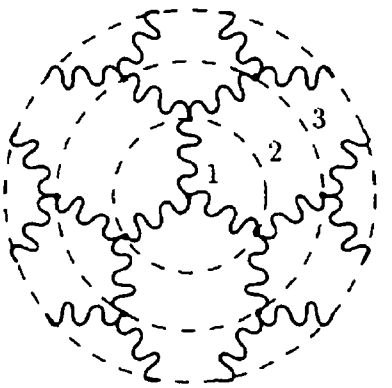

Figure 1.21 A three level Cayley Tree. This structure has been theoretically modeled for the intended use in structure property correlation studies in polymer melts.[97] Reproduced with permission from Macromolecules, 2001, 34, 2579. Copyright 2001 American Chemical Society.

Polybutadiene Cayley trees are reported by Hadjichristidis et al.[97] the rheology of these branched structures is investigated from materials formed using anionic polymerisation and silyl based DPE coupling reagents, for controlled polymers between branch points. The rheology is described as showing hierarchical relaxation, with signatures from each of the generations observed rheologically in the terminal region of the spectrum.

Recent review papers describing long chain branched structures in great detail include papers by Teertstra and Gauthier[99], Hirao et al.[100] and Tomalia[101].

1.7.2 References.

1. Young R.J., Lovell P.A. Introduction to Polymers, Chapman and Hall, 1997 2nd Edition.
2. Goodyear C. US Patent 240, 1837.
3. Crespy D., Bozonnet M., Meier M. *Angew. Chem. Int. Ed.,* 2008, 47, 3322.
4. Rane S.S., Choi P. *Chem. Mater.*, 2005, 17, 4, 926.
5. Szwarc M., Levey M., Milkovich R. *J. Am. Chem. Soc.,* 1956, 78, 2656.
6. Wang, J.S.; Matyjaszewski, K. *J. Am. Chem. Soc.* 1995, 117, 5614.
7. Chong Y.K., Le T.P.T., Moad G., Rizzardo E., Thang S.H. *Macromolecules*, 1999, 32, 2071. and Chiefari J., Chong Y.K., Ercole F., Kristina J., Jeffery J., Le T.P.T., Mayadunne R.T.A., Mejis G.F., Moad C.L., Moad G., Rizzardo E., Thang S.H., *Macromolecules*, 1998, 31, 5559.
8. Mitsukami Y., Donovan M.S., Lowe A.B., McCormick C.L. *Macromolecules*, 2001, 34, 2248.
9. Rizzardo E., Solomon D.H., *Polym. Bull.* 1979, *1*, 529. Moad G., Rizzardo E., Solomon D.H., *Macromolecules* 1982, *15*, 909, and Otsu T. *J. Polym. Sci. A: Polym Chem*, 2000, 38, 2121 .
10. Calderon N., *J Macromol Sci Rev Macromol Chem*, 1972, 7, 105.
11. Natta G., Pino P., Corrdini P., Danusso F., Mantica E., Mazzanto G., *J. Am. Chem. Soc.* 1955, 77, 1708.
12. Schrock R.R. (Nobel lecture), *Angew Chem Int Ed.*, 2006, 45, 3748.
13. Grubbs R.H., (Nobel lecture), *Angew Chem Int Ed.,* 2006, 45, 3760.
14. Kennedy J.P, Price J.L., Koshimura K. *Macromolecules*, 1991, 24, 6567.
15. Hsiech, H.L., Quirk, R.P. Anionic Polymerisation: Principles and Pracical Applications. Marcel Dekker, New York, 1996.
16. Hirao A., Hayashi M., Haraguchi N. *Macrom. Rapid Comm.*, 2000, 21, 17, 1171.
17. Hadjichristidis N., Roovers J.E.L. *J. Polym. Sci. B*, 1974, 12B, 2521.
18. Itrou H., Hadjischristidis N. *Macromolecules*, 1993, 26, 2479.
19. Larson R.G. 'The Structure and Rheology of Complex Fluids'; OUP, Oxford, 1999.
20. Gervasi J.A., Gosnell A.B. *J. Polym. Sci. A*, 1966, 6A, 1391.

21. Worsfold D.J., Zilliox J.G, Rempp P. *Can. J. Chem.*, 1969, 47, 3379.
22. Meunier J.C, Vanleemp R. *Makromol. Chem.*, 1971, 142, 1.
23. Hadjichristidis N., Guyot A., Fetters L.J. *Macromolecules*, 1978, 11, 889.
24. Hadjichristidis N., Fetters L.J. *Macromolecules*, 1980, 13, 191.
25. Higashihara T., Kitamura M., Haragushi N., Sugiyama K., Hirao A., Ahn J., Lee J. *Macromolecules*, 2003, 36, 6730.
26. Iatrou H., Hadjischristidis N. *Macromolecules*, 1992, 25, 4649.
27. Hirao A., Sugiyama K., Tsunoda Y., Matsuo A., Watanabe T. *J. Polym. Sci. A.*, 2006, 44, 6659.
28. Clarke N., Colley F.R., Collins S.A., Hutchings L.R., Thompson R.L. *Macromolecules*, 2006, 39, 1290.
29. Qian Z., Minnikanti V.S., Sauer B.B., Dee G.T., Archer L.A. *Macromolecules*, 2008, 41, 5007.
30. Roovers J., Toporowski P.M: *Macromolecules*, 1981, 14, 1174.
31. Roovers J., Graessley W.W. *Macromolecules*, 1981, 14, 3, 766.
32. Hakiki A., Young R.N, McLeish T.C.B. *Macromolecules*, 1996, 29, 3639.
33. McLeish T.C.B., Allgaier J., Bick D.K, Biswas P, Blackwell R.J., Blottiere B., Clarke N., Gibbs B., Groves D. J., Hakiki A., Heenan R.K., Johnson J.M., Kant R., Read D.J., Young R.N. *Macromolecules*, 1999, 32, 6734.
34. Daniels D.R., McLeish T.C.B., Kant R., Crosby B.J., Young R., Pryke N.A., Allgaier J., Groves D.J., Hawkins R. J. *Rheol. Acta*, 2001, 40, 403.
35. Heinrich M., Pyckhout-Hintzen W., Allgaier J., Richter D., Straube E., Read D.J,. McLeish T.C.B., Groves D.J., Blackwell R.J., Wiedernmann A. *Macromolecules*, 2002, 35, 6650.
36. Heinrich M., Pyckhout-Hintzen W., Allgaier J., Richter D., Straube E., Read D.J., McLeish T.C.B, Blackwell R.J, Wiedernmann A. *Macromolecules*, 2004, 37, 5054.
37. Iatrou H., Willner L., Hadjichristidis N., Halperin A., Richter D. *Macromolecules*, 1996, 29, 2, 581.
38. Roovers, J. *Polymer* 1979, 20, 843.
39. Gido S.P., Lee C., Pochan D.J., Pispas S., Mays J.W., Hadjichristidis N. *Macromolecules*, 1996, 29, 22, 7022.
40. Flory P.J. *J. Am. Chem. Soc.* 1952, 74, 2718.

41. Tomalia D.A., Baker H., Dewald J., Hall M., Kallos G., Martin S., Roeck J., Ryder J., Smith, P. *Polymer J*, 1985, **17**, 117.
42. Tomilia, D.A., Dewald, J.R. U.S. Patent 4507466, 1985
43. Tomilia, D.A., Dewald, J.R. U.S. Patent 4568737, 1986.
44. Newkome G.R., Yao Z., Baker G.R., Gupta V.K. *J Org. Chem.* 1985, **50**, 2004.
45. Young K.H. *J. Polym. Sci. A: Polym. Chem.*, 1998, **36**, 1685.
46. Tomalia D.A., Baker H., Dewald J., Hall M., Kallos G., Martin S., Roeck J., Ryder J., Smith P. *Polymer J*, 1985, 17, 117.
47. Frechet J.M.J., Hawker C.J., Philippides A.E. U.S. Patent 5041516, 1991.
48. Hawker C.J., Frechet J.M.J. *J. Am.Chem. Soc.*, 1990, 112, 7638.
49. Tomilia D.A. and Frechet J.M.J. *J. Polym. Sci. A: Polym. Chem.* 2002, 40, 2719.
50. Flory P.J. Principles of Polymer Chemistry, Cornell University Press, Ithaca, New York, 1953.
51. Uhrich K.E, Hawker C.J, Frechet J.M.J., Turner S.R. *Macromolecules*, 1992, 25, 4583.
52. Voit B. *J. Polym. Sci. A: Polym. Chem.*, 2005, 43, 2679.
53. Hutchings L.R., Roberts-Blemming S.J., *Macromolecules*, 2006, 39, 6, 2144.
54. Tomalia D.A., Hedstrand D.M., Ferritto M.S. *Macromolecules*, 1991, 24, 1435.
55. Gauthier M., Möller M. *Macromolecules*, 1991, 24, 4548.
56. Trollsås M., Hedrick J.L. *J. Am. Chem. Soc.* 1998, *120*, 4644.
57. Angot S., Taton D., Gnanou Y. *Macromolecules*, 2000, 33, 5418.
58. Li. J.M, Gauthier M. *Macromolecules*, 2001, 34, 8918.
59. Gauthier M., Li J.M., Dockendorff J. *Macromolecules*, 2003, 44, 36, 2642.
60. Feng X., Taton D., Chaikof E.L., Gnanou Y. *J. Am. Chem. Soc.*, 2005, 127, 10956.
61. Matsuo A., Watanabe T., Hirao A. *Macromolecules*, 2004, 37, 6283.
62. Matsuo A., Watanabe T, Hirao A. *Macromolecules*, 2005, 38, 8701.
63. Lepoittevin B., Matmour R., Francis R., Taton D., Gnanou Y. *Macromolecules*, 2005, 38, 3120.
64. Bernard J., Schappacher M., Viville P., Lazzaroni R., Deffieux A. *Polymer*, 2005, 46, 6767.
65. Kimani S.M., Hutchings L.R., *Macro. Rapid Comm.*, 2008, 29, 8, 633.
66. Orfanou K., Iatrou H., Lohse J.D., Hadjichristidis N. *Macromolecules*, 2006, 39, 4361.

67. Charlari I., Hadjichrisitidis N. *J. Polym. Sci. A*, 2002, 40A, 1519.
68. Hadjichristidis N., Pitsikalis M., Iatrou H., Pispas S. *Macro. Rapid Commun.* 2003, 24, 979.
69. Paulo C., Puskas J.E., *Macromolecules*, 2001, 34, 734.
70. Foreman E.A., Puskas J.E., Kaszas G. *J. Polym Sci A.: Polym Chem.*, 2007, 45, 24, 5847.
71. Hobson L.J., Feast W.J. *Polymer*, 1999, 40, 1279.
72. Wurm F., Lopez-Villanueva F.J, Frey H. *Macromol. Chem. Phys.*, 2008, 209, 675.
73. Knauss D.M., Al-Muallem H.A., Huang T.Z., Wu D.T: *Macromolecules,* 2000, 33, 3557.
74. Knauss D.M., Al-Muallem H.A. *J. Polym. Sci. A Polym Chem*, 2000, 38A, 4289.
75. Knauss D.M., Al-Muallem H.A. *J. Polym. Sci. A Polym Chem*, 2001, 39A, 3547.
76. Hutchings L.R., Dodds J.M., Roberts-Bleming S.J. *Macromolecules* 2005, 38, 5970.
77. Doraiswamy D. *Rheol. Bulletin*, 2002, *71, 1.*
78. Rohn C.L. 'Analytical Polymer Rheology – Structure-Processing-Property Relationships'; 1st Edition, Hanser, New York, 1995.
79. Goodwin J., Hughes R.W. Rheology for Chemists: An introduction. 2000. Royal Society of Chemistry. Cambridge.
80. Rouse P.E. *J. Chem. Phys.*, 1953, 21, 1272.
81. Larson R.G., Mead D.W., Doi M, *Macromolecules*, 1998, 31, 7895.
82. de Gennes P.G. *J. Chem. Phys.*, 1971, 55, 572.
83. Milner S.T., McLeish T.C.B. *Macromolecules*, 1997, 30, 2159.
84. Doi M., Edwards S.F. *J. Chem. Soc. Faraday Trans II*, 1978, 74:1789, 1802, 1818.
85. Ferry J.D. Viscoelastic Properties of Polymers, 3rd Edition, Wiley, New York.
86. Williams M.L., Landel R.F., Ferry J.D. *J. Am. Chem. Soc.* 1955, **77**, 3701.
87. Doi M., Edwards S.F. 'The Theory of Polymer Dynamics,' Oxford University Press: New York, 1986.
88. Marrucci G.J. *Non-Newtonian Fluid Mechanics*, 1996, 62, 279.
89. Milner S.T, McLeish T.C.B., Likhtman A.E. J. *Rheol*, 2001, 45, 539.
90. Dorgan J.R.; Knauss D.M.; Al-Muallem H.A.; Huang T., Vlassopoulos D. *Macromolecules*, 2003, 36, 380.

91. Wagner M.H., Hepperle J., Münstedt. H. *J. Rheol.* 2004, 48, 3, 489.
92. McLeish, T.C.B., *Macromolecules*, 1988, 21, 1062.
93. Marcos A. G., Pusel T. M., Thomann R., Pakula T., Okrasa L., Geppert S., Gronski W., Frey H. *Macromolecules*, 2006, 39, 3, 971.
94. Hempenius M.A., Zoetelief W.F., Gauthier M., Möller M. *Macromolecules*, 1998, 31, 2299.
95. McLeish, T.C.B. *Europhys. Lett.*, 1988, 6, 511.
96. Doi M., Graessley W.W., Helfand E. *Macromolecules*, 1987, 20, 1900.
97. Blackwell R.J., Harlen O.G., McLeish T.C.B. *Macromolecules*, 2001, 34, 2579.
98. van Ruymbeke E., Orfanou K., Kapnistos M., Iatrou H., Pitsikalis M., Hadjichristidis N., Lohse D.J., Vlassopoulos D. *Macromolecules*, 2007, 40, 16, 5941.
99. Teertstra S.J., Gauthier M., *Progress in Polymer Science*, 2004, 29, 4, 277.
100. Hirao A., Hayashi M., Loykulnant S., Sugiyama K., Ryu S.W., Haraguchi N., Matsuo A., Higashihara T. *Prog. Polym. Sci.*, 2005, 30, 2, 111.
101. Tomalia D.A. *Prog. Polym. Sci.*, 2005, 30, 294.

1.7 Aims and Objectives.

The aim of this research is to synthesize and characterize a range of polymers based on the HyperMac macromonomer approach reported by Hutchings et al.[76] for the construction of randomly branched polymers.

2.2.4 Modified Williamson Coupling Reactions.

Although it has been shown that improved stirring can have a beneficial effect on the coupling reaction, it was felt that carrying out the reactions in refluxing DMF might still be limiting the extent of the coupling reactions. To overcome this problem it was decided to try to increase the rate of the Williamson coupling reaction so the reactions could be carried out at lower temperatures – hopefully avoiding the degradation of the solvent. Two possible ways in which the Williamson reaction could be improved were considered; changing the leaving group and/or changing the base.

An AB_2 polystyrene macromonomer (M_n 28 000 $gmol^{-1}$) was synthesised in which the leaving group 'A' was bromine. The macromonomer synthesis was essentially identical to that described previously[1] for the synthesis of macromonomers with a chlorine leaving group except for the final step where the primary alcohol group is converted to bromine using carbon tetrabromide and triphenyl phosphine. To ensure fair comparison of the relative reactivity of chlorine and bromine as leaving groups, a large batch of macromonomer was synthesised and divided into two - one half was chlorinated and the other half brominated – avoiding any variation in reactivity due to molecular weight. Subsequent coupling reactions were carried out in DMF at 100 °C with 20% w/v solutions of macromonomer. Initially potassium carbonate was used as the base to deprotonate the phenol groups with 18-crown-6-ether (phase transfer agent) as potassium carbonate is insoluble in DMF.

2.2.4.1 Effect of Leaving Group.

Figure 2.6 shows that changing the leaving group from chlorine to bromine resulted in both an increase in the rate and extent of coupling reaction. At 100° C the chlorinated macromonomer (using potassium carbonate as the base) reacts very slowly. The extent of reaction, shown as Dp_w (M_w HyperMac/M_w macromonomer) increases steadily although very slowly to a value of Dp_w of about 4 after 7 hours. Previous reactions carried out in refluxing DMF (c. 160°C) produced HyperMacs with Dp_w values of 10-17 (depending on molecular weight of macromonomer) in much shorter times.[1] The brominated macromonomer of identical molecular weight showed a higher rate and extent of reaction under the same conditions. In Figure 2.5 it can be seen that the Dp_w

rises up to a value of about 11 during the first hour, gradually increasing up to 15.5 after 7 hours. After 24 hours (not shown on graph) the data indicated that the reaction was still proceeding, with a final value of Dp_w of just over 17. Replacing chlorine with bromine as the leaving group results in a obvious increase in both the rate and extent of reaction. However the results obtained for the brominated macromonomer are not really a significant improvement over the previous work – even though the reactions were carried at temperatures which were 60° C lower.

2.2.4.2 Effect of Base.

The next modification to try to improve the efficiency of these reactions was to look for an alternative to potassium carbonate as the base. In previous reactions 18-crown-6-ether (18-C-6) had been employed as a phase transfer agent due to the poor solubility of potassium carbonate in DMF, a likely limiting factor in the coupling reaction. The literature reports that cesium carbonate is a particularly efficient base for Williamson coupling reactions of this type in DMF due to the greater solubility of both cesium carbonate and the resulting phenolate[8]. To investigate this, a coupling reaction with cesium carbonate was carried out on the chlorinated macromonomer, shown in Figure 2.5 It can be seen that cesium carbonate in the absence of any phase transfer agent notably outperformed potassium carbonate/18-C-6. The reaction was slow in the early stages and for the first two hours proceeded only slightly faster than the reaction with potassium carbonate. The rate is seen then to increase and values of Dp_w of approaching 8.5 were obtained after 7 hours – approximately double that obtained with potassium carbonate. Although there was a marked improvement in the extent of reaction, it was not particularly impressive.

Combining the improvements in the coupling reaction seen with cesium carbonate and the bromine leaving group resulted in a significant improvement in the rate and extent of the reaction (Figure 2.5). There appears to be a synergistic relationship in action. After an hour the Dp_w had risen to nearly 60 after which there was little increase in Dp_w. The plateau observed in Figure 2.5, obtained via SEC after one hour, does not necessarily represent a halt in the growth of the HyperMacs, as the samples were filtered (0.2 micron) to remove small amounts of gel like polymer before being injected

into the SEC columns to prevent blockages. It is unlikely that these very high molecular weight HyperMacs (M_n ~ 400000 $gmol^{-1}$, M_w ~ 1.7 million $gmol^{-1}$) have formed insoluble networks, but it is likely that a very high molecular weight component exists in these samples that reduces the HyperMac solubility, causing a underestimate of the molecular weight of these materials.

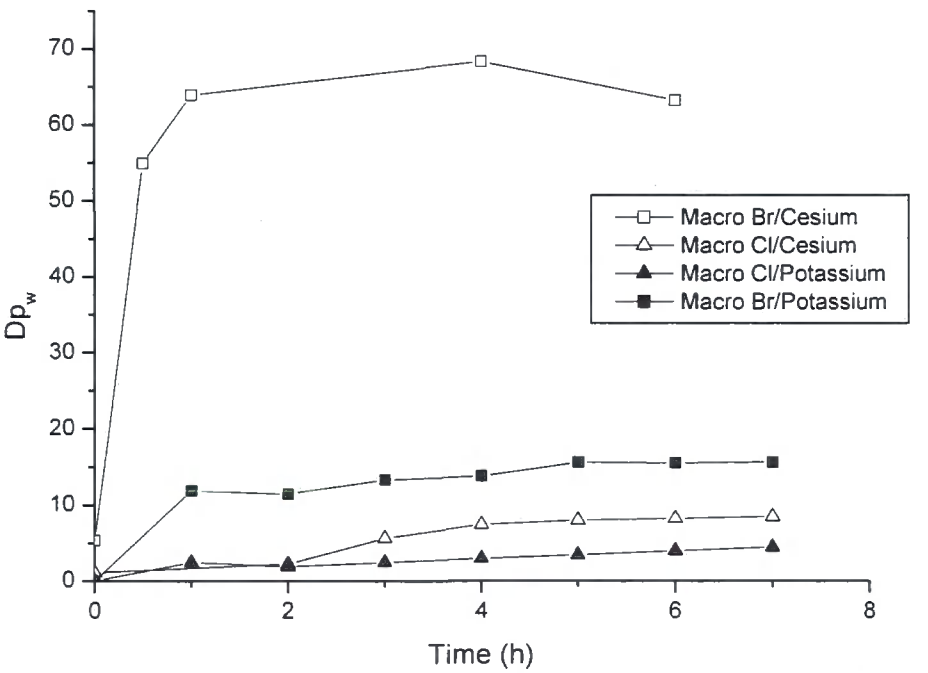

Figure 2.5 The effect of macromonomer leaving group and base on the extent of Williamson coupling reaction (DMF/100°C) used to prepare HyperMacs from polystyrene AB_2 macromonomer M_n 28000 $gmol^{-1}$.

2.2.4.3 Effect of Temperature.

Given the dramatic increase in the efficiency of the Williamson coupling reactions with the synergistic benefit of using both an alternative base and leaving group, and that the reactions appeared to be virtually complete within the first hour, it was decided to see if these reactions could be carried out to the same extent but at lower temperatures. One benefit of slowing the reaction down such that it proceeds over several hours, rather than less than one hour, is the possibility to stop the reaction at any given conversion – thereby offering some control/predictability over the final molecular weight of the HyperMac. A series of otherwise identical coupling reactions were carried out in which temperature was varied from 100°C to room temperature - the results are shown in Figure 2.6.

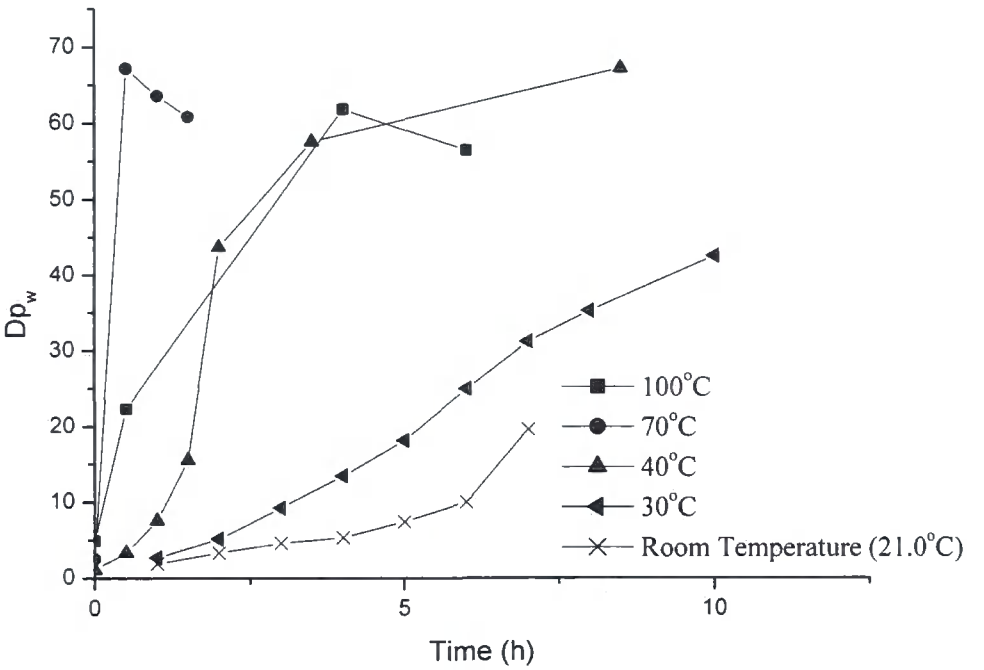

Figure 2.6 The effect of temperature on the extent of Williamson coupling reaction used to prepare HyperMacs from polystyrene AB_2 macromonomer M_n 28000 $gmol^{-1}$.

Reducing the temperature from 100° C to 70° C made no significant difference to the rate of reaction however further reductions in temperature to 40° C, 30° C and eventually to room temperature (21° C) progressively slowed the rate of coupling. For reactions carried out 40° C and higher the overall extent of reaction is similar - with final values of Dp_w in the range 60-70. There clearly is some variation in the final values of Dp_w. It is suspected that, at these very high molecular weights, filtration of the solutions for SEC analysis introduces a degree of error in the accuracy of this data; this being the likely source of error in the observed decreasing molecular weight with time for the 70° C data. At 30° C and at room temperature it appears that the reactions are slowed to the point that the reactions are incomplete within the times that they were followed. The trend in Dp_w is still upward; suggesting that given longer reaction times the extent of reaction would continue to increase, but issues with SEC characterisation mean this is still unknown.

The reactions appear to proceed in three distinct phases, clearly shown in the 40° C data (Figure 2.6). Firstly the Dp_w steadily increases, then after 1 – 2 hours the rate of this increase rises, lasting for a short period of time. The third and final phase shows a plateau being reached where the rate of DP_w increase slows down. Conceptually during the first phase, reaction occurs between individual macromonomers, then between

macromonomers and small HyperMacs comprising of only a few macromonomers. The period of the rapid increase in molecular weight observed in the second phase arises likely via the coupling of HyperMac to HyperMac; eventually resulting in the presence of a significant proportion of very high molecular weight species. The emergence of these "super" HyperMacs towards the end of the second phase can be seen in the SEC chromatograms (Figure 2.7).

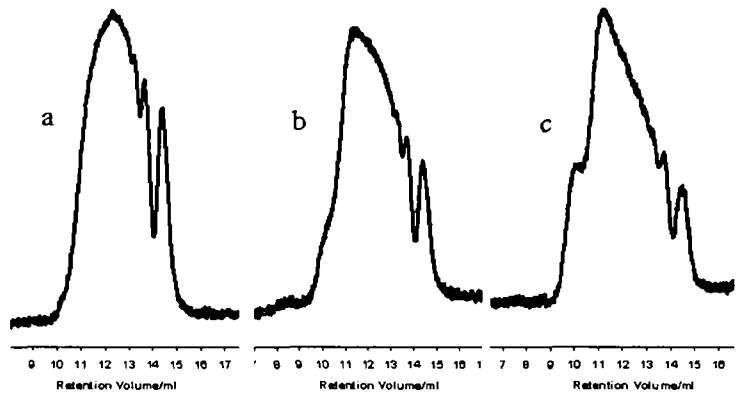

Figure 2.7 SEC chromatograms (RI trace) of HyperMac coupling reaction carried out at 40° C for a) 90 minutes, b) 120 minutes and c) 240 minutes.

The SEC chromatogram recorded 90 minutes into the coupling reaction (Figure 2.7a) indicates that there is still a significant amount of uncoupled macromonomer - as evidenced by the sharp peak with a retention volume of about 14.3 ml – as well as dimer and trimer with peaks at 13.7 ml and 13.2 ml respectively. From the data shown in Figure 2.7 it can be see that after 90 minutes the reaction is just entering the second phase where the rate of increase in molecular weight starts to dramatically increase. The SEC chromatogram obtained after 2 hours (Figure 2.7.b), shows the molecular weight distribution as the reaction is well into the second phase. The relative intensity of the peak at 14.3 ml has diminished indicating more macromonomer has been consumed and the main broad peak maximum has shifted from 12.2 ml to 11.5 ml indicating an increase in molecular weight. The emergence of a shoulder to lower elution volumes (between 10 and 10.5 ml) can be seen; likely a result of the coupling of HyperMac to HyperMac. This promising shoulder becomes more pronounced with time and after 4 hours (Figure 2.7) the relative intensity of this shoulder is greater than that of the macromonomer peak at 14.2 ml, indicating the presence of a significant proportion of the very high molecular weight "super" HyperMacs. The data in Figure 2.7 suggests

that after 4 hours the coupling reaction is into the final phase where the high molecular weight leads to very high solution viscosities, making efficient stirring/mixing a limitation. Here it is likely the reaction is inhibited by a reducing number of reactive 'A' halide functionalities and increasing viscosity, thus becoming diffusion controlled, resulting in the plateau seen in the third phase of the coupling reaction.

Time(h)	$M_n(gmol^{-1})$	$M_w(gmol^{-1})$	PDI	$[\eta]_{hyper}(dlg^{-1})^a$	$[\eta]_{lin}(dlg^{-1})^b$	g'^c
0	28000	28600	1.02	-	-	-
0.5	61300	103300	1.7	0.39	0.48	0.81
1	109400	231400	2.1	0.55	0.84	0.65
1.5	161800	483900	3.0	0.79	1.43	0.56
2	296700	1406000	3.5	1.04	2.47	0.42
2.5	419800	1465000	3.5	1.20	3.14	0.38
3	462400	1774000	3.8	1.27	3.60	0.35
4	473400	1756000	3.7	1.26	3.57	0.35
5	496200	1877000	3.8	1.30	3.75	0.35
6	471100	1792000	3.8	1.31	3.63	0.36
8.5	525100	1790000	3.4	1.30	3.62	0.36

Table 2.3 Molecular weight, polydispersity and intrinsic viscosity data for HyperMac synthesised from an AB_2 macromonomer where 'A' is bromine. Coupling reaction carried out in DMF, at 40° C with Cs_2CO_3.

[a] Measured by SEC viscometry.

[b] Calculated using the Mark-Houwink equation $[\eta] = KM^a$.

[c] $g' = [\eta]_{hyper}/[\eta]_{linear}$.

To demonstrate that these HyperMacs have a highly branched architecture and to get some idea of the degree of branching, the branching factor g' was calculated - g' being given by the ratio of the intrinsic viscosity of the branched polymer $[\eta]_{hyper}$ to the intrinsic viscosity of a linear polymer $[\eta]_{linear}$ of the same molecular weight. Table 2.3 shows data obtained for the HyperMac coupling reaction carried out in DMF, with cesium carbonate, at 40°C with the brominated macromonomer and showing intrinsic viscosity of the HyperMac, $[\eta]_{hyper}$, with time as well as the intrinsic viscosity of a series of linear polymers of the same M_w. The intrinsic viscosity of the linear polymers was

calculated using the Mark-Houwink equation with vales of a = 0.712 and K = 12.8 x 10^{-5} dl/g (supplied by American Polymer Standards Corporation). It can be seen that as the molecular weight of the HyperMac increases, so does the intrinsic viscosity, but at a much slower rate than would be expected for a linear polymer of identical molecular weight. This is to be expected due to the branched architecture, as branched polymers have smaller hydrodynamic volumes, are thus more compact than linear polymers of identical molecular weight and have relatively lower intrinsic viscosities. As the reaction proceeds the values of $[\eta]_{hyper}$ and $[\eta]_{linear}$ diverge and the value of g' decreases indicating increasingly compact, branched structures. HyperMac g' values calculated should be treated with caution since the intrinsic viscosity of the HyperMac is of a material which is polydisperse in both molecular weight and architecture, whereas the intrinsic viscosity of the linear polymer is calculated from the Mark-Houwink equation and therefore the value represents that of a monodisperse polymer. Despite this, the values of g' (as low as 0.35) undoubtedly confirms that this HyperMac is very highly branched and furthermore the values of g' are considerably lower than those observed for HyperMacs prepared by the original methodology[1] which had much lower values of Dp_n and Dp_w and g' values of between 0.65 and 0.53 (Table 2.1). This is not unexpected given the improvements seen in the extent of the synthesis of these 'super' HyperMacs.

2.2.5 Synthesis of HyperMacs in the Presence of B_3 Core.

It is well established that coupling reactions of AB_2 monomers in the presence of a B_n core molecule can result in significant changes in the properties of the resultant materials. Feast and Hobson carried out a series of AB_2/B_n (n = 2-6) copolymerisations to make poly(amidoamine) hyperbranched polymers.[9] They observed that the addition of such core (B_n) molecules led to a reduction in the molecular weight and that by varying either the functionality of B_n or the molar ratio of core to monomer – a degree of control over the molecular weight of the resultant polymers was possible.

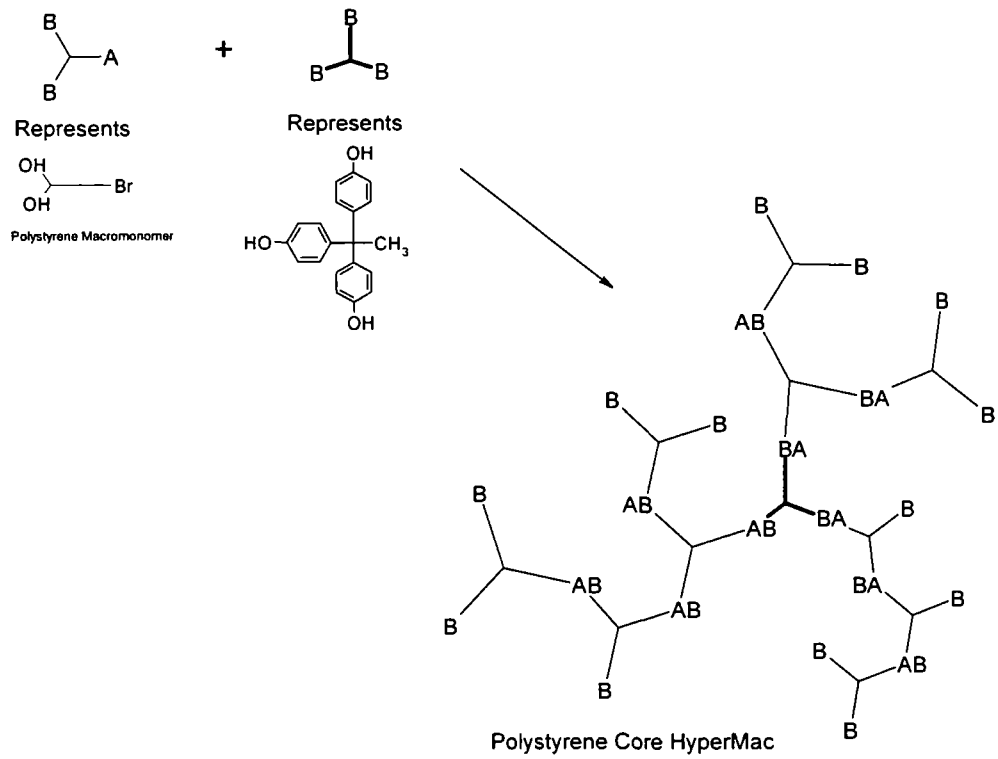

Figure 2.8 Synthesis of polystyrene core HyperMacs from an AB_2 macromonomer and a B_3 core.

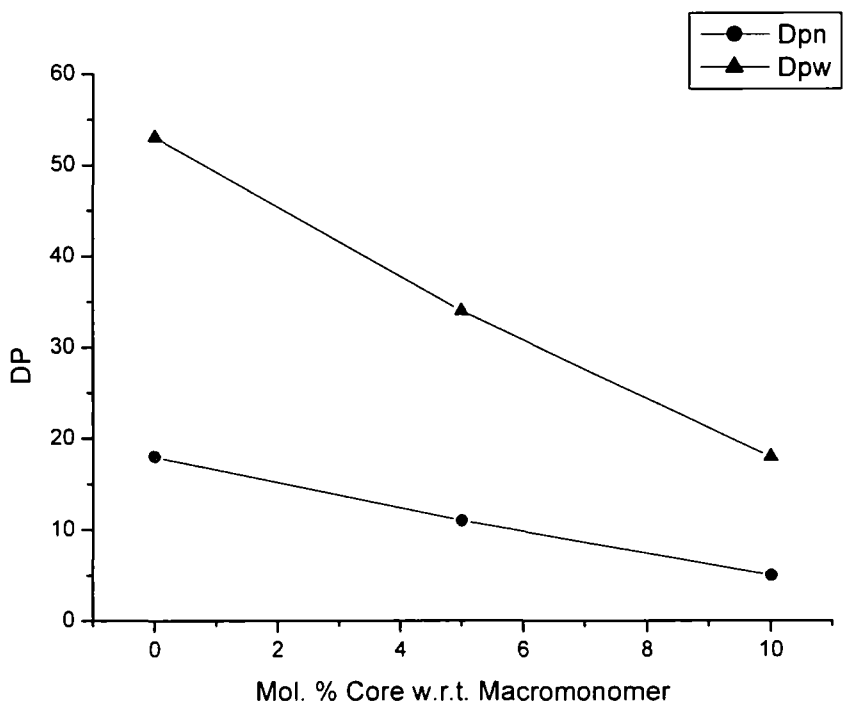

Figure 2.9 Effect of the addition of B_3 core on the extent of Williamson coupling reaction (Dp_n and Dp_w) used to prepare HyperMacs from polystyrene AB_2 macromonomer M_n 28000 $gmol^{-1}$. (Brominated macromonomer, at room temperature for 24 hours with Cs_2CO_3.)

They further postulated that addition of B_n core molecules could provide a single step route to produce pseudo-dendrimers. Analogous conclusions were drawn by Malmström and Hult[10] about the ability of B_n polyol cores to modify and 'control' the formation of hyperbranched polyesters based on 2,2-bis(methylol)propionic acid. In light of these observations and in an attempt to gain further insight into the synthesis of HyperMacs, a series of coupling reactions were carried out with an AB_2 macromonomer (M_n 28,000 $gmol^{-1}$) in the presence of 1,1,1-tris(4-hydroxyphenyl)ethane, a trifunctional B_3 core molecule. Initially a standard HyperMac coupling reaction (0% core) was performed for comparison with previous HyperMac synthesis. The data compared favourably. Addition of 5 and 10 % core (molar ratio) to the coupling reaction significantly decreases both the Dp_n and Dp_w of the core coupled HyperMacs (Figure 2.9). Indeed, this is expected from the work of Feast[9] where addition of core is described as decreasing the molecular weight of hyperbranched materials coupled in the bulk. One further notable feature in Table 2.4. is the increase in PDI of the HyperMacs with the increased addition of core to the reaction. Conceptually the addition of core molecules should decrease the PDI values of the material compared to standard molecular hyperbranched polymers predicted by Flory[11] who describes increasing polydispersity with molecular weight for the reaction of AB_2 monomers.

Here, in the case of core HyperMacs, the opposite is observed as the PDI increases. This is likely an effect of the increase in molecular weight of the macromonomers. Conventional hyperbranched polymers have much higher degrees of branching and inherently large PDIs compared to HyperMacs, which would noticeably decrease with addition of a core, as reported. HyperMacs are unlikely to ever branch to the degree of hyperbranched polymers due to the molecular weight between branch points and the inherent increase in viscosity. Addition of the core to this system does decrease the molecular weight, but with a PDI much lower than expected due to the chemistry of the system, a decrease in the PDI of an initially relatively low value anyway is likely to be negligible. Table 2.4 shows that the PDI reaches 3.6 with increasing addition of B_3 core; whereas a PDI of 3.8 is the maximum value observed in a typical HyperMac synthesis (Table 2.3). Consequently the trends opposite to those reported in the literature in terms of increasing PDI with addition of B_3 are likely due to differences in chemistry between HyperMacs and hyperbranched polymers, rather than more/less dendritic character in the core HyperMacs.

% Core	M_n(gmol^{-1})	M_w(gmol^{-1})	PDI	Dp_n	Dp_w	g'
0	510000	1527000	2.99	18	53	0.39
5	300000	993000	3.31	11	34	0.51
10	137000	505000	3.67	5	18	0.61

Table 2.4 SEC experimental values from a series of PS HyperMacs (AB_2, 28 kgmol^{-1}) coupled to a B_3 core after 24 h at room temperature in 20%w/v solution of DMF. g' = [η]hyperbranched/ [η] linear ;where [η] linear obtained using Mark-Houwink equation.[1]

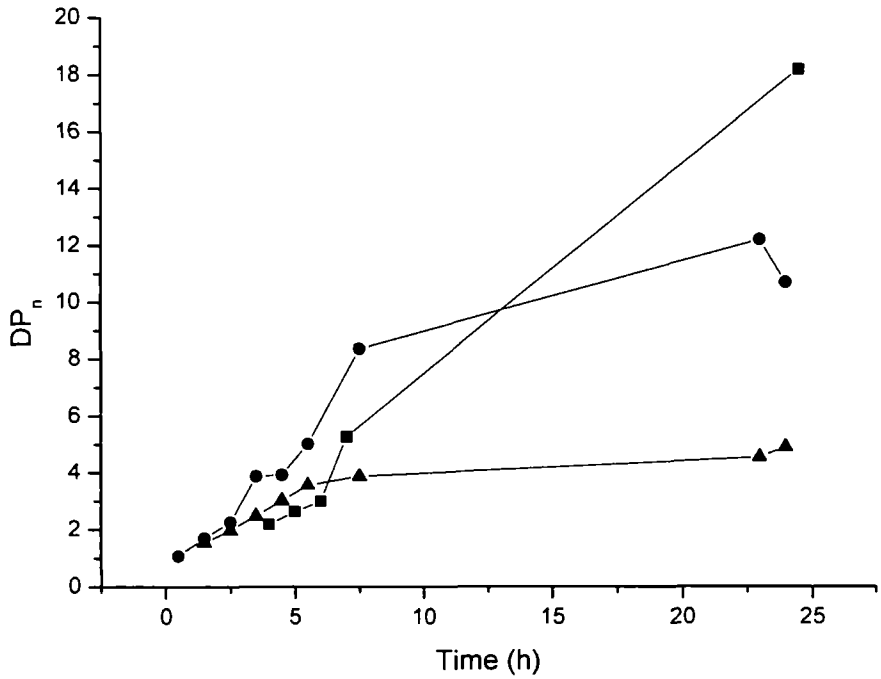

Figure 2.10 Extent of AB_2 polycondensation with addition of a % B_3 core to a HyperMac coupling reaction. ■ = 0%, ●= 5%, and ▲= 10%.

Figure 2.10 shows data for coupling reactions in the presence of a B_3 core and indicate the first two phases of reaction previously described for HyperMac coupling reactions; the lag and rapid growth. Towards the end of the reactions (24 hours), the addition of the core in different ratios to the reaction becomes obvious in the Dp_n values, where increasing the amount of B_3 significantly decreases the molecular weight. Addition of the core likely prevents the assembly of larger dendritic wedges towards the end of the reaction; where the coupling of smaller HyperMacs would normal dramatically increase the molecular weight forming 'super' HyperMacs. Clearly introducing the B_3 core prevents this from happening, and is to be expected as the B groups compete with the macromonomers for halide functionalities. If the coupling is diffusion controlled, as anticipated towards the end of the reaction, then cores are preferentially likely to couple to macromonomers due to their comparative low molecular weight. This agrees with the data from the material prepared by Feast, [9] with reasoning that the B_3 core acts more like a terminating agent than a core and seems entirely feasible in the case of core HyperMacs.

2.2.6 References.

1. Hutchings L.R., Dodds J.M., Roberts-Bleming S.J. *Macromolecules* 2005, 38, 5970.
2. Hawker, C.J., Frechet, J.M.J. *J. Am.Chem. Soc.,* 1990, 112, 7638.
3. Feast W.J., Stainton N.M. *J. Mater. Chem.* 1995, 3, 405.
4. Armarego W. L. F.; Perrin D. D. Purification of Laboratory Chemicals; Butterworth-Heinemann: Oxford, 1996.
5. Bertola A.; Cassarino S.; Raucq P., US Patent 6987191, 2006.
6. Brandrup, J., Immergut E.H. and Grulke, E.A. Polymer Handbook, 4th Edition; John Wiley and Sons, NewYork; 1999.
7. Konno J. *J. Polym Sci A: Polym. Chem.* 1997, 35, 605.
8. Martínez C.A., Hay A.S. *J.Poym. Sci A: Polym. Chem.*, 1997, 35, 1781.
9. Hobson L.J., Feast W.J. *Polymer*, 1990, 40, 1279.
10. Malmström E., Hult A. *Macromolecules*, 1996, 29, 1222.
11. Flory P.J. Principles of Polymer Chemistry, Cornell University Press, Ithaca, New York, 1953.

3. Polybutadiene HyperMacs.

3.1 Introduction.

The synthetic route to HyperMacs in which branched polymers are produced from the coupling of well-defined AB_2 macromonomers is extremely versatile and as such can be used to synthesise HyperMacs from polymers other than polystyrene. However some minor modifications to the exact chemistry are required. Here the improvements discussed in the previous chapter for polystyrene HyperMacs are combined with modifications to construct polybutadiene HyperMacs.

3.2 Results and Discussion.

Well defined dendrimer-like branched polymers constructed from polybutadiene have been reported by Hadjichristidis[1] who used a combination of diphenylethylene (DPE) derivatives and silyl coupling agents to produce a two level dendrimer type branched polybutadiene. Hutchings and Kimani[2] report the synthesis of a 2 level G1 polybutadiene DendriMac from a 3 arm mikto star coupled via an ether linkage to a trifunctional core. Both of these routes describe methods for the construction of very well-defined materials in terms of polydispersity, for structure-property correlation studies. The principle disadvantage of both of these methodologies is the time consuming synthesis and purification steps resulting in low yields for these well-defined materials.

It has already been demonstrated[3] that the synthesis of HyperMacs offers an alternative strategy for the synthesis of highly (albeit less perfectly) branched polymers in a facile, one-pot polycondensation reaction, allowing the production of useful amounts of branched polymer in a relative short period of time. The same philosophy is applied here for the synthesis of polybutadiene HyperMacs via a slightly modified route to that described previously for polystyrene structures. This reinforces both the versatility and facile nature of the macromonomer approach for constructing branched polymers.

3.2.1 Polybutadiene Macromonomers.

The anionic polymerization of dienes, such a butadiene, is well understood and has been successfully used for many years in both industrial and academic environments.[4] Two polybutadiene macromonomers (Table 3.1) were synthesised using a modified version of the already established route to polystyrene macromonomers.[3] (Figure 3.1)

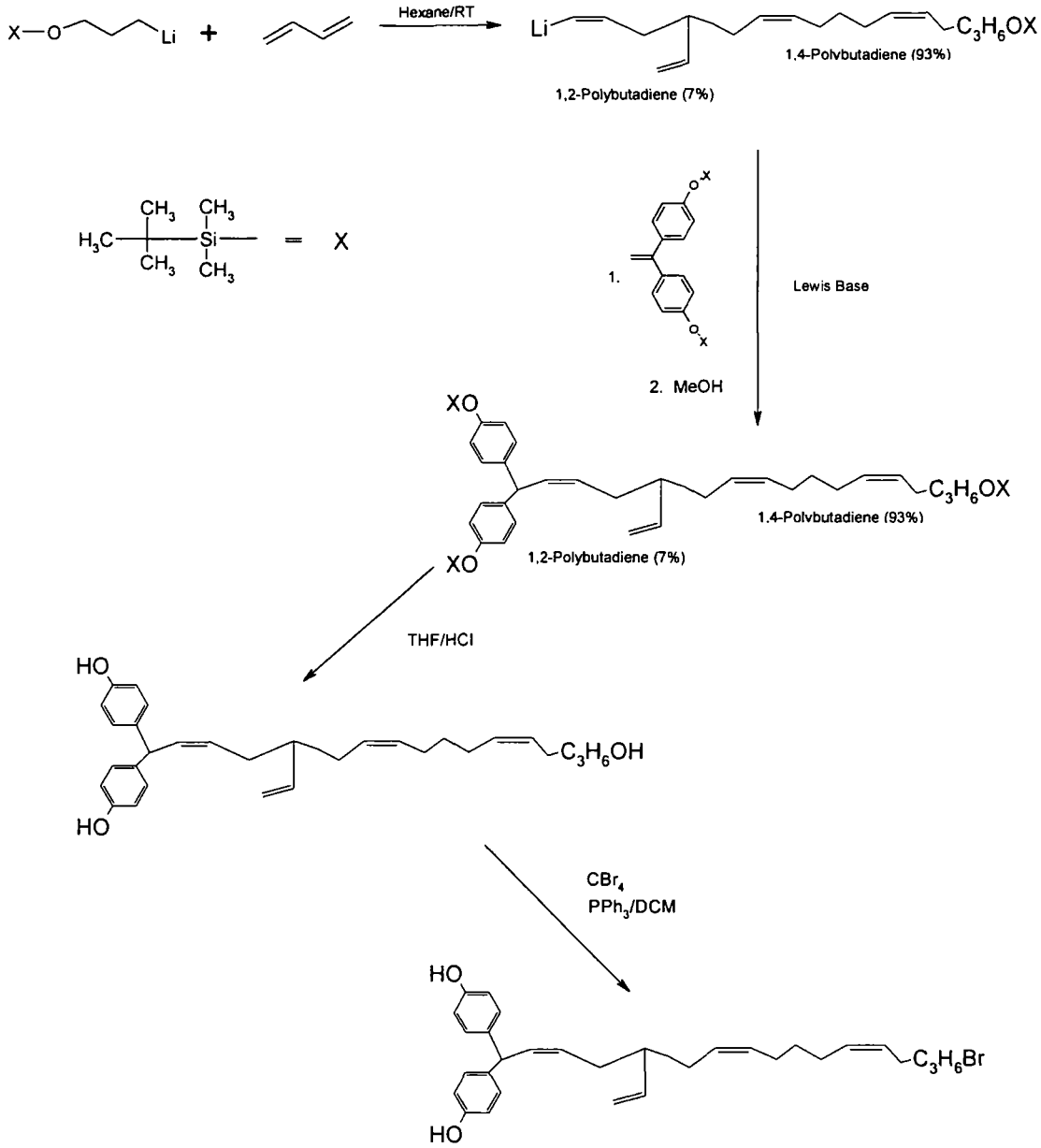

Figure 3.1 Synthesis of polybutadiene AB_2 macromonomer under high vacuum conditions.

Macromonomer	M_n (gmol^{-1})	M_w (gmol^{-1})	PDI
PBM 1	6500	7200	1.09
PBM 2	15600	16200	1.03

Table 3.1 Polybutadiene AB_2 macromonomers.

The chemistry used for the synthesis of polybutadiene macromonomers is similar to that previously reported by the Hutchings group for the construction of polybutadiene DendriMacs.[2] Polybutadiene macromonomers were synthesised as shown in Figure 3.1. Anionic polymerisation under high vacuum conditions of butadiene in n-hexane was performed to maintain high 1,4 polybutadiene microstructure. The living polybutadiene chain end was end-capped with a functionalised diphenylethylene derivative (DPE) (1) and the reaction quenched with methanol. The protected polymers (macromonomers) were deprotected in a rapid acid hydrolysis reaction, and the primary alcohol groups brominated with carbon tetrabromide and triphenylphospine, producing an AB_2 macromonomer. High 1,4 microstructure is desirable to maintain the potential for hydrogenation of the polybutadiene to polyethylene, a route to well-controlled model branched polyethylenes. Molecular weight data for the two polybutadiene macromonomers constructed in this study are shown in Table 3.1.

3.3.2 Polybutadiene HyperMacs.

Synthesis of polybutadiene macromonomers using anionic polymerisation provides the building blocks for HyperMacs. Chapter 2 described modifications to the original polystyrene HyperMac synthesis,[3] with the aim of improving the extent of branching by increasing the numbers of macromonomers coupling to one-another in a polycondensation reaction. It was noted for polystyrene HyperMacs that solubility of HyperMacs decreased in dimethylformamide (DMF) with increasing molecular weight. It was anticipated the solubility of polybutadiene would also be an issue. A series of reactions were conducted to investigate.

Initial coupling reactions were carried out using conditions developed for the synthesis of polybutadiene DendriMacs. In that case the initial coupling reactions using N,N-

dimethylacetamide (DMAc) as the solvent had undeniably suffered from solubility problems. This limitation was overcome by the addition of a cosolvent tetrahydrofuran, (THF), in a 50:50 by volume mixture (Figure 3.2). Although the addition of THF reduces the dipole moment of the coupling solution, which in itself may reduce the extent of the reaction, good solubility was seen to be more important. The same solvent mixture was used in these studies.

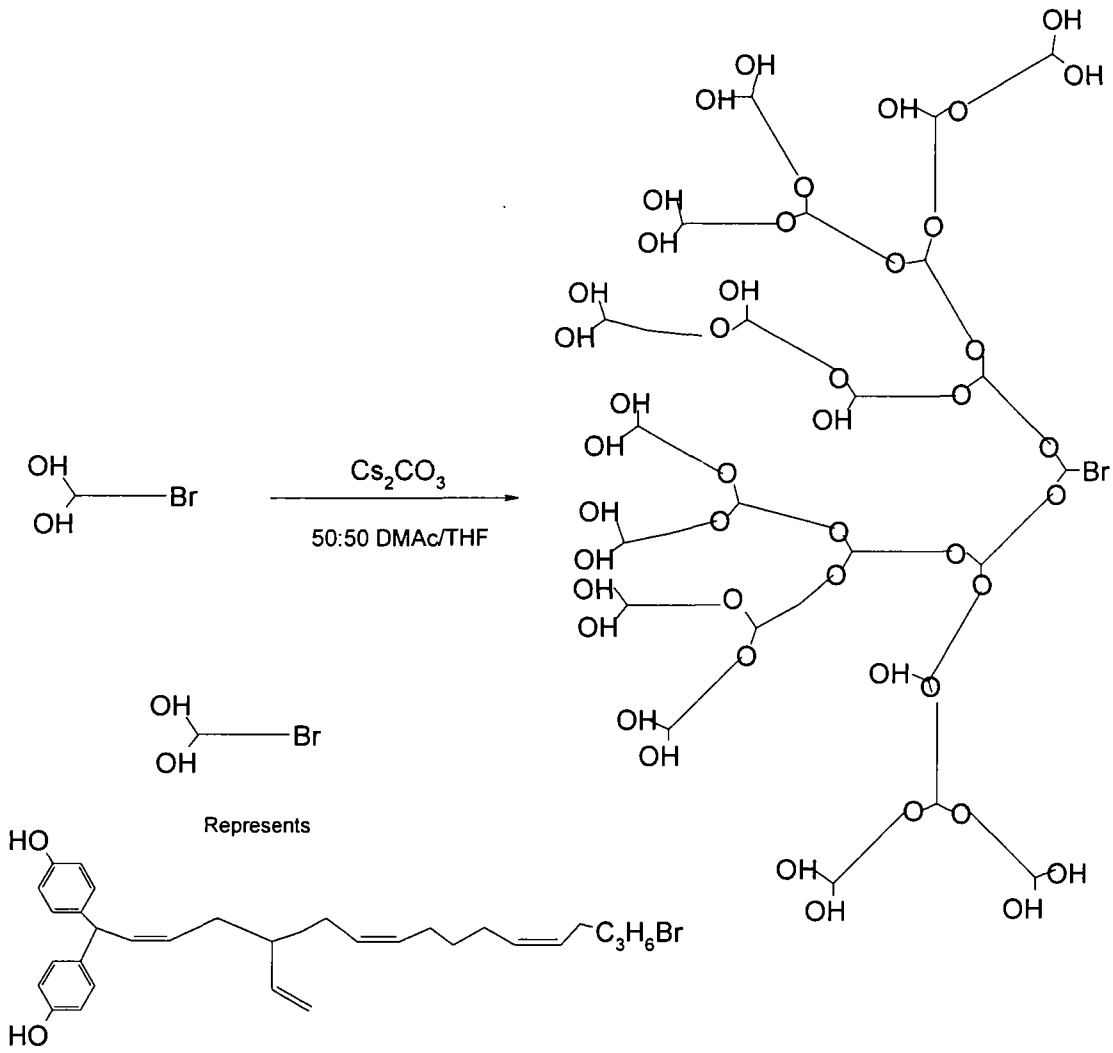

Figure 3.2 Synthesis of Polybutadiene HyperMac.

Molecular weight data for the coupling reaction of macromonomer PBM2 shows that the reaction proceeds successfully and after 6 hours at 60°C the Dp_w has reached a value approaching 45. This is a similar extent of reaction to that achieved for polystyrene HyperMacs. Concerns about changes in reaction solvent appear unfounded, as the coupling strategy undoubtedly works, albeit that the reactions proceed more slowly than for polystyrene macromonomers in DMF.[3]

Time (h)	M_n (gmol^{-1})	M_w (gmol^{-1})	Dp_n	Dp_w	PDI
1	34400	75900	2.21	4.68	2.20
2	74000	229400	4.74	14.16	3.10
3	163600	672700	10.49	41.52	4.10
4	184900	648900	11.85	40.05	3.50
6	188400	692500	12.08	42.74	3.70

Table 3.2 Synthesis of polybutadiene HyperMac. Coupling reaction carried out at 60°C, 50:50 DMAc/THF from PBM 2 macromonomer (M_n 15600 gmol^{-1}). 93% 1,4 PB.

Coupling reactions of the lower molecular weight macromonomer (PBM 1) show a significant increase in the Dp_w compared to the higher molecular weight macromonomer, with the HyperMac having a Dp_w approaching 80 after 2 hours coupling (Figure 3.3).

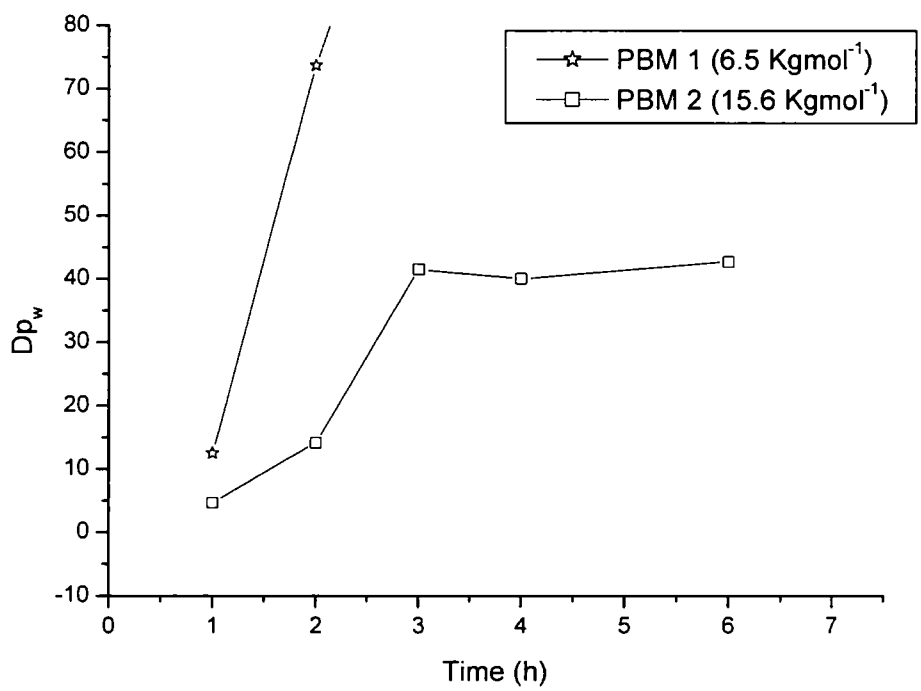

Figure 3.3 Polybutadiene HyperMac coupling reactions of the macromonomers of varying molecular weight.

It should be noted at this point the absence of data for Dp_w after 2 hours for the coupling of the lower molecular weight macromonomer, this is due to the decreasing solubility of the polymer in THF, required for SEC analysis. Samples of this HyperMac collected for analysis after 3 hours reaction were agitated for 14 days in THF with antioxidant 3,5-di-

t-butyl-4-4-hydroxytoluene (BHT). After this time the material was still not soluble but instead resembled a swollen gel. Reduced solubility of the materials causes problems for the characterization of these highly branched HyperMacs, as both NMR and SEC require solubility of the materials for characterization. It could be suggested that this gel like behavior arises from the presence of very high molecular weight (> 1000000 $gmol^{-1}$), highly branched polymers which may indeed have reduced solubility in THF.

One other possible explanation is oxidative coupling as dienes are susceptible to thermal oxidation[5]. The Williamson coupling reactions have to be carried out in the absence of an antioxidant such as BHT. The antioxidant would inhibit the Williamson coupling reaction due to its free phenolic OH group which would compete with the phenol functionalities on the macromonomer and therefore cannot be used in this reaction, increasing potential for oxidative coupling of the polybutadiene. However, similar observations of gel like material have been made for polystyrene HyperMacs with very high molecular weight. These also begin to become insoluble towards the end of reactions. Oxidative coupling is not however an issue for polystyrene due to its aromatic nature and there is no other obvious cross-linking mechanism for an AB_2 coupling reaction.

It seems most likely therefore that the insoluble gel like behavior of PBM1 is a consequence of the very high molecular weight and highly branched architecture. Lowering the molecular weight of the macromonomers in the original series of polystyrene HyperMacs appeared to reduce somewhat the extent of the coupling reaction. An increase in the probability of intramolecular coupling reactions was proposed as an explanation; the opposite appears to occur in this case. Clearly there are a number of factors affecting the coupling reactions of these polymers; however one of the dominating features seems to be a limitation imposed on the reaction by high molecular weight and high viscosity towards the end of the reaction.

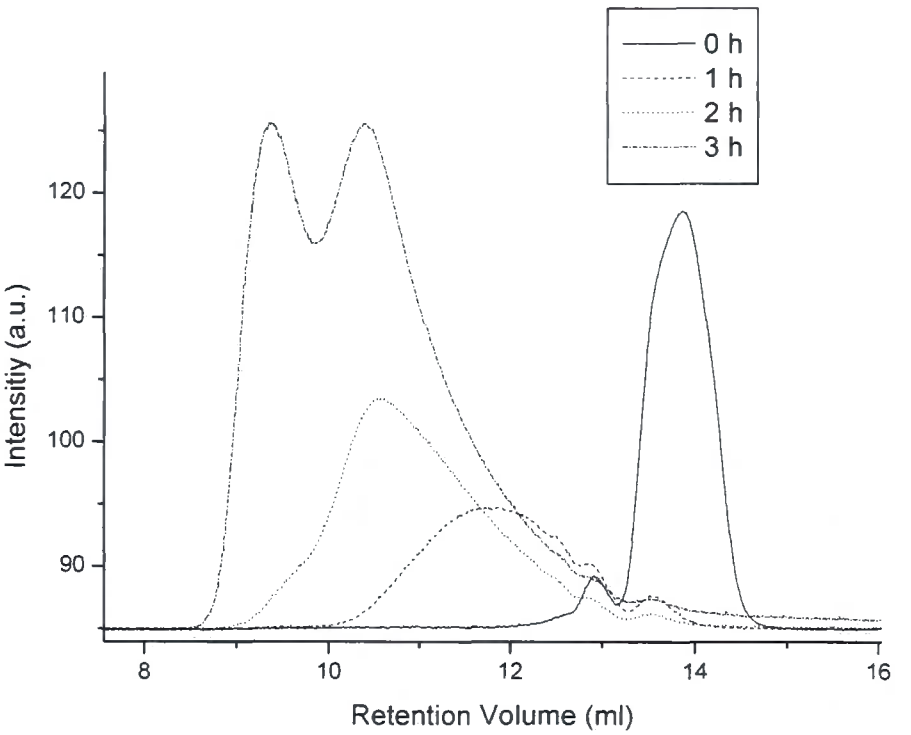

Figure 3.4 SEC RALLS data for synthesis of Polybutadiene HyperMac PBH2 after coupling reaction had proceeded for 0, 1, 2 and 3 hours.

Figure 3.4 shows light scattering SEC data for the synthesis of PBH2 with molecular weight increasing to the left. The major component of the first sample taken as the reaction reached the desired temperature-60°C- (0 hours) is unreacted macromonomer with a peak elution volume of approximately 14ml. The small peak at 13ml when the reaction has reached a temperature of 60°C (0 h) indicates that even heating the reaction not much above room temperature causes coupling to occur. As the reaction proceeds the macromonomer is consumed with time and the molecular weight distribution broadens and shifts to lower retention volumes (higher molecular weights). Appearance of a second peak with a retention volume of approximately 9.25ml after 3 h at 60°C indicates the formation of very high molecular branched polymer resulting from the coupling of HyperMac to HyperMac. The rapid growth of the HyperMac and the production of a bimodal curve in the SEC trace are also observed in polystyrene HyperMacs. The emergence of this high molecular weight shoulder/peak is also accompanied by a dramatic increase in viscosity of the solution and in some cases a loss of solubility that ultimately appears to inhibit the further growth of the HyperMacs, irrespective of macromonomer type.

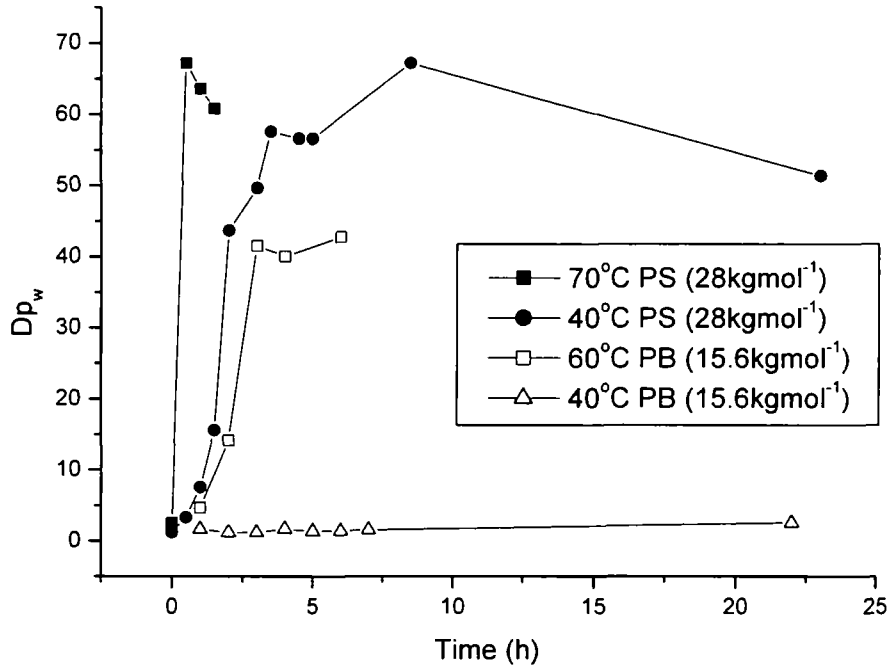

Figure 3.5 Polybutadiene and polystyrene HyperMac coupling reactions.

A comparison of the polystyrene (PS) and polybutadiene (PB) HyperMac coupling reactions (Figure 3.5) shows that the rate of coupling is significantly slower for polybutadiene macromonomers compared to polystyrene macromonomers. The PB reaction at 40°C appears to couple at a very conservative rate, with the Dp_w well below 5 after 24 h. Compare this with the PS coupling reaction at the same temperature with a Dp_w of over 60 after 7.5h - the rate of reaction is obviously slower for polybutadiene. The reason for this is likely due to the reduction of the dielectric constant of the reaction solvent with the addition of THF. In the pursuit for a suitable coupling solvent in the original PS HyperMac synthesis[3], a reaction in pure THF was reported to proceed very slowly (if at all) compared to solvents with a higher dielectric constant (7.58 and 36.71 for THF and DMF respectively). It stands to reason that this is the factor behind the reduced coupling of PB materials in Figure 3.5.

Polybutadiene is possibly a more attractive candidate than polystyrene for rheological investigations given that its entanglement molecular weight (M_e) (<1800 gmol^{-1}) is much lower than polystyrene (<16000 gmol^{-1}).[6] Useful rheological investigations usually require branched polymers with several entanglements between branch points[7,8]. Furthemore the hydrogenation of polybutadiene HyperMacs would provide a route

towards model long-chain branched polyethylene, with some control of molecular weight between the branch points. Importantly the controlled molecular weights of the macromonomer and AB_2 coupling strategy, result in a somewhat predictable model material.[9] A possible application of this methodology is to synthesize 'model' systems for molecular rheology. The rheology of polymer melts may be tailored by controlled addition of long-chain branches using 'open-site' metallocene catalysts, and the molecular mechanism of vinyl-group reincorporation leads statistically to the same one-parameter topological family of branched structures as the AB_2 HyperMac polycondensation. The only difference lying in the exponential polydispersity of the molecular weight between branches in the case of the metallocene catalyzed system.
Thus HyperMacs may be useful 'model' materials for metallocene catalyzed polymers and their use for property-structure correlation studies is ongoing.

3.3.3 References.

1. Orfanou K., Iatrou H., Lohse D.J., Hadjichristidis N. *Macromolecules*, 2006, 39, 4361.
2. Kimani S.M., Hutchings L.R. *Macromole. Rapid Commun.*, 2008, 29, 8, 633.
3. Hutchings L.R., Dodds J.M., Roberts-Bleming S.J. *Macromolecules*, 2005, 38, 14, 5970, and Clarke N., De Luca E., Dodds J.M., Kimani S.M., Hutchings L.R. *Euro. Polym. J.*, 2008, 44, 665.
4. Hsiech H. L. and Quirk R.P. Anionic Polymerisation: Principles and Practical Applications. Marcel Dekker, New York, 1996.
5. Coquillat M., Verdu J., Colin X., Audouin L, Nevière R. *Polym. Degrad. Stab.*, 2007, 92, 1343.
6. Larson R.G. 'The Structure and Rheology of Complex Fluids', Oxford University Press, Oxford, 1999.Ch 3.
7. Lohse D.J., Milner S.T., Fetters L.J., Xenidou M., Hadjichristidis N., Mendleson R.A., Garcia-Franco C.A., Lyon M.K. *Macromolecules*, 2002, 35, 3066.
8. Hadjichristidis N., Xenidou M., Iatrou H., Pitsikalis M., Poulos Y., Avgeropoulos A., Sioula S., Paraskeva S., Velis G., Lohse D.J., Schulz D.N., Fetters L.J., Wright P.J., Mendelson R.A., Garcia-Franco C.A., Sun T., Ruff C.J. *Macromolecules*, 2000, 33, 2424.
9. Read D.J., McLeish T.C.B. *Macromolecules*, 2001, 34, 1928.

4. Rheological Characterisation of HyperMacs.

4.1 Introduction.

Synthesis of polystyrene HyperMacs described previously produced a wide range of branched materials with varying molecular weights. Here the rheology of these materials is investigated to gain insight into how branching affects the physical properties of these polymers.

4.2 Results and Discussion - Unfractionated HyperMacs.

Anionic polymerisation was used for the production of well-defined AB_2 macromonomers with molecular weights of 6500, 16400 and 104200 $gmol^{-1}$ which are below, approximately equal to and above the entanglement molecular weight (M_e) of polystyrene. The macromonomers were then converted via a one-pot polycondensation reaction into HyperMacs (Table 4.1).

	Macromonomer			HyperMac		
Sample	**$M_n(gmol^{-1})$**	**$M_w(gmol^{-1})$**	**PDI**	**$M_n(gmol^{-1})$**	**$M_w(gmol^{-1})$**	**PDI**
HM UN 1	6200	6500	1.05	43700	91000	2.10
HM UN 2	16100	16400	1.02	91800	226700	2.46
HM UN3	93900	104200	1.11	324500	682800	2.10

Table 4.1 Molecular weight and polydispersity data for HyperMacs used in unfractionated rheological studies.

Qualitative rheological analysis was carried out on three samples of HyperMac prepared by the 'original' synthetic methodology.[1] The HyperMacs in question had macromonomers with molecular weights below (HM UN 1), approximately equal to (HM UN 2) and above (HM UN 3) the entanglement molecular weight for polystyrene[2] see Table 4.1.

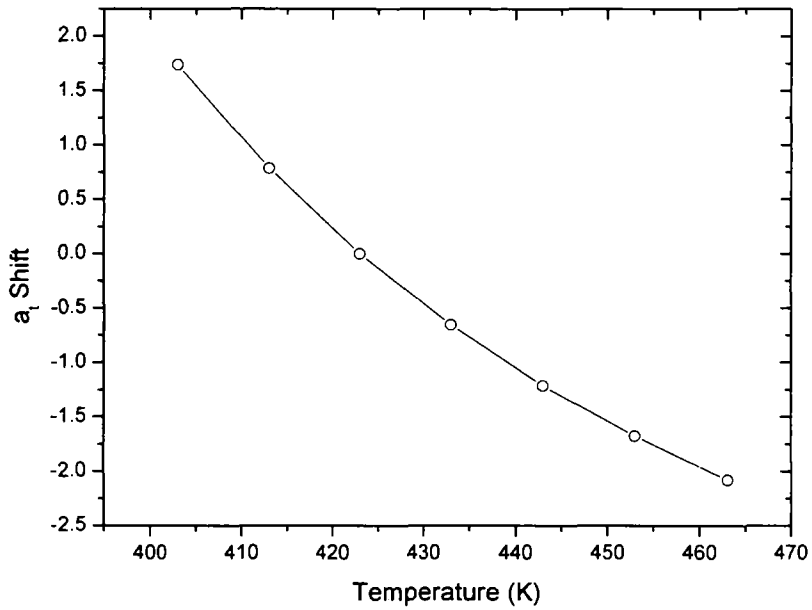

Figure 4.1 Horizontal shift values a_t as a function of temperature, fitted to WLF parameters (solid line) with a reference temperature of 150 °C (HM 12) $M_w = 92800$ gmol^{-1}.

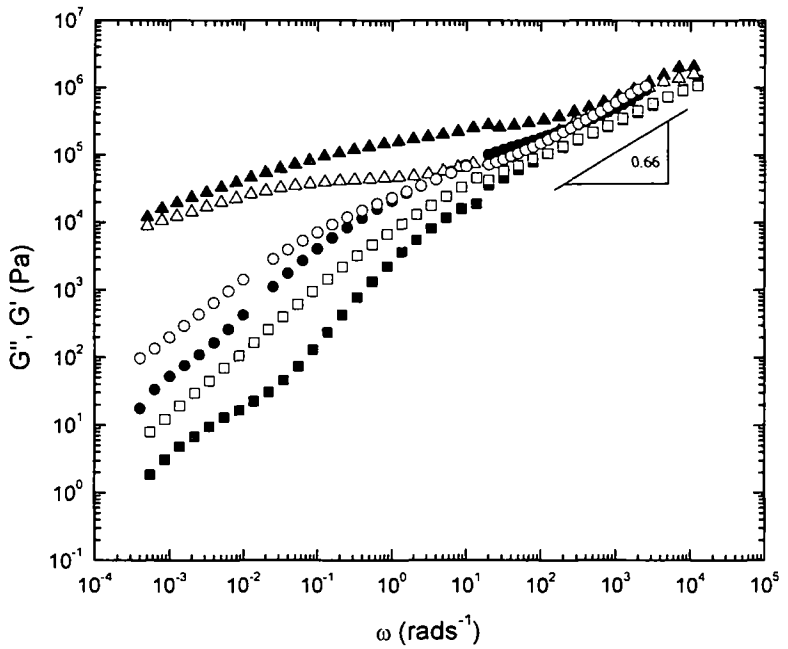

Figure 4.2 Storage moduli generated from varying the molecular weight between branch points from unfractionated HyperMacs shown in Table 4.1. (□ = HM UN 1, o = HM UN 2, Δ = HM UN 3; where G' =□, G'' =■.) (T_0 = 150 °C.)

Linear rheology measurements demonstrate that HyperMacs obey time-temperature superposition with the vertical shifts in the moduli response being negligible (Figure 4.1). Figure 4.2 shows the storage (G') moduli curves for the three HyperMacs with different molecular weight macromonomers and the variation between the samples is worth noting. Theory predicts that at high frequencies, G' for polydisperse randomly branched polymers should have a slope of approximately 0.66 at the gel point.[3] Figure 4.5 confirms that in the case of all three HyperMacs, the storage modulus versus frequency at frequencies above 1000 $rads^{-1}$ varies accordingly suggesting the onset of gel like behaviour. Interestingly, in the case of HM UN 1 and HM UN 2, the absence of a true rubbery plateau suggests that these materials are essentially unentangled despite having molecular weights significantly above M_e for linear polystyrene. M_n (HM UN 1) is approximately $3M_e$ and M_n (HM UN 2) is approximately $6M_e$. This is consistent with the work of Knauss *et al.*[4, 5] who reported a similar behaviour for hyperbranched polystyrenes with M_w in excess of 10^6 $gmol^{-1}$. Clearly the apparent absence of entanglements is the result of the highly branched architecture. However in the case of HM UN 3 in which the molecular weight of the macromonomer is close to 100000 $gmol^{-1}$ the slope of G'' – the loss modulus – is much more shallow than in the case of HM UN 1 and HM UN 2, indicating the presence of some chain entanglement. Furthermore, for HM UN3, in contrast to HM UN 1 and HM UN 2, across the entire frequency range the storage modulus is greater than the loss modulus, which is also indicative of an entangled viscoelastic regime. Since we were not able to observe a low frequency crossover between G' and G'', the longest relaxation time must be greater than 10^3 s. It is also worth noting that the magnitude of the storage modulus is comparable to that of the longer relaxation time. It is apparent that it is possible to prepare high molecular weight polymers which are essentially unentangled provided that the molecular weight of the linear segments between branch points is below M_e.

A more detailed analysis of the rheology of the unfractionated HyperMac is not quantitatively possible because of the high polydispersity of the material. To overcome this issue, material prepared from macromonomers with M_w approximately = M_e (HM UN 2) was fractionated to produce a range of materials with a wide range of molecular weights and narrower polydispersity (Table 4.2).

4.3 Fractionated HyperMac Rheology.

The fractionation results in series of HyperMac fractions with a range of molecular weights and lower polydispersity values than the unfractionated material. Figure 4.3 shows the SEC trace of the unfractionated HyperMac in bold, with a relatively high polydispersity and the presence of low molecular weight material (dimers and trimers) towards the higher retention volume. SEC of the HyperMac fractions show a decrease in polydispersity of the fractionated material and a more monomodal distribution. The unfractionated material is multimodal.

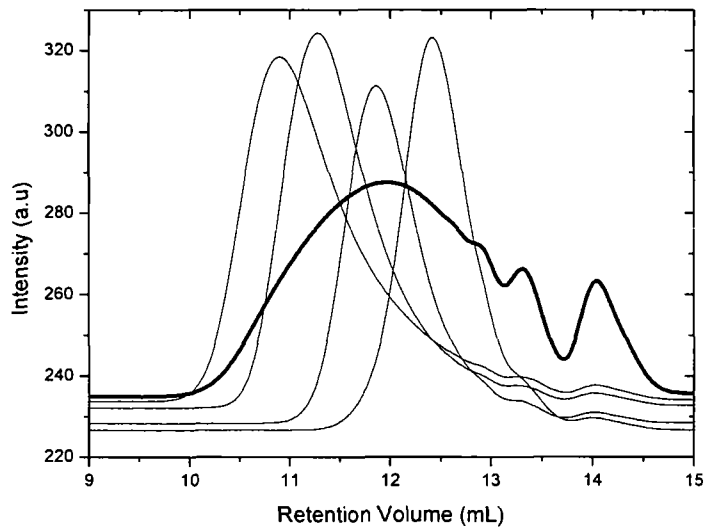

Figure 4.3 SEC traces of selected fractions HM2, HM6, HM10, HM10 (left to right) from the HM UN 2 (in bold) unfractionated HyperMac.

The William-Landen-Ferry (WLF) expression,[6] $\log(a_T) = -C_0(T - T_{ref})/(C_1 + T - T_{ref})$, was used to construct master curves with shift values shown in Figure 4.2. The data is well fit with the values, C_0 = 3.5 ± 0.25 K and C_1 = 81.1± 15.05 K, which within the experimental error, closely match previously reported values for star polystyrene.[7]

In Figures 4.5 and 4.6 the G' and G'' master curve for some example fractions are shown. The dependence of G' and G'' in the terminal region of each HyperMac fraction was modelled by a power-law type relationship, $G=A\omega^b$ where ω is the angular frequency and A, b are experimentally determined constants. Linear regressions were performed on the terminal region of each of the fractions master curves to determine the fitting parameters

(Figures 4.5 and 4.6). The slopes determined from this simple linear regression were used to compare the experimental data with terminal region behaviour described in theoretical models. The G' terminal gradients data in Table 4.2 show an array of values between 1.25 and 1.73, with the average value for all the fractions being 1.5 ± 0.05. It is interesting to note that this is the theoretical value predicted by McLeish[8] for the relaxation of entangled branched polymers (Cayley trees). His work extends the tube model for linear polymer relaxation by de Gennes[9] and introduces the effect of branching which prevents reptation from occurring in branched melt systems. Above the plateau region, the G' modulus gradient averages 0.49, close to the predicted[8] value of 0.5 for randomly branched entangled polymers. Hadjichristidis et al.[10] report relaxation in sparsely branched asymmetric star polymers, with structures that resemble Cayley trees; both indicate that the model proposed shows good agreement with this data.

Sample	M_w ($gmol^{-1}$)	M_n ($gmol^{-1}$)	PDI	Av mon N. (Dpn)	τ_{long} (s)	τ_e (s)	G' (slope1)	G' (slope2)
HM 1	694700	421200	1.65	26	508.35	1.38E-03		0.34
HM 2	519300	347600	1.49	22	160.94	1.74E-03	1.26	0.52
HM 3	462700	313900	1.47	19	100.05	3.96E-03	1.38	0.51
HM 4	412300	296300	1.39	18	52.53	5.07E-03	1.25	0.49
HM 5	354900	258800	1.37	16	38.79	5.22E-03	1.54	0.46
HM 6	318400	238700	1.33	15	31.54	1.97E-03		0.59
HM 7	274800	210900	1.30	13	14.37	6.63E-03	1.73	0.48
HM 8	235300	178700	1.32	11	9.86	6.33E-03	1.48	
HM 9	190600	153100	1.24	10	1.87	9.76E-03	1.62	0.45
HM 10	162900	126100	1.29	8	0.72	1.19E-02	1.32	0.53

Table 4.2 M_w, M_n, polydispersity (PDI), average number of macromonomers, high and low frequency relaxation times and *G'* terminal region slopes of the fractions from HM UN 2 HyperMacs.

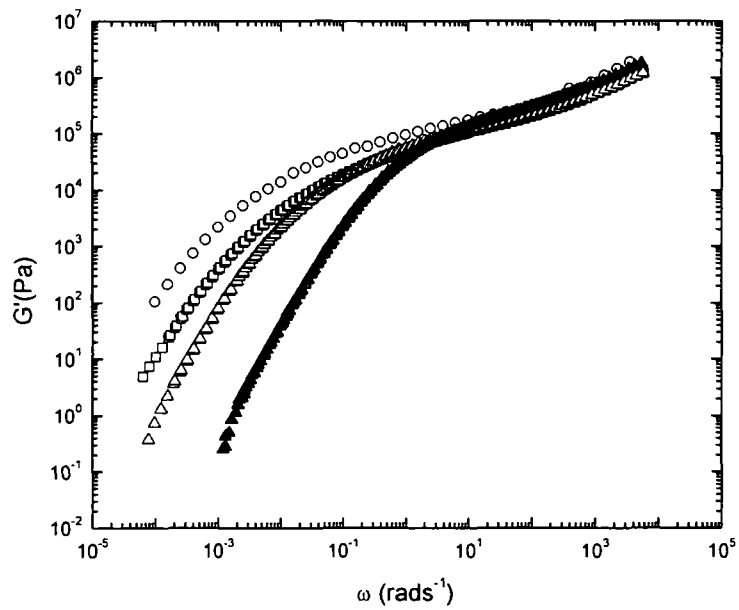

Figure 4.5 *G'* for fractions HM2○, HM6□, HM8Δ and HM10▲ (T_0=150°C).

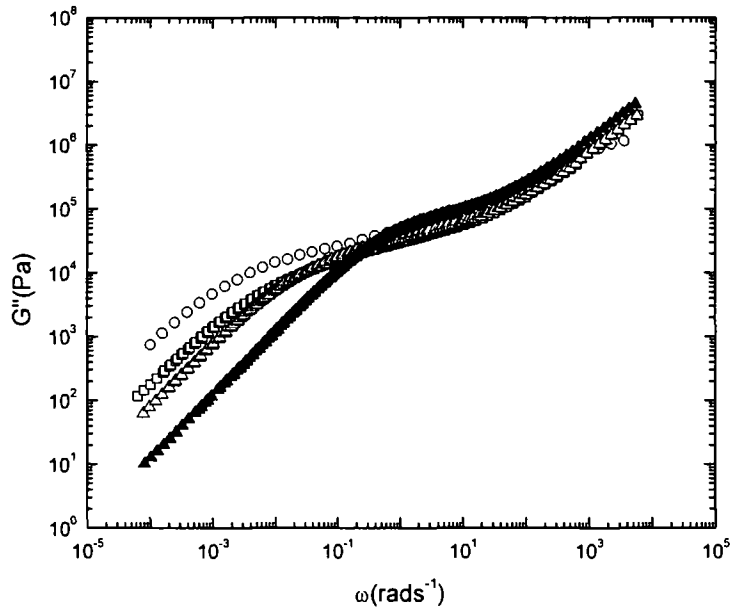

Figure 4.6 *G''* for fractions HM2○, HM6□, HM8Δ and HM10▲ (T_0=150°C).

It should be considered that due to the strategy involved in the synthesis of HyperMacs, each fraction contains a distribution of branched structures. Figure 4.7, constructed using the principles outlined by Flory[11], shows a few examples of branched structures constructed from macromonomers. Fractionation separates mainly by molecular weight. In the case of lower molecular weight fractions, such as HM 12 with the Dp_n value of 5, the structures are either almost linear with one branch point or H-shaped with 2 branch points. Cyclic products from the branching reaction will also be present but are more probable at low molecular weight as the probability of cyclisation increases when the two chain ends are closer.

It can be noted that the gradients predicted[8] (1.5 and 0.5 for the high and low frequency regions respectively) for the branched structures are more readily shown by the higher molecular weight fractions. One exception to this is HM 1, where the deviation from the theoretical values is likely to be due to polydispersity, as low molecular weight material may act to dilute the entanglement network. Our fractions do not show a plateau in the storage modulus, in agreement with the work of Namba et al.[12] who reported the dynamic shear moduli of multi-branched polystyrenes.

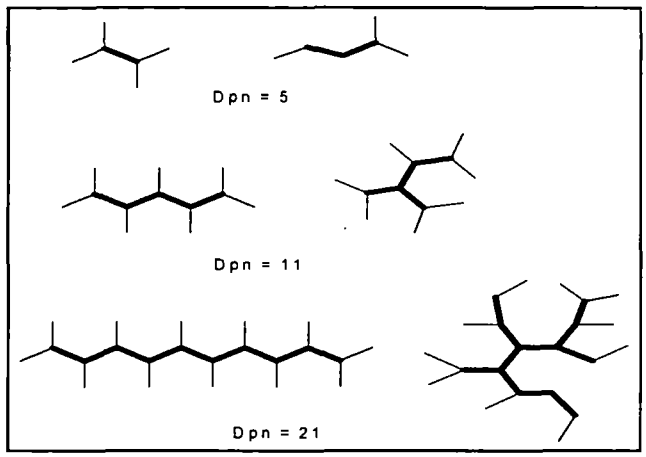

Figure 4.7 Possible structures of HyperMacs from the fractions of HM 2. Number of branches determined from the Dp_n determined using SEC. Note that the cartoon examples shown here are a small selection of possible HyperMac structures due to the random synthetic route. (Interior relaxation segments bold – seniority >1.)

The molecular rheology of long chain branched structures is discussed by Read and McLeish[13] and Larson[14] for metallocene catalyzed polyolefins. An important concept introduced is seniority which identifies the order in which the branched polymer is likely to relax in terms of interior and exterior segments. In the lower molecular weight fractions, the application of seniority is limited due to the reduced number of branch points; however at the increased level of branching (Dp_n=21 in Figure 4.7), this terminology becomes more valid. The different relaxation processes observed (Figure 4.8) may be accounted for with the application of seniority, as the gradients could conceivably correspond to the relaxation of exterior and interior segments[9]. Read and McLeish[13] also discuss the statistics of the branching probability formed from long-chain branched materials with metallocene catalysts, however due to the inherent differences in synthetic routes between the commercial and HyperMac material, it seemed inappropriate for the branching probabilities to be applied in the case of HyperMacs.

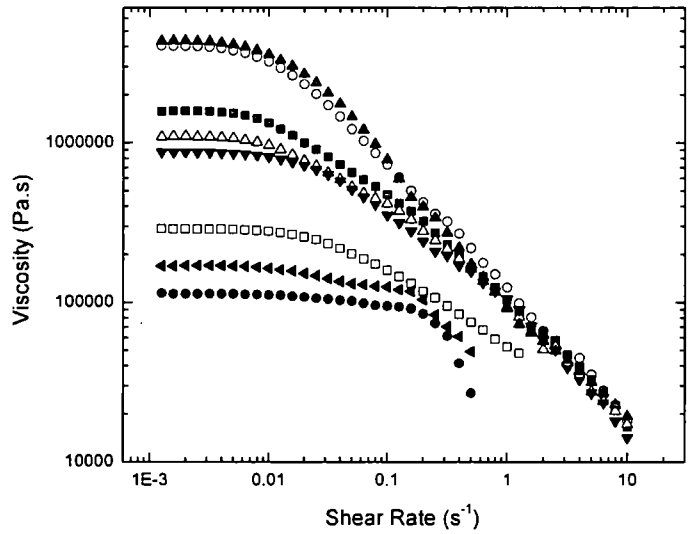

Figure 4.8 Shear thinning of fractionated HyperMacs in the melt. HM 2 UN□, HM1▲, HM2○, HM5■, HM6Δ, HM7▼, HM9◀, HM10● (T_0=150 °C).

Relaxation times were extracted from the rheology data and their molecular weight dependence is shown in Figures 4.9 and 4.10. The longest relaxation time increases with increasing molecular weight $\tau_{long} \propto Mw^{3.2 \pm 0.1}$ showing a remarkably similar trend to linear entangled polymers[11] ($\tau_{long} \propto Mw^{3.4}$). For comparison we note that Lusignan and co-workers[15] found a slope of 2.28 in the case of randomly branched polyester, also Müller et al.[16] observed a value of 2.61 for randomly branched polymethylmethacrylate.

Unusual molecular weight dependence was found for the entangled Rouse time, which decreases with increasing molecular weight according to $\tau_e \propto Mw^{-1.0 \pm 0.1}$. This relaxation time is proportional to the length of an entanglement strand of N_e monomers and it is well documented that for linear polymers, τ_e is independent of molecular weight. It appears that a dilution effect is playing an important role and that the effective N_e increases with decreasing weight average molecular weight, due to the corresponding increase in the fraction of lower molecular weight unentangled chains.

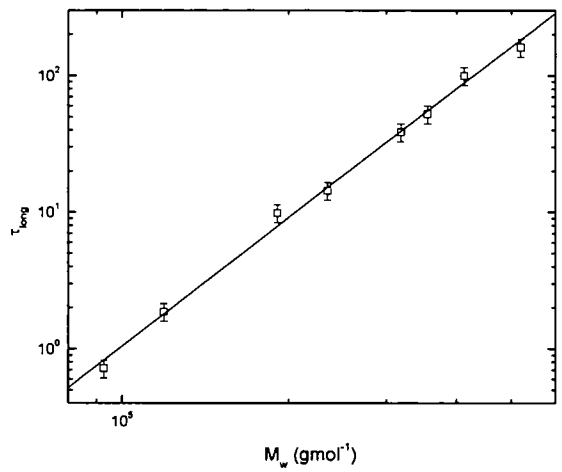

Figure 4.9 Linear fit of the longest relaxation time τ_{long} versus M_w.

Unsurprisingly, the zero shear viscosities (η_0) increase with molecular weight of the HyperMac. The significance of even small amounts of long chain branching in polyethylene is described by Gabriel et al.[17] where the zero shear viscosity significantly increases, compared to linear polyethylene. The shear rate dependent viscosity measurements showed typical shear-thinning behavior (Figure 4.8) as in the case of irregularly long-chain branched polypropylenes.[11]

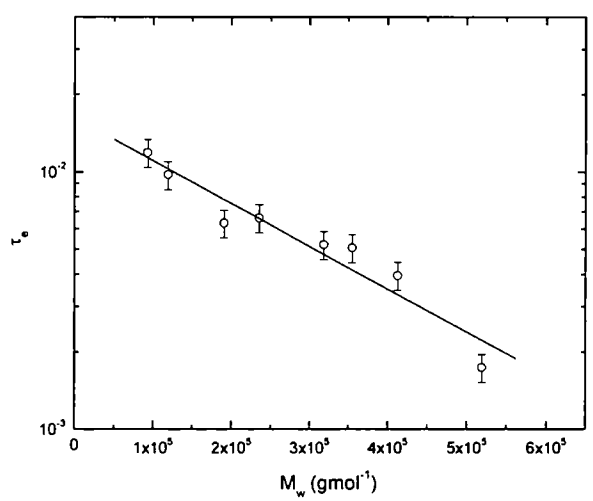

Figure 4.10 Linear fit of the entanglement Rouse relaxation time τ_ε versus M_w.

The effect of branching type on zero shear viscosity is discussed by Larson[14] with a theory that predicts zero-shear viscosities from the degree of branching in mono-disperse polybutadiene melts. It is hypothesised that the conversion of unbranched to branched molecules with fixed molecular weight will cause the viscosity of the melt to rise until there is roughly one branch per molecule, and then decrease beyond this point as the overall effect of arm entanglements is reduced. Figure 4.8 shows an increase in zero-shear viscosity with molecular weight for each of the fractionated HyperMac samples, therefore the HyperMacs are likely to be below the threshold of the one branch per molecule, exhibiting imperfect branching. It is also to be noted that this may explain the unusual trends in τ_e for increasing molecular weight described above.

Larson[2] also reports that zero-shear viscosities are very sensitive to branching distributions, however the relationship between molecular weight and zero shear viscosity is described as being less than perfect for the estimation of the degree of polymerisation for long chain branched materials. In this sense it accounts for the anomalies observed in the highest molecular weight fraction due to the higher polydispersity of the HM 1 material.

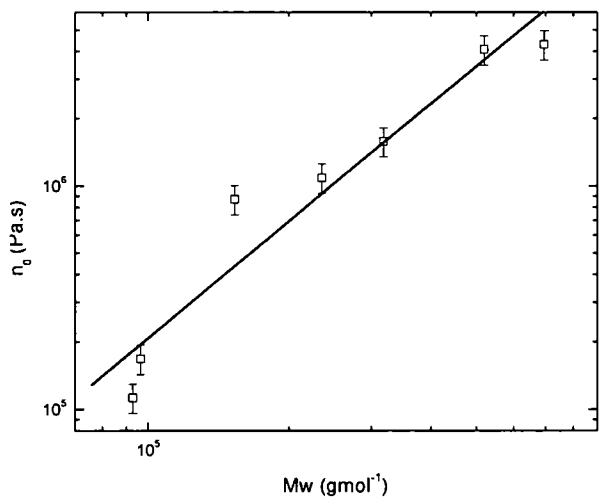

Figure 4.11 Zero shear viscosity against M_w for HM fractions (T_0=150°C).

Figure 4.11 shows that $\eta_0 \propto M_w^{-1.74 \pm 0.15}$. This value is significantly lower than that anticipated for linear polymers which relax via reptation[2]. The deviation of this value is not too unexpected given the unusual relation between the entangled Rouse relaxation time and molecular weight. Mechanisms such as constraint release, or contour length fluctuations[2]

are more likely to dominate relaxation due to its branched architecture. The deviation in the gradient observed for the HyperMac material is also seen for long chain branched polyethylenes[17], model combs[18] and highly branched polymethylmethacrylates,[16] materials with essentially comb type architectures and increased degree of branching.

Recently, the melt rheology of monodisperse comb polymer melt has been reported by Gabriel et al.[17] where the largest zero shear viscosities are obtained for combs that have few long arms and a long backbone. Highly branched materials with short arms and shorter backbones are reported to show linear gradients with values below the 3.4 expected for entangled linear polymers which would relax via reptation. The zero shear viscosity of HyperMacs with such diverse architectures from the one-pot synthetic route are inherently difficult to predict, however the appearance (Figure 4.8) of two gradients in the high molecular weight material suggests good agreement with viscoelastic prediction in long-chain branched materials.

4.4 Core HyperMac Rheology.

HyperMac rheology from both fractionated and unfractionated materials inherently shows correlation between molecular weight and branching. Addition of a B_3 core to the one-pot polystyrene HyperMac synthesis described in the previous synthetic chapter is not only shown to lower molecular weight, but also affect the material properties in the melt.

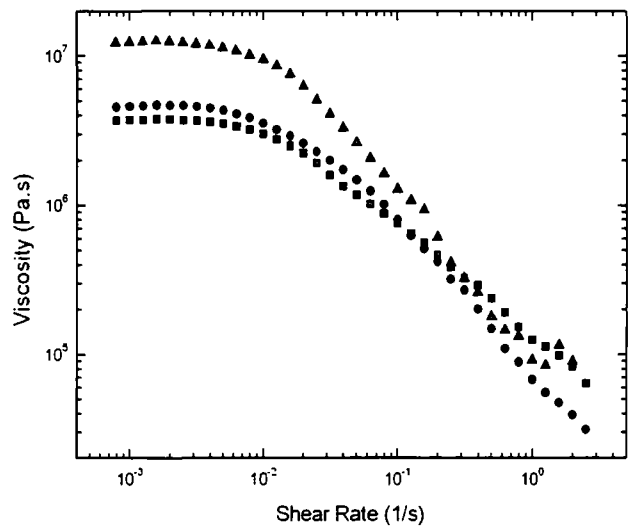

Figure 4.12 Shear rheology of a series of polystyrene HyperMacs (28 $kgmol^{-1}$, AB_2) with a B_3 core. ▲ = 0%, ●= 5%, and ■= 10% (T_0=150°C).

Figure 4.12 shows that the increasing content of core not only decreases molecular weight, but also decreases the zero shear viscosity of the core HyperMac. Compare this for instance with the section describing the addition of a pseudo B_2 core to a HyperMac coupling reaction. The introduction of more linear material (less branching) would affect the zero shear viscosity compared to HyperMacs of the same molecular weight, with or without a core. If it is assumed that the HyperMacs themselves are essentially unentangled, then the addition of the core, hence giving more linear sections, would result in more entanglements and an increase in the zero shear viscosity, (neglecting changes in molecular weight) observed in Figure 4.12.

Notably, the polydispersity of this type of material and the presence of low molecular weight materials (assumed due to the similarities in synthesis from standard polystyrene HyperMacs) means that the rheology data itself may be difficult to interpret for direct comparison in this circumstance. The material shear thins in the melt, as seen with the original polystyrene HyperMacs – confirming the presence of some entanglements and likely branching in the material.

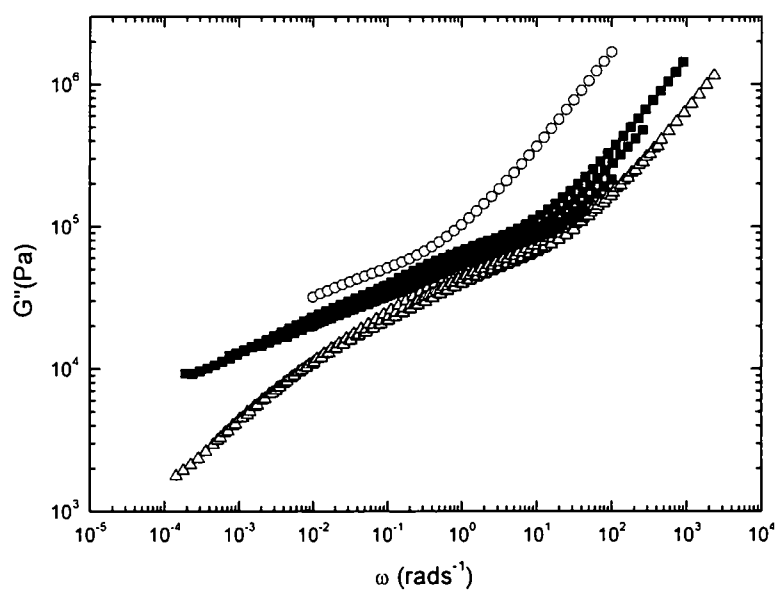

Figure 4.13 Loss modulus (G'') from a series of HyperMacs with B_3 cores. Symbols correspond to Δ = 0%, ○= 5%, and ■= 10% molar ratios of AB_2 macromonomer to B_3 core (T_0=150°C).

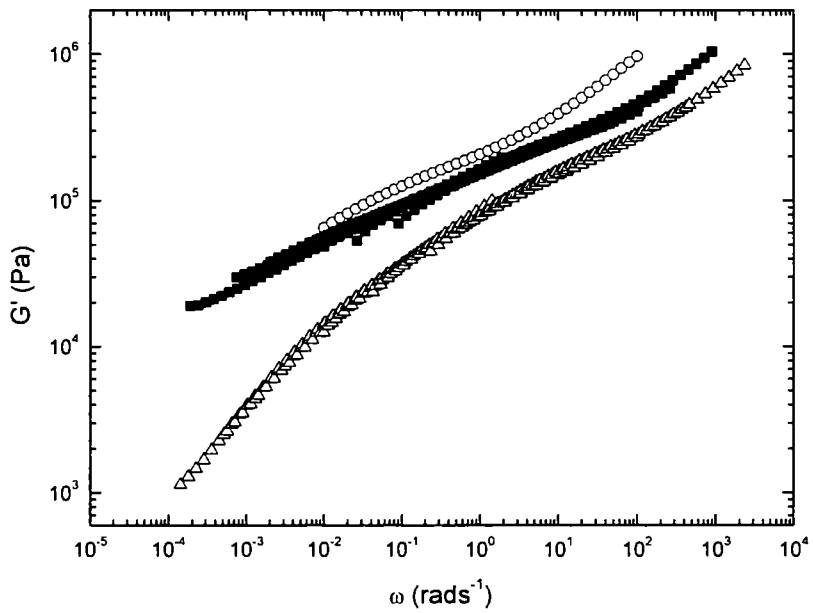

Figure 4.14 Storage modulus (G') from a series of HyperMacs with B_3 cores where Δ = 0%, ○= 5%, and ■= 10% molar ratios of AB_2 macromonomer to B_3 core (T_0=150°C).

% Core	η_0 (Pa s)	Low ω Gradient G'	High ω Gradient G'	Low ω Gradient G''	High ω Gradient G''
0	1.23 x 10^7	0.63	0.38	0.44	0.65
5	4.55 x 10^6	0.31	0.42	0.21	0.68
10	3.71 x 10^6	0.28	0.40	0.22	0.78

Table 4.3 Rheology data from the series of AB_2 HyperMacs with B_3 core, gradients refer to a power-law fitted to the linear regions shown in Figures 4.13 and 4.14.

Figures 4.13 and 4.14 show the storage and loss moduli for the range of core HyperMacs. One notable point observed in both of these figures is the positioning of the three mastercurves with respect to molecular weight. Increasing the molecular weight generally shifts the positioning of matercurves to the upper left corner of figures such as 4.6 and 4.7. In the case of core HyperMac, the reverse of the general trend is observed – the higher molecular weight HyperMac with no core added is seen in the lower right of the mastercurve figures. These observations are likely due to changes in architectures on the addition of the core to branched material.

Time-temperature superposition[6] is also seen to fail, particularly in the addition of 10% of the B_3 core in the G'' (Figure 4.13), suggesting heterogeneity. Failure of time-temperature superposition in star branched hydrogenated polybutadiene has been reported by Graessley et al.[19] where viscosity temperature coefficients of four star arms are shown to be different to those of the core, creating the breakdown. The addition of the B_3 core to polystyrene HyperMacs potentially has the same effect, thus explaining the deviation from time-temperature superposition.

Speculatively, the low and high frequency gradients (Table 4.3) observed for the HyperMac without a core correlate well with the Cayley tree model for branched polyethylenes by McLeish,[8] which considers well defined branched materials and observes gradients of 0.5 for the high ω G' (storage) moduli. One of the trends also observed in the G' gradients for the material with a core present results in values roughly half that seen for the HyperMac without a core.

It is difficult to speculate too much on the significance of these results due to the high polydispersity and variation in molecular weight between the different materials. However, it appears that the addition of a core to a one-pot AB_2 HyperMac synthesis alters the architecture and subsequent material properties.

4.5 References.

1. Hutchings L.R., Dodds J.M., Roberts-Bleming S.J. *Macromolecules* 2005, 38, 5970.
2. Larson R.G. 'The Structure and Rheology of Complex Fluids', Oxford University Press, Oxford, 1999.
3. Rubinstein M., Colby R.H. 'Polymer Physics', Oxford University Press, Oxford, 2003.
4. Knauss D.M., Al-Muallem H.A., *J. Polym. Sci., Part A: Polym. Chem.* 2000, 38: 4289.
5. Dorgan J.R., Knauss D.M., Al-Muallem H.A., Huang T., Vlassopoulos D. *Macromolecules* 2003, 36: 380.
6. Williams M.L., Landel R.F., Ferry J.D. *J. Am. Chem. Soc.* 1955, 77, 3701.
7. Clarke N., Colley F.R., Collins S.A., Hutchings L.R., Thompson R.L. *Macromolecules* 2006; 39, 1290.
8. McLeish T.C.B. *Europhys. Lett.* 1988; 6, 511.
9. de Gennes P.G. *J. Chem. Phys.*, 1971; 55: 572.
10. Kapnistos M., Koutalas G., Hadjichristidis, N., Roovers J., Lohse D.J., Vlassopoulos D. *Rheol. Acta.* 2006; 46: 273.
11. Flory P.J. Principles of Polymer Chemistry, Cornell University Press, Ithaca, New York, 1953.
12. Namba S., Tsukahara Y., Kaeriyama K., Okamoto K., Takahashi M. *Polymer* 2000; 41: 5165.
13. Read D.J., McLeish T.C.B. *Macromolecules* 2001; 34, 1928.
14. Larson R.G. *Macromolecules* 2001; 34, 4556.
15. Lusignan C.P., Mourey T.H., Wilson J.C., Colby R.H. *Phys. Rev. E.* 1995; 52, 6271.
16. Simon P.F.W., Müller A.H.E., Pakula T. *Macromolecules*, 2001, 34, 1677.
17. Gabriel C., Kokko E., Löfgren B., Seppälä J., Münstedt H. *Polymer* 2002; 43, 6383.
18. Inkson N.J.; Graham R.S., McLeish, T.C.B., Groves, D.J., Fernyhough, C.M. *Macromolecules* 2006; 39, 4217.
19. Raju V.R., Greassley W.W. *J. Polym. Sci: Polym. Phys*, 1979, 17, 1223.

5. HyperMacs from Block Copolymeric Macromonomers - HyperBlocks.

5.1 Introduction.

The macromomer approach for assembling branched polymers is versatile in many ways. In previous chapters the ability to modify the chemistry used to produce polystyrene HyperMacs for other monomers, such as butadiene, has been successful. This concept is further extended using the inherent ability of living anionic polymerisation to form diblock, triblock or multiblock copolymers.

Block copolymers are of interest due to their self-assembly and solid state morphologies which have many applications in the commercial and academic worlds. One of the applications of particular interest arises when block copolymers are constructed from rubbery and glassy polymers to give polymers called thermoplastic elastomers (TPEs).[1] Thermoplastic elastomers contain blocks of rubbery (e.g. polybutadiene or polyisoprene) and glassy (typically polystyrene) polymers. They combine two thermodynamically immiscible polymers into one material by covalently bonding each constituent to the other. The bonding of two (or more) immiscible polymers is just one of the important factors which allow TPEs to be used in many commercial applications as it allows the beneficial components of each polymer to be exploited. The main advantages of TPE materials over other thermosoftening plastics includes the ability to stretch the material which then returns to almost their original shape when the applied stress is removed, the ability to be melt processed as they are not crosslinked and their resistance to creep.[1]

Properties of TPEs generally depend on two main criteria, the volume fraction of each component - the major factor in controlling the morphology, and the molecular weight of each block. Typically a TPE will be designed so that the morphology comprises of a rubbery matrix with domains of glassy polymers, such as a polyisoprene matrix with polystyrene domains. The domains of glassy polymers act as physical crosslinks at room temperature provided the molecular weight of the glassy block is above the entanglement molecular weight M_e,[2] whilst the rubbery polyisoprene gives the material the desired flexible properties.

Commercial examples of this type of material include the Kraton family of polymers[1] typically consisting of polyisoprene or polybutadiene as the rubbery block and polystyrene as the glassy. The original commercial aim when developing these materials was to introduce strength into polyisoprene made by lithium initiated anionic polymerisation. This led to a family of linear and branched block-copolymeric materials which are commercially available with applications in adhesives, bitumen modifiers and structural materials.

Further examples of TPE formed from branched block copolymers include those described by Puskas et al.[3] where a series of hyperbranched polymers of polyisobutylene and polystyrene were prepared. The molecular weights of the polystyrene blocks were varied to give compositions of between 26 and 34%, with the resulting branched materials having phase-separated spherical, cylindrical and lamellar morphologies. The physical properties of these polymers are reported to depend on the number of branching points and mechanical analysis of the materials suggests they are comparable with commercial materials.

Hadjichristidis et al. [4] report 4-miktoarm A_2B_2 star copolymer materials constructed from polystyrene and polybutadiene using living anionic polymerisation with chlorosilane coupling chemistry. Branching is shown to influence the phase separated structures observed in these materials, including those of tetra block copolymers constructed from polystyrene, poly(4-methylstyrene), polyisoprene and polybutadeiene.

Branched block copolymers synthesized by anionic polymerisation are reported by Mays et al.[5, 6, 7] where the effect of architecture, principally the number of branch points and chains connected to them is investigated (Figure 5.1).

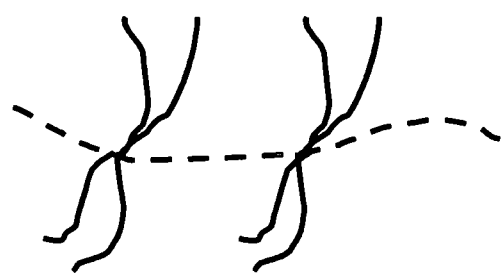

Figure 5.1 Barbed wire type architectures prepared by Mays et al. [5, 6, 7] with hexa functional branch points constructed with polystyrene backbones (dashed line) and polyisoprene arms (solid line).

Polyisoprene backbones containing tri, tetra and hexa functional branch points with polystyrene arms are synthesised. The two parameters that influence the mechanical

properties of these materials are reported to be the functionality of the branch points and number of branch points per molecule. The functionality of the branch points changes the morphology of the polymers and those displaying cylindrical and lamellae morphologies were shown to have improved tensile strength over those with spherical domains. Elastomeric properties of these materials are good; elongation at break is reported to exceed 2000% for some of these materials, almost twice that for commercially available TPEs.[6] The number of branch points influences physical properties of the materials such as the domain size in the phase separated morphology. It was found that more highly branched examples still undergo microphase separation but on a much smaller length scale as the junction points frustrate the morphological ordering

The following chapter investigates the effect of branched architectures on the solid state morphology of HyperMacs made from ABA triblock copolymeric macromonomers – HyperBlocks.

5.2 Results and Discussion.

In order to successfully synthesize HyperMacs in which the macromonomers are themselves block copolymers, a few modifications to the routes established for the synthesis of polystyrene and polybutadiene macromonomers are required.[8] Anionic polymerisation however is probably the optimal methodology for the synthesis of block copolymers and lends itself perfectly to the synthesis of macromonomers which are ABA triblock copolymers.

It was decided to prepare ABA triblock copolymers of polystyrene-polyisoprene-polystyrene rather than diblocks for two reasons. Firstly to minimize the number of modifications required to the existing chemistry as the initiation and end capping reactions would be identical to those used to make polystyrene macromonomers and secondly to allow direct comparison of the resulting HyperBlocks to commercial materials such as the Kraton range of thermoplastic elastomers.

5.2.1 Synthesis of ABA Triblock Macromonomer.

Synthesis of the macromonomer was carried out using standard high vacuum techniques as previously reported[8], with the following modifications (Figure 5.2). Initiation of the first block (polystyrene) with the protected initiator was carried out in benzene at room

temperature without any added TMEDA. The omission of TMEDA was crucial to maintain a high degree of 1,4 enchainment in the second (polyisoprene) block.[9] As expected this resulted in a slow rate of initiation with the characteristic orange/red colour of polystyryllithium developing over a few hours. The polydispersity of this polystyrene block was 1.48, higher than would normally be expected for a well-controlled/living polymerisation. However it was preferred to omit the TMEDA and accept a relatively high polydispersity rather than jeopardize the 1,4 microstructure preferred in the second (polyisoprene) block for good thermoplastic elastomeric properties. Addition of isoprene monomer to the living polystyrene chain resulted in a marked colour change from orange/red to an almost colourless solution. An increase in viscosity of the solution due to increased coordination of living polyisoprene chain ends around the lithium cation also indicated successful sequential monomer addition for this crossover reaction. Addition of a second batch of styrene monomer to form the final block was preceded by the addition of TMEDA (1:1 with respect to lithium initiator) before the sequential addition of the styrene. The amine was added for quick initiation of the final block of polystyrene by the living polyisoprene - the red colour of living polystyryllithium was observed immediately after the addition of styrene to the reaction vessel. This suggests a rapid crossover reaction.

Introduction of the B functionalities onto the macromonomer was achieved using a controlled end capping reaction with functionalized DPE, as reported in the initial HyperMac synthesis.[8]

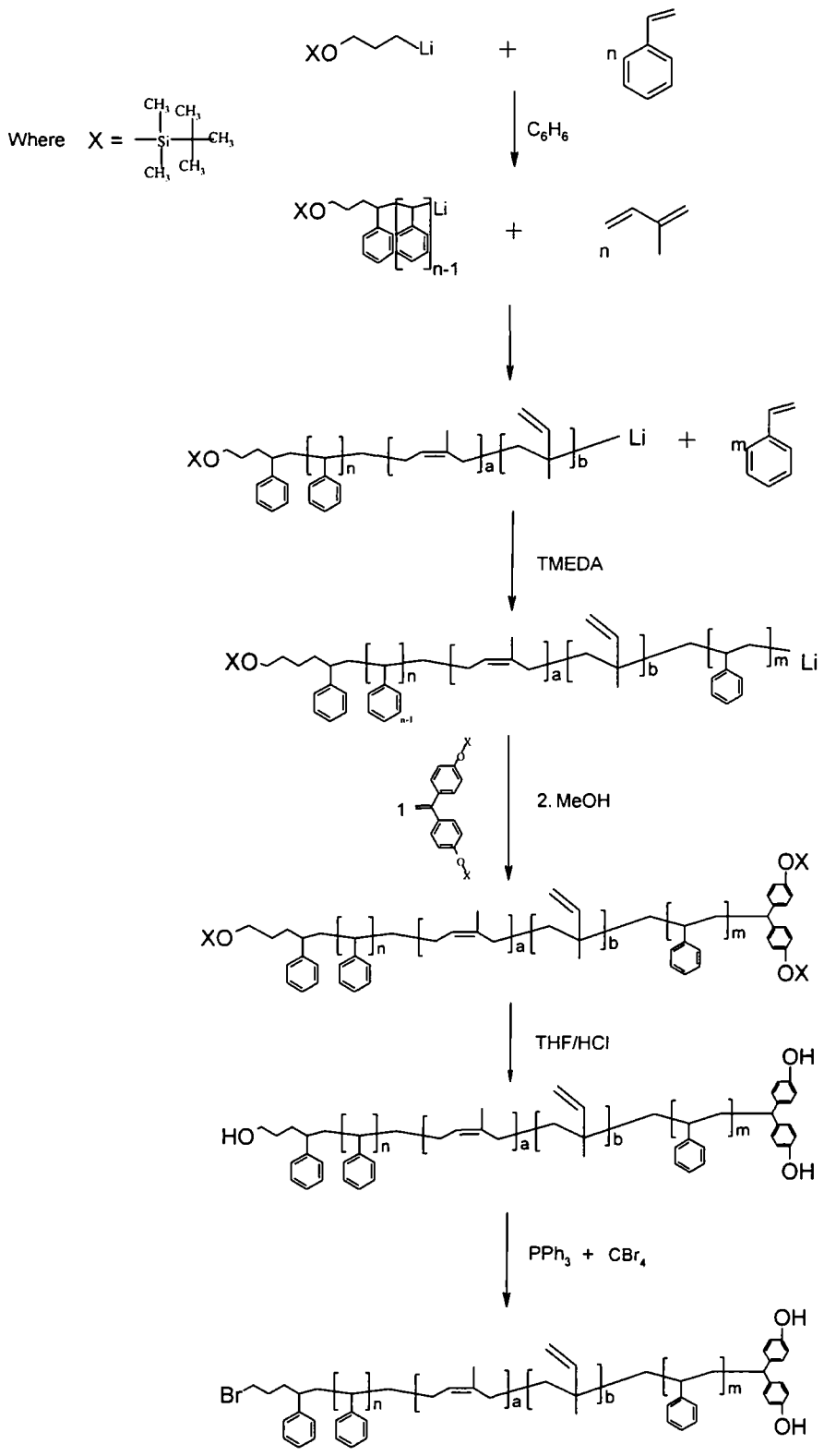

Figure 5.2 Synthetic scheme of polystyrene-b-polyisoprene-b-polystyrene HyperBlock AB_2 macromonomer.

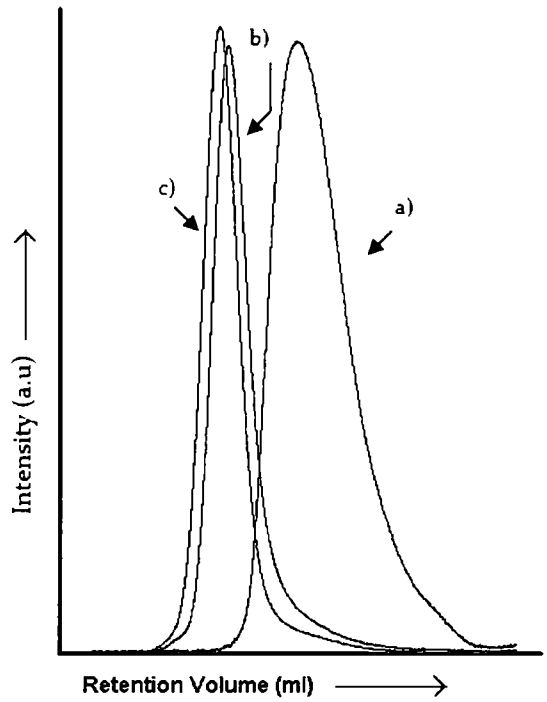

Figure 5.3 Size Exclusion Chromatograms (RI) of the various stages of HyperBlock macromonomer formation from sequential monomer addition. (right to left) (a) PS block 1(1.48); (b) PS-b-PI block 2 (1.21) and (c) PS-b-PI-b-PS block 3.(1.19) PDI values in brackets.

SEC traces were obtained by sampling the living polymer solution before each sequential addition of monomer (Figure 5.3) and are all monomodal. As expected the chromatogram from the first PS block is broader than the other peaks due to slow initiation in the absence of TMEDA (as previously discussed) and consequently has a high polydispersity value (1.48). The polydispersity narrowed following subsequent monomer additions, indicating rapid crossover reactions and good control over the polymerisation. Molecular weight data obtained both by SEC and NMR for this macromonomer are shown in Table 5.1.

The discrepancy between some of the NMR and SEC data arises from the method in which the SEC data has been calculated. The first set of data shown in Table 5.1 (central column) uses an assigned value of 0.185 for the *dn/dc* of the polymer; 0.185 is the *dn/dc* for polystyrene in THF[10]. The second set of SEC data (right hand column) uses a calculated value of *dn/dc* for each sample. The calculated value was obtained using the number fractions of polystyrene and polyisoprene (from NMR) and the actual

dn/dc values for each homopolymer – 0.185 for polystyrene[10a] and 0.124 for polyisoprene[10b].

The microstructure of polyisoprene was calculated using NMR by comparing the ratios of 1,4 and 3,4 polyisoprene at 5.3 and 4.9 ppm[11] respectively in C_6D_6. The high 1,4 microstructure (93%) as calculated is predicted for a polymerization carried out in non polar solvents with the absence of polar additives.

Material	NMR M_n ($gmol^{-1}$)[a]	SEC M_n ($gmol^{-1}$) [b]	SEC M_n ($gmol^{-1}$) [c]
1st PS Block	14600	14600	14600
2nd PI Block	38600	20000	30800
3rd PS Block	10900	11500	12700
PS-PI-PS Macromonomer	64100	46100	58100

Table 5.1 HyperBlock Macromonomer. Overall PDI=1.19, 1,4-polyisoprene=93%, polystyrene=40%.

a) Polystyrene 1st block obtained by triple detection SEC in THF using a value of dn/dc of 0.185 (polystyrene). The polystyrene proton integral was used to in conjunction with the SEC data to compare the polymer (polystyrene and polyisoprene) signature protons to generate values shown above. Polyisoprene microstructure determined by comparing signature peaks from 1,4 and 3,4 polyisoprene for ratios.

b) SEC data obtained by triple detection SEC in THF using a value of dn/dc of 0.185 (polystyrene).

c) SEC data obtained by triple detection SEC in THF using adjusted values with respect to polystyrene content of dn/dc of 0.185 (Polystyrene 1st block, 100% PS), 0.141(Diblock, 27%PS) and 0.148(Triblock, 40%PS).

Values in Table 5.1 determined by NMR show significantly increased M_n values compared to those determined using SEC with the two different calibrations. NMR values were calculated from the spectra using the signals from the silane protected functionalized initiator integrals; comparing these with the signals from the constituent polystyrene or polyisoprene blocks. Removal of the protection groups is achieved under relatively mild acidic conditions (Chapter 2) therefore hypothetically a small quantity of these groups may be removed when the polymer is precipitated into methanol before being fully characterised. Clearly comparing the intensity of peaks arising from a small number of polymer end groups for M_n determination is itself a possible source of

inaccuracy and could account for the elevated molecular weights for the macromonomer determined using NMR.

Deprotection and functional group modification to prepare the block copolymer AB_2 macromonomers was achieved as previously described (Chapter 2) for brominated polystyrene macromonomers. Slight modifications were made to prevent oxidative degradation and/or coupling of the polyisoprene block. Consequently, deprotection of the alcohol functionalities by acid hydrolysis reaction was carried out for a much shorter time, one hour rather than overnight as previously for polystyrene macromonomers.[8] It would have been advantageous to add the antioxidant, 3,5-di-t-butyl-4-hydroxytoluene (BHT), to prevent oxidative degredation.[12] However BHT could not be added to the material at this point for fear that it would be difficult to remove, as traces of BHT inhibits, via competition, the final Williamson ether coupling reaction.

5.2.2 HyperBlock Coupling Reactions.

Although the overall coupling strategy for converting block copolymeric macromonomers into HyperBlocks via a Williamson coupling reaction is unchanged,[8] experience suggests that solvent choice and solubility of the macromonomer will be crucial. Having investigated several solvents for the coupling of polystyrene macromonomers, DMF emerged as the most appropriate choice – provided the temperature was controlled to prevent degradation of the solvent. Dimethylacetamide (DMAc) with a 50/50 mixture (by volume) of tetrahydrofuran (THF) proved the most suitable solvent for the successful coupling of polybutadiene macromonomers (Chapter 3); it was expected that some combination of these solvents would be suitable for HyperBlock reactions.

5.2.2.1 Effect of Solvent, Solution Concentration and Temperature.

A series of coupling experiments were carried out to ascertain the optimal solvent and temperature choice for the successful coupling of the ABA polystyrene-b-polyisoprene-b-polystyrene macromonomer into HyperBlocks.

An initial reaction (HBlock 1) carried out at room temperature in DMF resulted in no significant coupling (Table 5.2). HyperBlock 1 had a Dp_n of 1.4, a Dp_w of 2.5. Since the composition of the macromonomer is approximately 40% PS the incorporation of the polyisoprene block into the macromonomer made them less soluble in DMF. Addition

of THF (a good solvent for both polyisoprene and polystyrene) in a 50:50 ratio to DMF at an elevated temperature of 40°C (HBlock 2) resulted in improved solubility whilst still maintaining a high polarity environment required for the Williamson coupling reaction to proceed. The extent of coupling was slightly improved with a value of Dp_n of 2.7 and Dp_w of 5.1 however the reaction didn't proceed to the extent seen for pure polystyrene HyperMacs (Chapter 2).

Sample	Solvent	Temp. (°C)	Conc. (% w/v)	$M_n(gmol^{-1})$	Dp_n	$M_w(gmol^{-1})$	Dp_w	PDI
HBlock 1	DMF	20	20	65500	1.4	137900	2.5	2.1
HBlock 2	50:50DMF/THF	40	20	125000	2.7	280200	5.1	2.2
HBlock 3	50:50DMF/THF	40	10	245900	5.3	619700	11.3	2.5
HBlock 4	50:50DMF/THF	40	5	242700	5.3	654300	11.9	2.7
HBlock 5	50:50DMAc/THF	40	10	129400	2.8	292000	5.3	2.3
HBlock 6	50:50DMAc/THF	40	20	186200	4.0	503000	9.2	2.7
HBlock 7	50:50DMF/THF	50	10	366400	7.9	1780000	32.4	2.7
HBlock 8	50:50DMF/THF	60	10	286400	6.2	1463000	26.6	3.3
HBlock 9	50:50DMF/THF	80	5	285200	6.2	684000	12.5	2.4
HBlock 10	50:50DMF/THF	80	10	154400	3.3	253900	4.6	1.7

Table 5.2 Effect of solvent, temperature and solution concentration on the extent of HyperBlock coupling reactions carried at for 24h. Data obtained by triple detection SEC in THF using a value of dn/dc of 0.185 (polystyrene).

Having previously determined that the solubility of the macromonomer appears to be a major factor and given the limited success of the first two reactions, further modifications were considered. It was assumed that increasing the temperature would increase the rate of reaction and might improve solubility, but could also increase the possibility of inducing undesirable degradation. It was also observed that the high molecular weight and high concentration were resulting in very viscous solutions. So a subsequent reaction was carried out at a lower solution concentration (10% w/v), HBlock 3. Table 5.2 shows that decreasing the solution concentration from 20% to 10 and 5 weight % increases the extent of reaction at 40°C from Dp_w of 5.3 to 11.3. Although the improvements compared to polystyrene HyperMacs[8] were still modest.

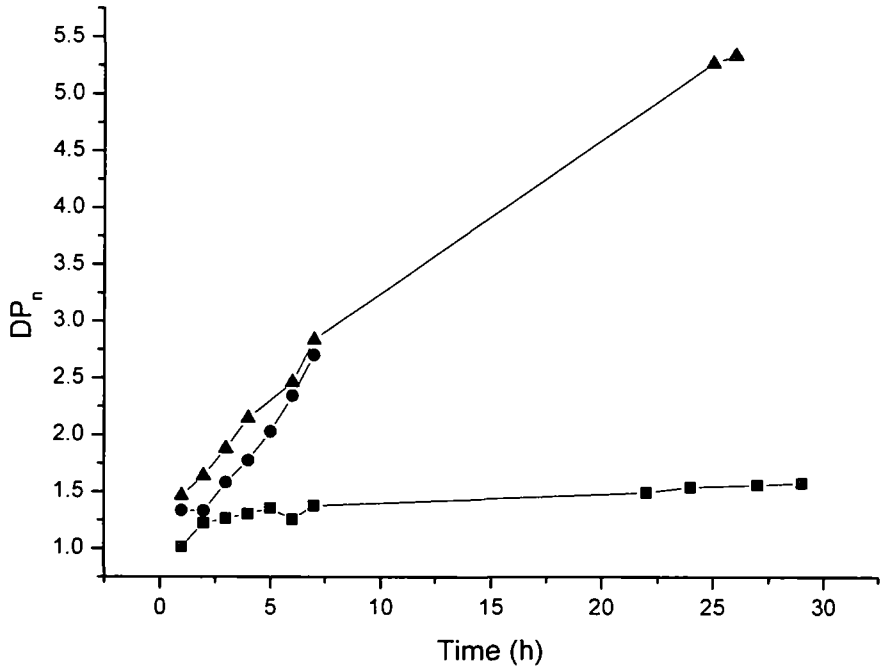

Figure 5.4 Effect of solution concentration on the extent of HyperBlock coupling reactions in 50:50 DMF/THF solutions at 40°C. HBlock 2 ■(20% w/v), HBlock 3 ●(10% w/v) and HBlock 4 ▲(5% w/v).

The data in Figure 5.4 shows that reactions carried out at in 5 and 10% w/v solutions are almost identical while reaction carried out at 20% w/v solution progresses significantly slower. This implies that solubility/viscosity of the macromonomer is one dominant factor in this reaction.

By raising the temperature of the reaction it was anticipated that the extent of reaction would similary increase; therefore further reactions were conducted at 50°C and 60°C (Figure 5.5). The Dp_w values for these reactions (HBlock 7 and 8) were 32.4 and 26.6 respectively – clearly a significant improvement over the reactions at lower temperature of 40°C (Hblock 3) which gave the best results up to this point. The decrease in the Dp_w of HBlock 7 at 50°C after 2 hours is a likely artifact of the reduced solubility of the growing HyperBlock making characterization via SEC difficult, rather than a reduction in molecular weight of the polymer.

The values of Dp_w of 32.4 and 26.6 showed a significant improvement over all reactions up to this point and are comparable with the original polystyrene HyperMacs.[8] Increasing the temperature further to 80°C gave values of Dp_w of around 12 (HBlock 9), somewhat disappointing in respect of the extent of the reaction. One explanation for this result at the highest temperature (80°C) is loss of THF from the reaction vessel, which

would decrease the solubility, retarding the extent of the coupling reaction. The materials obtained at 50 and 60°C were perfectly acceptable for further characterisation studies.

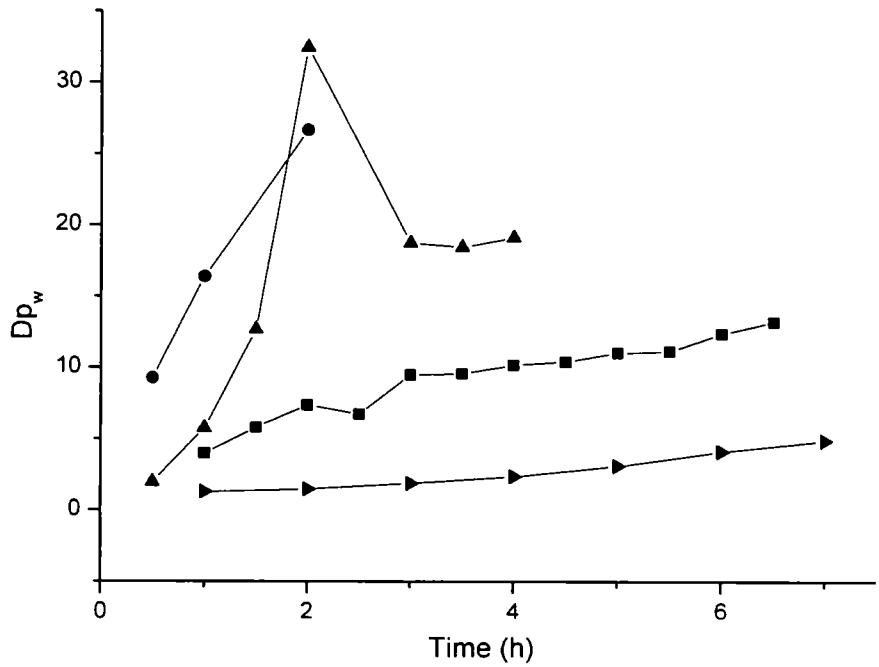

Figure 5.5 Effect of temperature on the extent of HyperBlock coupling reactions in 50:50 DMF/THF at 10% w/v solutions. HBlock 10■ (80°C), HBlock 8● (60°C), HBlock 7 ▲ (50°C) and HBlock 3 ► (40°C).

Determining the optimal reaction concentration of 10% w/v and temperature of 50°C, the next parameter investigated was the coupling solvent. HyperMacs constructed from polybutadiene were prepared successfully in 50:50 volume blend of N,N-Dimethylacetamide (DMAc) and tetrahydorfuran (THF) at 10 weight % solutions (Chapter 3). The syntheses of HBlock 5 and 6 were carried out in this mixed solvent. Dp_w values of 5.3 and 9.2 for these reactions were lower than reaction in the 50:50 DMF/THF blends used in HBlock reactions 2, 3 and 4. No real benefit was observed using DMAc rather than DMF, therefore the original 50:50 blend of DMF/THF was used as the default coupling solution.

5.2.2.2 Scale up of HyperBlock Synthesis.

In order to characterise the physical properties of HyperBlocks it was necessary to carry out a larger scale coupling reaction to produce sufficient material for a full set of characterization experiments on one batch of polymer. The synthetic route to HyperBlock macromonomers can easily be scaled up to allow the synthesis of batches of around 50 grams. A coupling reaction (Table 5.3) was subsequently conducted on a moderately large scale of ca. 20 grams under the optimal conditions established above (50:50 DMF/THF 10% w/v solutions with Cs_2CO_3 at 50°C).

Sample	M_n ($gmol^{-1}$)	Dp_n	M_w($gmol^{-1}$)	Dp_w	PDI
HBlock 12	287700	6.3	1363000	24.8	4.7

Table 5.3 Large scale HyperBlock coupling reaction at 24h constructed from the macromonomer in Table 5.1. (SEC data obtained by triple detection SEC in THF using a value of *dn/dc* of 0.185 (polystyrene)).

The extent of the coupling in HBlock 12 reaction in Table 5.3 is not quite as high as the best small scale reaction (HBlock 7 Dp_w 32.4, Table 5.2) under identical reaction conditions. However the degree of coupling is more than adequate.

5.3 Characterisation of Physical Properties of HyperBlocks.

In this section HBlock 12 (Table 5.3) was characterized using a wide variety of techniques with a view in particular of gaining some insight into the effect of the branched architectures on the properties of block copolymeric HyperBlocks. These included differential scanning calorimetry (DSC), dynamic mechanical analysis (DMA), small angle x-ray scattering (SAXS) and transmission electron microscopy (TEM).

5.3.1 Commerical Thermoplastic Elastomers.

Commercially available thermoplastic elastomers prepared by the anionic polymerization of polystyrene and polyisoprene (linear and star-branched) were obtained from Kraton Polymers (Table 5.4). These materials provide useful comparisons to the HyperBlock polymers prepared in this project.

	Kraton Linear	Kraton Star
Manufacture Code	D-1160	D-1124P
M_n ($gmol^{-1}$)[a]	145700	97400
M_w ($gmol^{-1}$)[a]	164600	148800
PDI[a]	1.13	1.28
M_n ($gmol^{-1}$)[b]	99200	73500
M_w ($gmol^{-1}$)[b]	123500	156500
PDI[b]	1.25	1.50
Polystyrene Content (%w)	17.4 to 20.5	28.4 to 31.6
Elongation at Break (%)	1300	1100
Tensile Strength (MPa)	32	14.5

Table 5.4. Molecular characteristics of commerical available thermoplastic elastomers obtained from Kraton Polymers.[13]

[a] SEC data using conventional calibration.[10a]

[b] SEC data obtained by triple detection SEC in THF using a value of dn/dc of 0.185 (polystyrene).[10a]

5.4 Thermal Analysis.

Thermal analysis is used to investigate the properties of a polymer as a function of temperature. Various techniques (discussed below) exist for the characterisation of block copolymers to obtain the glass transition temperature(s) (T_g); a point where amorphous polymers change from a brittle to pliable structure.[14] The two main techniques used for thermal analysis are differential scanning calorimetry (DSC) which uses small changes in heat capacity to investigate these types of transitions and dynamic mechanical analysis (DMA) which measures changes in mechanical properties with temperature.

5.4.1 Differential Scanning Caliorimetry (DSC) of HyperBlocks.

A typical example of a DSC thermogram of a polystyrene/polyisoprene HyperBlock macromonomer is shown in Figure 5.6. Two thermal transitions are clearly observed

corresponding to the low temperature polyisoprene transition (-73°C) at -60°C and the smaller high temperature polystyrene transition (110°C) at 94°C (numbers in brackets literature glass transition temperatures).[14]

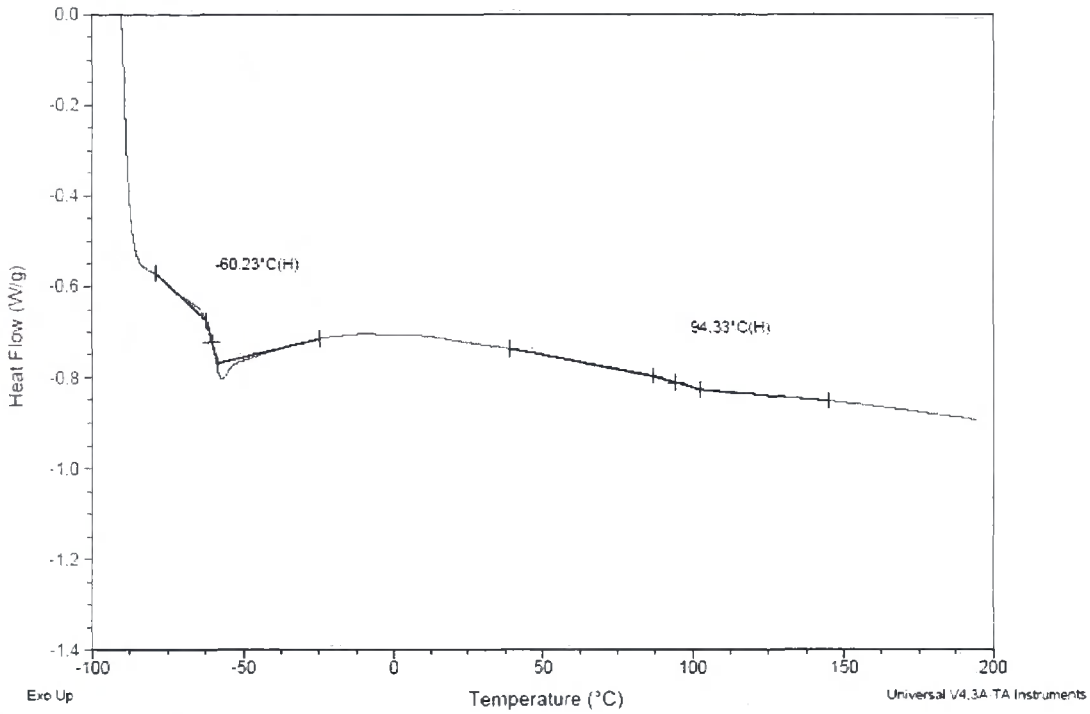

Figure 5.6 DSC thermogram from SIS HyperBlock macromonomer.

The discrepancy between the temperatures of the observed transitions and the literature values particularly that of the polyisoprene, should be noted. The elevation in this value is likely due to the variable polyisoprene microstructures the; literature reports T_gs for 1,4-cis polyisoprene as -70°C, 1,4-trans polyisoprene as -63°C and 1,2-polyisoprene as -7°C.[15] Anionic polymerisation of isoprene in benzene results in mainly (~65%) 1,4-cis polyisoprene[16] which would favour the lower T_g value for the HyperBlock and macromonomer materials. The (~28%) 1,4-trans polyisoprene could account for the observed increase in the polyisoprene T_g due to the relatively high values obtained for the purely 1,4 trans material, as well as the influence due to the 7% 1,2 polyisoprene constituent. There are undoubtedly many other influences on the glass transition values observed in these materials, probably the major one being the other polymer block in the material. This theory is demonstrated more clearly for the commercial Kraton polymers (Table 5.5) that show a significant decrease in values of up to 45°C in the polystyrene transition in the Kraton linear material with a significantly low (18.7%) content of polystyrene. The literature reports this phenomenon, hypothesising dynamic

interactions between the two polymer microdomains, where smaller separate domains are created that decrease the observed polystyrene T_g. More simply the movement of polyisoprene in the block copolymer above its T_g is transmitted to the polystyrene at polymer interfaces, lowering the T_g value.[17] Kim et al.[18] come to similar conclusions as Morèse-Sèguèla[19], as they also observe a reduction in the polystyrene T_g for a series of polyisoprene/polystyrene block copolymers.

Sample	Description	Low T_g (°C)	High T_g (°C)	Styrene %
1st PS Block Macromonomer 1	PS 1st block	-	98	100
PS-PI Block Macromonomer 1	PS-PI 2nd block	-59	78	27
HBlock macromonomer 1	Macromonomer	-60	94	40
HyperBlock HBlock 12	HBlock 12	-52	103	40
Kraton Star	Commercial SIS (Kraton) Star	-55	74	31.6
Kraton Linear	Commercial SIS (Kraton) Linear	-57	65	18.7

Table 5.5 DSC T_gs from constituent parts of HBlock 12 and commercial Kraton materials.

The effect of the polymer constituents on the T_gs of diblock copolymer of linear materials has been described above; however polymer architecture must also play a roll. Glass transitions determined using DSC are dependent on small endothermic transitions caused by the increase in motion and the free volume associated with each polymer chain end. In HyperBlock macromonomers, the polyisoprene has no free chain ends as they are bonded to the polystyrene constituents. It is likely that the polyisoprene will influence the movement of the polystyrene polymer chain ends and alter (decrease) the T_g values associated with the material, more clearly seen in the Kraton linear materials (Table 5.5).

Coupling macromonomers into HyperBlocks introduces branching into these materials which constrains the polystyrene macromonomer chain ends. Significantly the polystyrene T_g values have a difference of 9°C between the macromonomer and HyperBlock architectures with the same polystyrene content. This demonstrates the influence of branching and polymer chain ends on these thermal transitions, as a higher

temperature is required for the movement of a reduced number of chain ends in the branched material, increasing the glass transition temperature.

The reverse trend is observed for the commercial Kraton materials (Table 5.5) as the star polymer, with more chain ends, has a higher upper T_g value than the linear material with fewer chain ends. Undoubtedly the polystyrene content of the commercial polymers is different (~10%) which combined with changes in architecture make comparative investigation into branching effects on commercial materials difficult.

DSC relies on relatively small changes in heat flow/capacity for determining T_g values, hence more sensitive techniques investigating the thermomechanical properties of these phase separated materials has been used for further characterization.

5.4.2 Dynamic Mechanical Analysis (DMA) of HyperBlocks.

The DSC analysis in the previous section clearly identified the glass transition temperature of the polyisoprene, the glass transition temperature of the polystyrene blocks were sometimes difficult to identify with confidence, therefore a complementary technique was used.

Dynamic mechanical analysis (DMA) is often far more sensitive for the detection of glass transition temperatures (T_gs) as it relies on changes in the mechanical properties of the materials rather than the changes in heat capacity, as in the case of DSC.

DMA involves sinusoidally applying stress to a sample and recording dynamic storage moduli (E′) and dynamic loss moduli (E″), corresponding to the ability to store and dissipate energy by the material. The phase angle is the loss modulus divided by the storage modulus ($\tan\partial = E''/E'$) with peaks corresponding to phase transitions which include glass transition temperatures. A typical DMA trace is shown in Figure 5.7.

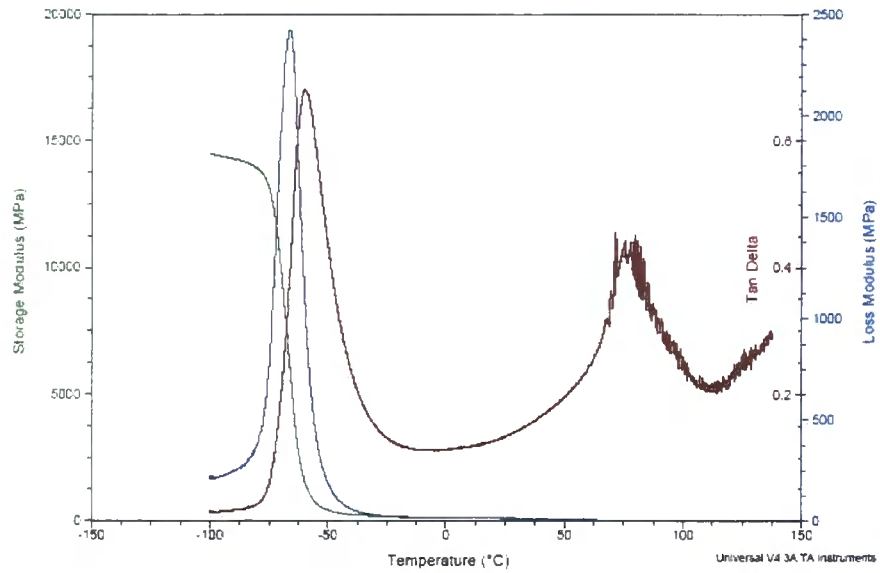

Figure 5.7 DMA trace from HyperBlock HBlock 12.

Figure 5.7 shows two peaks in the tan delta curve, the lower around -65°C and the upper around 75°C corresponding to the T_gs of polyisoprene and polystyrene.[14] The presence of two distinct peaks indicates the polymer blocks are phase separated corresponding to the constituent polymers.

The DMA results (Table 5.6) compare well with those in Table 5.5 from the DSC, apart from the upper polystyrene glass transition temperature which at 75 °C is 28°C lower than previously observed. This artifact is likely due to the effect of branching on the HyperBlock in relation to the reduction of the number of chain ends which influence the DSC thermal analysis.

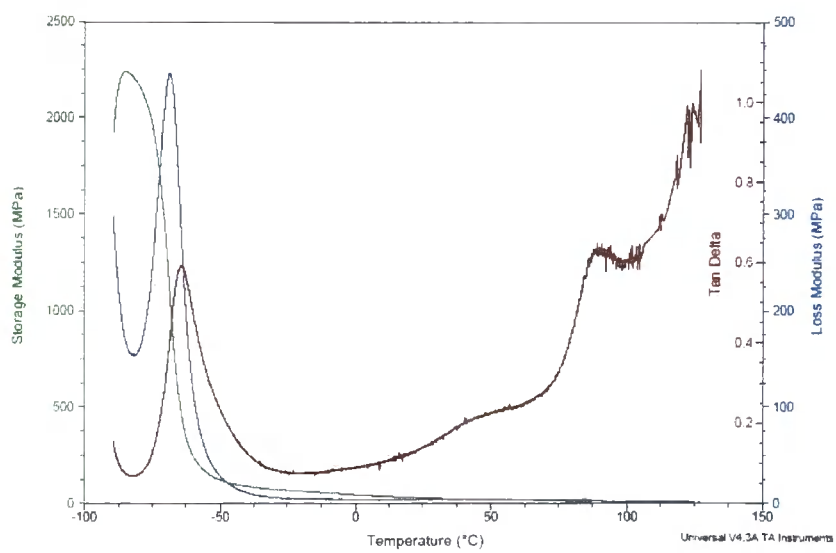

Figure 5.8 DMA data from Kraton Star.

Figure 5.8 shows the commercial Kraton star sample. The two peaks in tanδ appear for the polyisoprene and polystyrene glass transitions, but significantly a very broad peak is observed between approximately 10 °C and 60°C. The origin of this peak could be imperfections in the star architecture; for example block copolymers with variable polystyrene content and/or architecture. This feature, combined with the depressed upper T_g, agrees with the hypothesis of the creation of small interactions at the interface between polymer domains which cause the reduction in the polystyrene T_gs observed[17] due to more polyisoprene character being present.

Sample	T_{g1} (°C)	T_{g2} (°C)
HBlock 12	-55	75
Kraton Linear	-64	73
Kraton Star	-71	80

Table 5.6 Glass transition temperature from DMA experiments. (T_gs observed from the peaks in tan delta where $\tan\partial = {}^{E''}/_{E'}$.)

Values in Table 5.6 indicate the depression of the upper (T_g2) glass transition temperatures in all of the samples compared to the DSC results in Table 5.5, however the third broad peak observed in the commercial star material is not clearly seen in the two other samples.

In agreement with the DSC (Table 5.5), the DMA results shows phase separated materials in each case with two distinct glass transition temperatures corresponding to the glass transition temperatures for each of the constituent polymers. Slight variation in these temperatures occurs according to block constituents, microstructures and architectures.

Clearly further characterization using techniques such as transition electron microscopy (TEM) could allow more insight into the morphologies of the materials described above.

5.5 Small Angle X-ray Scattering (SAXS)

SAXS is used to characterize macroscopically ordered materials and is a technique to help determine the morphology in structured materials. Whilst TEM gives a visual guide to the morphology, SAXS relies on the scattering of X-rays for characterization.

The technique uses a monochromatic x-ray beam which irradiates a sample at relatively small angle (typically <10°) causing scattering from the material, creating signals for the detector. Data analysis uses Bragg's Law for structure determination:

$$q = 4\pi Sin\theta / \lambda$$

where, q = scattering vector, 2θ = angle between x-ray beam and detector and λ = wavelength of x-rays.

After the application of Bragg's Law, data takes the form shown in Figures 5.9, 5.10 and 5.11 from which peaks may be assigned corresponding to structural features in the materials. For example scattering from Kraton linear materials (Figure 5.9) suggests a cylindrical based morphology:

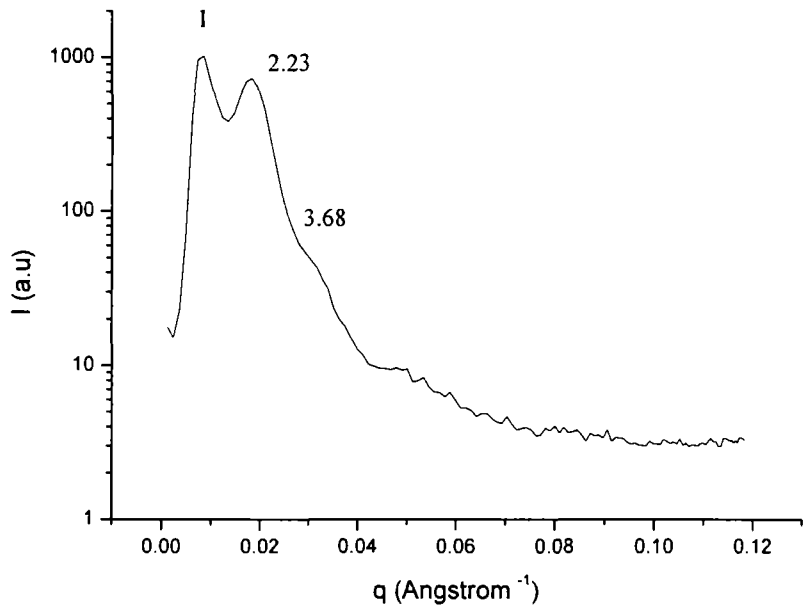

Figure 5.9 SAXS scattering from Kraton linear material.

The three peaks in the trace above indicate the material is not disordered as scattering is seen from ordering in the material. The numbers shown above the peaks in the SAXS data (Figures 5.9, 5.10, 5.11) correspond to possible reflections from Bragg spacing. The ratios of the initial peak with the lowest scattering angle, q*, and subsequent peaks q_n, where $PeakRatio = q_n / q^*$ correspond to a series of peaks in the scattering pattern characteristic of the lattice symmetry and can be used for morphology determination[17]. In the case of the Kraton linear material (Figure 5.9) this corresponds reasonably well with hexagonally packed cylindrical morphology, derived from the 1, 1.83, 2.65, 3.48,

4.30... Bragg scattering pattern, although the absence of the second peak in the expected range is puzzling.[18]

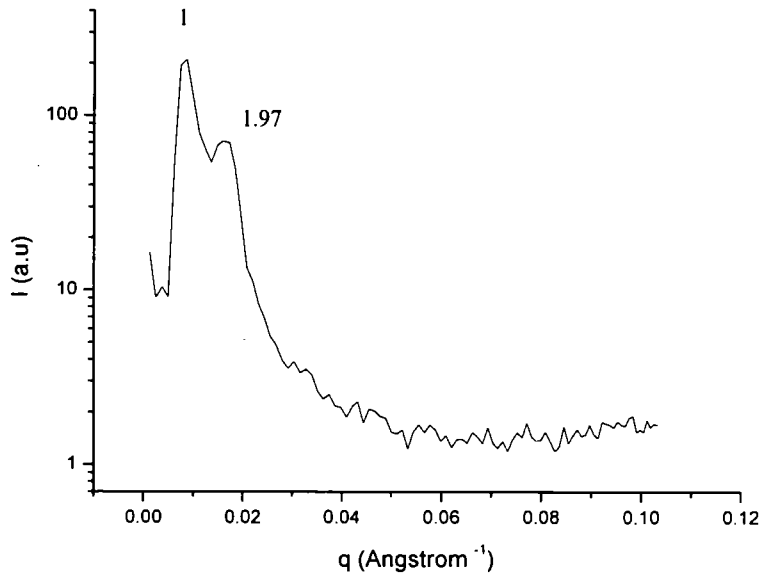

Figure 5.10 SAXS scattering from Kraton Star polymer.

The scattering of the Kraton star sample in Figure 5.10 shows two distinct reflections at 1 and 1.97, suggesting some ordering in the material at lower q values. The branched architecture of the star sample appears to be less ordered than the linear material from the SAXS scattering patterns. Using the two reflection peaks to estimate the morphology also suggests a hexagonal cylindrical structure, although undoubtedly more observed scattering peaks would make this assignment more robust.

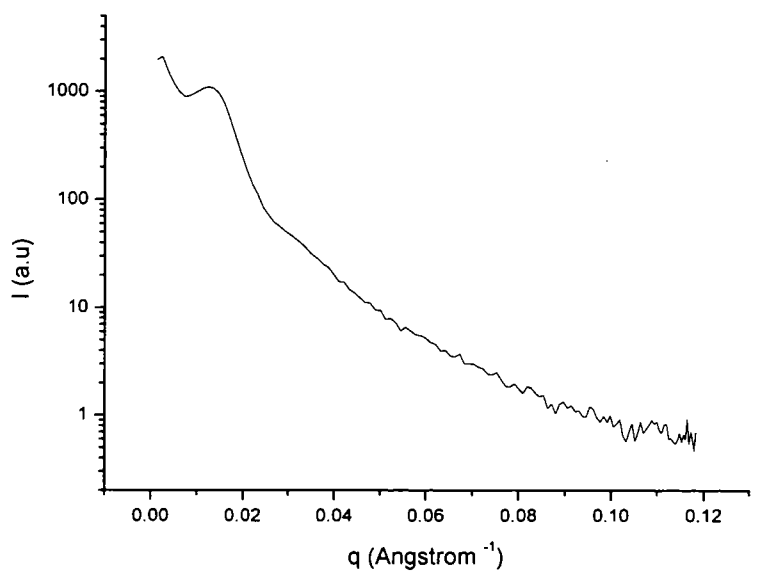

Figure 5.11 SAXS scattering from HyperBlock HBlock 12.

Figure 5.11 shows the scattering from a HyperBlock synthesized in house. The presence of a weak peak around 0.018 q (Angstrom^{-1}) suggests the HyperBlock exhibits a focal point ordering only, with no long range ordering. This is unsurprising as coupling linear ABA triblock macromonomers into HyperBlocks is likely to disrupt any order present due to the branched architecture.

5.6 Transition Electron Microscopy (TEM).

The morphologies of the Kraton materials and HyperBlocks were explored using TEM, typical data is shown in Figures 5.12, 5.14, 5.16 for the Kraton linear, branched and HyperBlock block copolymers.

Samples for TEM were solution cast from toluene (3% w/v) onto aluminum plates which were dried at room temperature for 14 days, and then annealed at 393 K for 7 days to equilibrate the morphologies. Samples were prepared for imaging by cryo-ultramicrotomy and stained with osmium tetroxide.

Block copolymer composition is one of the dominant factors influencing polymer morphologies and therefore it is important to consult Table 5.1 and 5.5 for the corresponding content. The polystyrene content is approx 20% for the Kraton linear polymer (Figure 5.12), 30% for the Kraton branched polymer (Figure 5.14) and 40% for the HyperBlock (Figure 5.16).

Figure 5.12 shows Kraton linear material is microphase separated with a small degree of short range ordering. The morphology is likely to be hexagonally packed cylindrical morphology due to the low polystyrene content of around 17.4 - 20%. Nevertheless this material is clearly significantly more disordered than one would expect from a linear triblock – this could be due to poor sample preparation, or contamination with diblock copolymers or other impurities from the manufacturing process, however regions of order can be seen.

The phase diagram of ABA triblock copolymer melts (Figure 5.13) is reported by Matsen[22, 23] where symmetric and asymmetric ABA triblocks are considered using self-consistant field theory. It is noted that although the diblock and triblock materials exhibit similar phase behaviour, the extra portion of block in a triblock means mechanical properties can be improved with bridging polymer segments which impart strength into the structure.

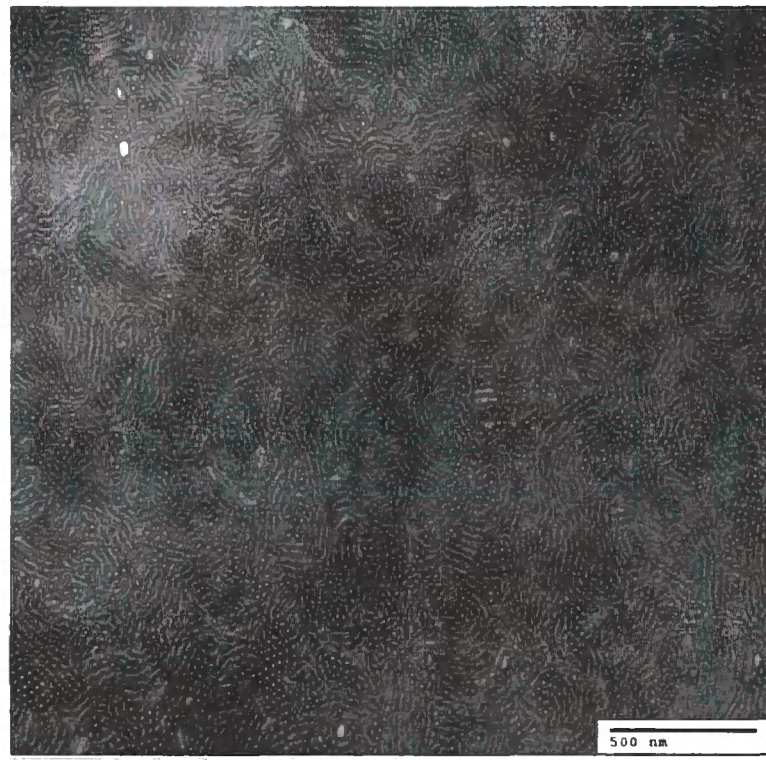

Figure 5.12 TEM image of Kraton Linear.

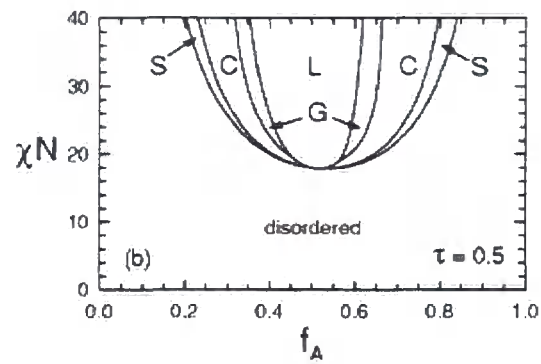

Figure 5.13 Phase diagram of a symmetric ABA block copolymer. S = spherical, C = cylindrical, G = gyroid and L = lamellar morphologies. Plotted in terms of χN segregation (Flory interaction parameter χ for polymer is 0.141 and N is the degree of polymerization)and f_A volume fraction from SCFT calculations. [22] Reproduced with permission from M.W. Matsen, J. Chem. Phys. 113, 5539 (2000). Copyright 2000 American Institute of Physics.

The commercial star polymer (Figure 5.14) clearly shows a cylindrical morphology as indicated by the circles of polystyrene in a polyisoprene matrix transverse to material appearing to be of a lamellar structure. The higher polystyrene content (~30%) in this material clearly pushes the morphology of the material into the cylindrical regime (Figure 5.13). Compare this to the Kraton linear material (Figure 5.12) where a less ordered (disordered) morphology is observed, and indeed predicted,[22] with a

polystyrene content of ~20%. This demonstrates the polystyrene content, as well as the χ value and architecture are the main driving forces for the observed morphologies in the TEM images. Undoubtedly the branching when comparing the commerical star with linear polymers must affect the structures observed in these materials, but with changes in both polystyrene content and polymer architecture means this can only be speculated.[4]

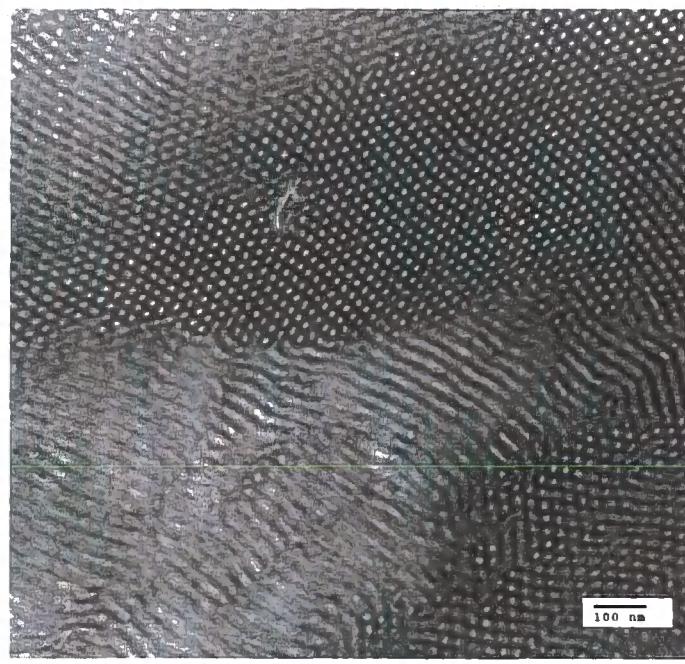

Figure 5.14 TEM image of Kraton Star.

Whilst Figures 5.12 is not of particularly good quality, the morphologies observed in the two commercial materials favourably agree with the SAXS data in Figures 5.9 and 5.10. The general trend from the materials appears to be a phase separated cylindrical morphology showing reasonable long range order. Kraton polymers are used as adhesives and bitumen modifiers, both classical applications of thermoplastic elastomers, where both strength and flexibility are required. A cylindrical morphology as seen in the two Kraton materials (Figures 5.12 and 5.14) logically suggests improved mechanical properties from this morphology[1] as the diene matrix provides flexibility whilst the polystyrene cylinders provide the strength for the desired material properties. This suggests Kraton polymers are designed for cylindrical morphologies with commercially desirable properties.

Comparison of the PS-PI-PS macromonomer and HyperBlock (with identical polystyrene composition) allows an investigation into the effect of branched architecture upon morphology.

Figure 5.15 shows TEM of the triblock copolymer macromonomer which shows a cylindrical morphology of polystyrene cylinders in a matrix of polyisoprene; clearly seen by the cylinders in head-on orientation in the upper central part of the figure, and side on in much of the figure. Although the cylinders of polystyrene are clearly distinct the distance between cylinders is relatively small suggesting that for this block copolymer composition the morphology is on the cusp of cylindrical and lamellar structure.

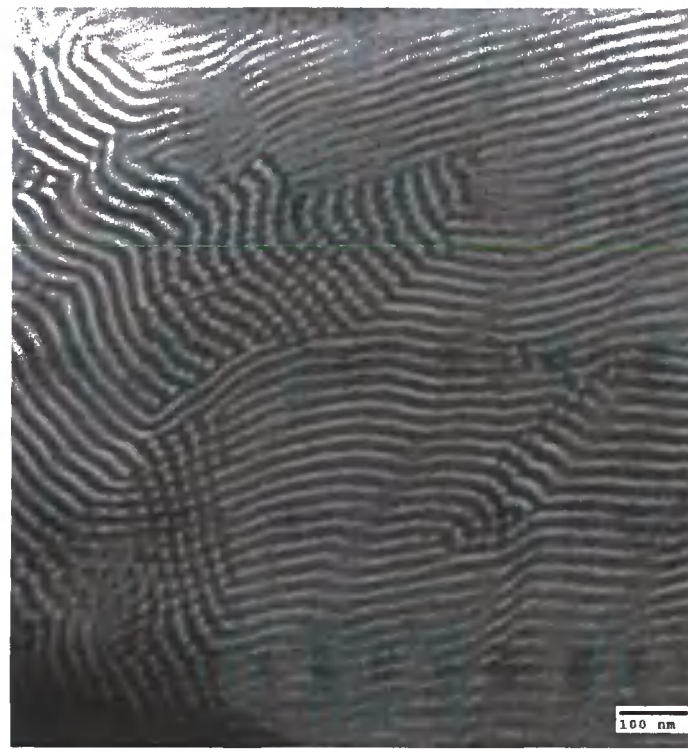

Figure 5.15 TEM of ABA HyperBlock Macromonomer.

The cylindrical morphology of the HyperBlock macromonomer suggests, as it has been seen for the two commercial Kraton polymers, that the structures formed due to the polystyrene content of the material would have desirable mechanical strength.

Coupling of the HyperBlock macromonomer into a HyperBlock results in a change in the observed phase separated morphology from a long range cylindrical structure to a much more disordered state. Comparing the two TEM micrographs (Figures 5.15 and 5.16), the HyperBlock structures show no long range order in agreement with the SAXS

data, compared to that seen for the macromonomer. Clearly, and as shown previously in the commercial Kraton materials, the volume fraction of polystyrene was seen to have a big influence over the block copolymer morphology. However it is equally clear that the highly branched molecular architecture also plays a major role in determining morphology. Undoubtedly the assembly of cylindrical morphology is thermodynamically favourable, but the constraints imposed on the system by the branching means this can only be achieved on a much shorter length scale – hence the disorder seen in Figure 5.16.

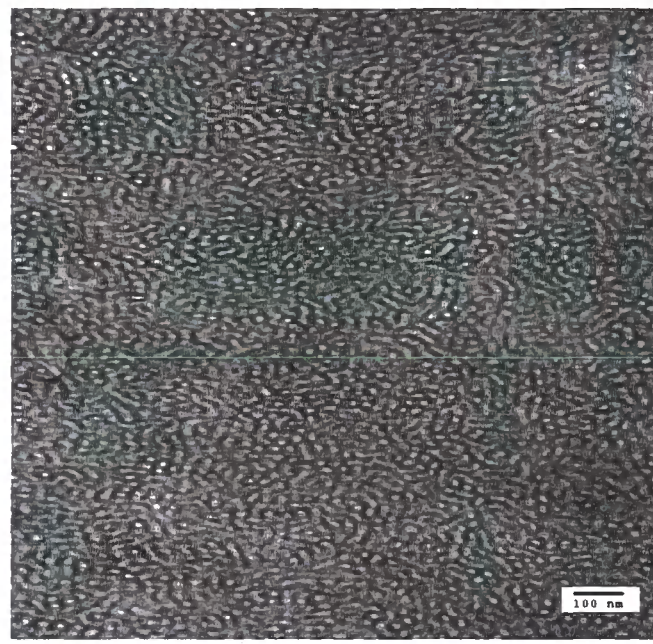

Figure 5.16 TEM of HyperBlock HBlock 12.

Changes in architecture as well as polystyrene content clearly have a role to play in the morphologies of thermoplastic elastomeric materials. Mays et al.[7] (Figure 5.1) describe the introduction of branch points into 'barbed wire' type materials constructed from polyisoprene backbones and polystyrene arms described previously. They reported that increasing the number of branch points along the backbone, for polymers with the same composition, resulted in a decrease in the long range order of the polymer (Figure 5.17). This agrees favourably with the effect of branching on the change from macromonomer to HyperBlock with increasing disorder.

Figure 5.17 shows TEM data for three compositional identical 'barbed wire' branched polymers produced by Mays,[7] each with a different degree of branching. In each case the polymers are clearly phase separated with vastly differing long range order. It is

important to remember that the polymer architectures in Figure 5.17 are the same (as shown in Figure 5.1), only the number of branch points differs.

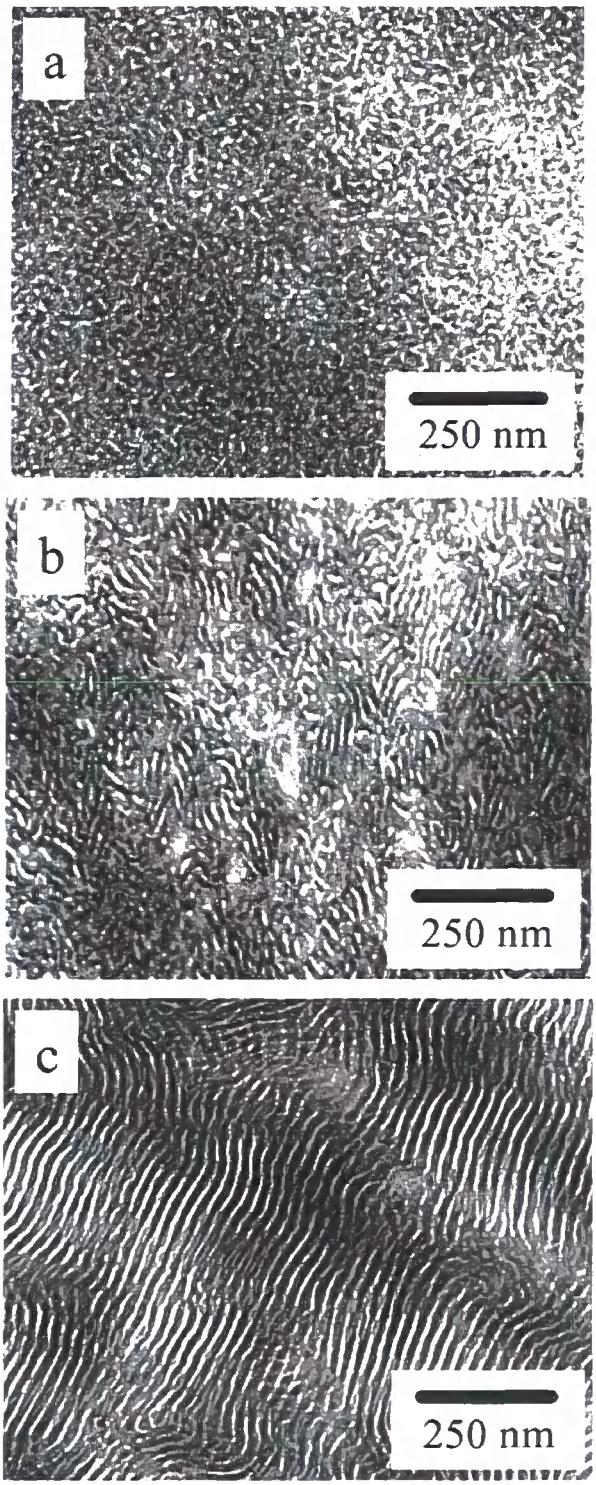

Figure 5.17 TEM images of Polyisoprene/Polystyrene 'barbed wire' polymers with increasing number of branch points per molecule, composed of 21% PS, with 4 arms grafted from the PI backbone (6 junction point functionality). Number of junction points per molecule (a), 5.3; (b), 3.6; (c), 2.7. Reproduced with permission from Macromolecules, 2006. 39, 4428. Copyright 2006 American Chemical Society.

Sample 'a' in Figure 5.17 is phase separated with limited ordering as it is the most highly branched material in this series, and bears a striking resemblance to the HyperBlock material shown in Figure 5.16. Sample 'b' shows disordered lamellar structures as the branching decreases, and more ordered lamellar structures are seen in sample 'c'. These barbed wire materials show some similarities with the HyperBlocks; increasing the branching of the materials reduces the long range order seen in the TEM images in Figure 5.17. Sample c in the figure shows well-ordered lamellar or cylindrical structures with a small amount of branching (2.7 junction points per molecule), demonstrating that branching can exist in ordered morphologies under certain conditions. An important point to note when comparing these materials is that the HyperBlock and macromonomer materials are branched and linear, whereas the Mays materials are all branched to different degrees, with differing numbers of branches, functionality and composition.

5.7 HyperBlocks Summary/Conclusion.

HyperBlocks constructed from macromonomers offer unique control of copolymer composition between branch points in HyperMac polymers. The ability to characterize both linear and highly branched polymers with the same copolymer composition enables the effect of branching on morphology to be investigated without concern for changes in polymer composition.

Clearly it has been seen that in the case of polystyrene/polyisoprene ABA copolymers and HyperBlocks that polystyrene content is a major factor in determining the morphology observed for each material. Branching is seen to reduce the extent of the ordering and to dominate the morphologies observed in the TEM images of the HyperBlocks, Kraton star polymers and 'barbed wire' materials.

HyperBlocks show promise as thermoplastic elastomers (TPEs) as the polystyrene content can promote the favoured cylindrical morphology of the macromonomers, whilst the HyperBlocks still retain a phase separated morphology but in a disordered state. The ability for HyperBlocks to be controlled in composition and branching, as well as introducing covalent bonds between polymer chains suggests a combination of the advantages of both linear and star TPEs in HyperBlock materials. HyperBlocks are therefore likely to have improved strength and durability compared to linear and branched TPEs available today.

5.8 References.

1. Hsiech H.L., Quirk R.P. Anionic Polymerisation: Principles and Practical Applications. Marcel Dekker, New York, 1996.
2. Kraton Polymers technical booklet 'Introduction to polymers', 2008.
3. Puskas J.E., Kwon Y., Anthony P., Bhowmick A.K. *J. Polym. Sci. A: Polym. Chem.* 2005, 43, 1811.
4. Iatrou H., Hadjichristidis N., *Macromolecules*, 1993, 26, 2479.
5. Pochan D.J., Gido S.P., Pispas S., Mays J.W., Ryan A.J., Fairclough P.A., Hamley I.W., Terrill N.J. *Macromolecules*, 1996, 29, 5091.
6. Weidisch R., Gido S.P., Uhrig D., Iatrou H., Mays J.W., Hadjichristidis N. *Macromolecules*, 2001, 34, 6333.
7. Zhu Y., Burgaz E., Gido S.P., Staudinger U., Weidisch R., Uhrig D., Mays J.W. *Macromolecules*, 2006, 39, 4428.
8. Hutchings, L.R., Dodds, J.M., Roberts-Bleming S.J. *Macromolecules*, 2005, 38, 5970, and Clarke N., De Luca E., Dodds J.M., Kimani S.M., Hutchings L.R. *Euro. Polym. J.*, 2008, 44, 665.
9. Lopez-Villanueva F., Wurm F., Kilbinger A.F.M, Frey H. *Macromol. Rapid Commun.* 2007, 28, 704.
10. a) Obtained from Viskotek technical literature. b) Calculated in house.
11. Tanaka Y., Takeuchi Y., Kobayashi M., Tadokoro H. *J. Polym. Sci A2*, 1971, 9, 43.
12. Armarego, W.L.F.; Perrin, D.D. Purification of Laboratory Chemicals; Butterworth-Heinemann: Oxford, 1996.
13. Kraton Polymers technical publications for polymer. Data sheets D-1160 and D-1124P.
14. Hatakeyama T., Quinn F.X. Thermal Analysis. Fundamentals and Applications to Polymer Science. 2nd Edition. John Wiley and Sons, Chichester. 1994.
15. Larson R.G. 'The Structure and Rheology of Complex Fluids'; OUP, Oxford, 1999.
16. Boyer R.F. *Macromolecules*, 1992, 25, 5326.
17. Park T., Park K., Chang T. *Polymer (Korea),* 1992, 16, 1, 79.
18. Han C.D., Baek, D.M., Kim J.K. *Macromolecules*, 1995, 28, 5886.

19. Morèse-Sèguèla B., St-Jacques M., Renaud J.M., Prud'homme J. *Macromolecules*, 1980, 13, 100.
20. Xu F., Li T., Xia J., Qiu F., Yang Y. *Polymer*, 2007, 48, 1428.
21. Förster S., Timmann A., Konrad M., Schellbach C., Meyer A., Funari S.S., Mulvaney P., Knott R. *J. Phys. Chem. B*, 2005, 109, 1347.
22. Matsen M.W. *J Chem. Phys.*, 2000, 113, 13, 5539.
23. Matsen M.W., Thompson R.B., *J. Chem Phys*. 1999, 111, 15, 7139.

6. Experimental

6.1 Materials.

6.1.1 HyperMac Synthesis.

Benzene (HPLC grade, Aldrich) and styrene (Aldrich) were both dried and degassed over CaH_2 (Aldrich; ≥ 97.0% powder), styrene was further purified with dibutylmagnesium immediately prior to use. *N,N,N',N'*-Tetramethylethylenediamine (Aldrich) and 3-*tert*-butyldimethylsiloxy-1-propyllithium, 0.7 M in cyclohexane (InitiaLi 103, FMC corporation) were used as received. 1,1-*Bis*(4-*tert*-butyldimethylsiloxyphenyl)ethylene was synthesised in two steps from dihydroxybenzophenone according to the procedure of Quirk and Wang[1]. DCM (dichloromethane) (Innovative Technology Inc. solvent purification system), methanol (Fischer, AR grade.), PPh_3 (triphenyl phosphine), (Aldrich, 99%), CBr_4 (carbon tetrabromide), (Aldrich, 99%), Cs_2CO_3 (cesium carbonate), (Aldrich, 99.995%) , K_2CO_3 (Aldrich, 325 mesh), thionylchloride (99+%, Aldrich), pyridine (anhydrous, Aldrich), THF (Aldrich, anhydrous 99.9%), DMF (dimethyl formamide) (Aldrich, ≥ 99.9%), NMP (Aldrich, biotech grade ≥99.5%), DMAc (Aldrich, 99%) were used as received. 4 Angstrom molecular sieves (Aldrich) were activated before use.

6.1.2 Core HyperMacs.

B_3 core (1,1,1,-tris(4-hydroxyphenyl)ethane) (Aldrich, 99%) was used as received. All other materials were used as reported in the previous material section.

6.1.3 SIS/ Polybutadiene HyperMacs.

Isoprene (Aldrich, 99%) was freshly distilled from CaH_2, 1,3-butadiene (Aldrich, 99+%) was purified by passing through columns of Carbosorb (Aldrich), BHT (3,5-di-t-butyl-4-4-hydroxytoluene) (Aldrich, 99%) were used as received. All other materials were used as reported in the previous material sections.

6.2 Synthetic Procedures.

6.2.1.1 Anionic Polymerisation of Polystyrene AB_2 Macromonomers.

Synthesis of macromonomers was achieved using anionic polymerisation in a 'christmas tree' reaction vessel (Figure 6.1) under standard high vacuum conditions[2].

Figure 6.1 Christmas tree vessel used for anionic polymerisation.

The synthesis of polystyrene HyperMacs has been previously reported by Hutchings and Dodds,[3] with improvements and modifications to this synthetic route described in this chapter.

A typical polymerisation is as follows; benzene (500ml) and styrene (45g, 0.48mol) were freshly distilled under vacuum into a 1-litre reaction flask. To the monomer solution tetramethylethylenediamime (TMEDA) in 1 molar equivalent with respect to initiator, and then the initiator, 3-tert-butyldimethylsiloxy-1-propyllithium in 0.7M cyclohexane, was injected into the solution. For a target M_n = 15000 $gmol^{-1}$, 0.45 ml (3 mmole) of TMEDA and 4.26ml (3 mmole) initiator were used. Addition of the initiator resulted in the deep red colour of living polystyryllithium. The reaction was stirred at room temperature for 1 hour

before the addition of a 1.5 molar excess (with respect to initiator) solution of 1,1-bis(4-tert-butyldimethylsiloxyphenyl)-ethylene (functionalized DPE) as a solution in benzene was added to the living polymer solution. The reaction was stirred at room temperature for 5 days and the reaction terminated with nitrogen sparged methanol. The polymer was precipitated into a 10 volume excess of methanol, redissolved in benzene and precipitated for a second time into methanol before being dried under vacuo. Yield > 95%. M_n 19200 $gmol^{-1}$, M_w 20700 $gmol^{-1}$, PDI 1.07. ^1H NMR (500MHz, C_6D_6): CH_2OSi δ 3.36, $HC(Ph)_2$ δ 3.5, $Si(CH_3)_2C(CH_3)_3$ δ 1.0, $ArOSi(CH_3)_2C(CH_3)$ δ 0.1, $CH_2OSi(CH_3)_2C(CH_3)_3$ δ 0.0.

Similar reactions to make further polystyrene macromonomers follow the same procedures, but with varying amounts of reactants:

For a target of M_n 20000 $gmol^{-1}$, 55.21g (0.47 moles) styrene, 0.41ml (0.29mmol) of TMEDA and 3.94 ml of initiator were used. Resulting polymer: M_n 27000 $gmol^{-1}$, M_w 28600 $gmol^{-1}$, PDI 1.05. Yield > 95%.

For a target of M_n 20000 $gmol^{-1}$, 48.94g (0.42 moles) styrene, 0.36ml (0.25mmol) of TMEDA and 3.49 ml of initiator were used. Resulting polymer: M_n 28000 $gmol^{-1}$, M_w 28600 $gmol^{-1}$, PDI 1.02. Yield > 95%.

For a target of M_n 16000 $gmol^{-1}$, 28.75g (0.24 moles) styrene. 0.27ml (0.16mmol) of TMEDA and 3.45 ml of initiator were used. Resulting polymer: M_n 14900 $gmol^{-1}$, M_w 15800 $gmol^{-1}$, PDI 1.05. Yield > 95%.

6.2.1.2 Macromomomer Deprotection.

Deprotection or removal of the tert-butyldimethylsilyl (TBDMS) from the protected macromonomer was achieved using an acid hydrolysis reaction. The protected macromonomer (45.0g, 3.00 x 10^{-3} moles) was dissolved in THF (450ml, 10% w/v solution) and concentrated HCl in a 10:1 molar ratio with respect to macromonomer (37 wt%) (0.009 moles, 9.56ml) was added dropwise to the solution. The solution was then stirred under reflux overnight. The deprodected polymer solution was precipitated into a 10 w/v excess of methanol (4.5L), redissolved into benzene (450ml) and reprecipitated and

dried under vacuo. Yield > 95%. ^{1}H NMR (500MHz, C_6D_6): CH_2OH δ 3.15, **HO**-Ph δ 3.7-3.8.

All deprotection reactions were carried out as described, with variations in volumes according to the material quantity.

Macromonomer M_n 27000 gmol^{-1}, M_w 28600 gmol^{-1}, PDI 1.05, mass 57.75g. HCl (0.00639 moles, 6.39ml) Yield > 95%.
Macromonomer M_n 28000 gmol^{-1}, M_w 28600 gmol^{-1}, PDI 1.02, mass 52.19g. HCl (0.00589 moles, 5.59 ml). Yield > 95%.
Macromonomer M_n 14900 gmol^{-1}, M_w 15800 gmol^{-1}, PDI 1.05. mass 29.65g HCl (5.629 x 10^{-3} moles, 5.63 ml). Yield > 95%.

6.2.1.3 Macromonomer Chlorination.

In a 500 ml round bottom flask, 44g of the deprotected macromonomer (20700 gmol^{-1}, 2.125 x 10^{-3} moles) was dissolved in 450ml of benzene under an atmosphere of nitrogen. To this 1.34g pyridine (0.0169 moles, 1.37ml) was added and the mixture stirred for 15 minutes before the solution was cooled to 0°C with an ice water bath. Thionyl chloride 2.52g (0.0212 moles, 1.54ml) was added drop wise to this solution over a period of five minutes. The stirring solution was allowed to warm to room temperature over an hour then heated to 55°C overnight. A small sample was taken for ^{1}H NMR (in C_6D_6), where the CH_2-OH signal (3.15ppm) had been replaced by a signal of CH_2-Cl (2.9ppm). The remaining solution was precipitated into a x10 excess of methanol (4.5L), collected by filtration and redissolved into toluene in a 10% w/v solution (450ml). This solution was passed down an alumina column (20g) to remove residual pyridine or thionyl chloride and precipitated into x10 excess methanol. The polymer was dried to constant mass under vacuo.
Yield > 85%, M_n 19200 gmol^{-1}, M_w 20700 gmol^{-1}, PDI 1.07. ^{1}H NMR (500MHz, C_6D_6): CH_2Cl δ2.9, **HO**-Ph δ 3.7-3.8.

The chlorination of other macromonomers followed the procedure described above. Note that the final macromonomer (M_n 28000 $gmol^{-1}$) batch was halved, one batch being chlorinated and the other brominated.

Macromonomer: M_n 27000 $gmol^{-1}$, M_w 28600 $gmol^{-1}$, PDI 1.05, Mass 54.13g. Pyridine (1.26g, 0.0160 moles, 1.29ml) and thionyl chloride (2.39g, 0.0201 moles, 1.46ml). Yield >90%.

Macromonomer: M_n 28000 $gmol^{-1}$, M_w 28600 $gmol^{-1}$, PDI 1.02. Mass 23.0g. Pyridine (0.52g, 6.57×10^{-3} moles, 1.52ml) and thionyl chloride (0.976g, 8.21×10^{-3} moles, 1.59ml). Yield >90%.

6.2.1.4 Macromonomer Bromination.

Bromination of AB_2 macromonomers is based on a modified Appel reaction[4] described by Baughman et al.[5] All reactions were conducted under high vacuum conditions.

In a 1 litre round bottom flask, 24.3g (1.78×10^{-3} mol) of the 28,000 $gmol^{-1}$ AB_2 macromonomer and a 2.2 molar excess of triphenylphosphine (0.501g, 1.91×10^{-3}moles) was dissolved in 250ml of dried benzene. The deprotected macromonomer was azeotropically dried by distilling the benzene out of the solution and dry benzene into the flask. This procedure was repeated twice to dry the materials, before 250ml (10%w/v solution) of dichloromethane (DCM) was distilled into the flask.

The macromonomer solution was cooled in an ice/water bath and carbon tetrabromide (0.576g, 1.738×10^{-3} mol) added in a solution of dichloromethane. The mixture was stirred at room temperature and the progress of the reaction followed by ^{1}H-NMR (in C_6D_6) until (24 hours) the signal for the CH_2-OH (3.26 ppm) had been completely replaced by a new signal for CH_2-Br at 2.75 ppm. The polymer was recovered in quantitative yield by precipitation into methanol, redissolved and reprecipitated once more, collected by filtration and dried to constant mass in vacuo.

6.2.2. Macromonomer Williamson Coupling Reactions.

Coupling reactions were carried out under an inert atmosphere of either argon or nitrogen. A generic coupling reaction is described below, with modifications being described as the

chemistry evolved. Modifications include altering the reaction temperature, solvent, concentration, leaving group and base, and were all investigated during this project.

6.2.2.1 HyperMac Synthesis.

Initial coupling reactions were based on the chemistry reported by Hutchings and Dodds[2] using polystyrene macromonomers. A typical reaction is as follows:

2.00g of M_n 20000 $gmol^{-1}$ chlorinated macromonomer (1.037×10^{-4} moles), 0.057g (4.148×10^{-4} moles) potassium carbonate and 0.109g (4.148×10^{-4} moles) 18-crown-6 ether were dissolved in 10ml (20% w/v solution) of DMF (Figure 5.2.2). The reaction temperature was raised to reflux and the solution vigorously stirred with a magnetic stirrer. The progress of this reaction was monitored by removing small samples and subjecting the sample to size-exclusion chromatography. The reaction was considered complete when no increase in molecular weight was observed. The mixture was then cooled and precipitated into methanol and dried under vacuo.

Yield 70%, M_n 86700 $gmol^{-1}$, M_w 221900 $gmol^{-1}$, PDI 2.55.

Further reactions were carried out using this standard procedure with the modifications to the reaction scheme described below: It should be noted yields reported below are systematically low due to small samples being taken throughout the course of each reaction.

Chlorinated macromonomer: M_n 20000 $gmol^{-1}$; HyperMac M_n 85700 $gmol^{-1}$, M_w 206400 $gmol^{-1}$, PDI 2.41. Yield 63%.

Chlorinated macromonomer: M_n 20000 $gmol^{-1}$; HyperMac M_n 180900 $gmol^{-1}$, M_w 668400 $gmol^{-1}$, PDI 2.41. Yield 45%.

6.3 Effect of Coupling Solvents.

6.3.1 N-Methyl-Methylpyrrolidone (NMP).

One other possible suitable solvent for this reaction is N-Methyl-Methylpyrrolidone (NMP) Using the original magnetic flee method, NMP was used as a coupling solvent. A typical reaction is as follows:

2.00g of M_n 20000 $gmol^{-1}$ chlorinated macromonomer (1.037 x 10^{-4} moles), 0.057g (4.148 x 10^{-4} moles) potassium carbonate and 0.109g (4.148 x 10^{-4} moles) 18-crown-6 ether were dissolved in 10ml (20% w/v solution) of NMP. The reaction temperature was raised to reflux and the solution vigorously stirred with a magnetic flea. The progress of this reaction was monitored by removing small samples and subjecting the sample to size-exclusion chromatography. The reaction was considered complete when no increase in molecular weight was observed. The mixture was then cooled and precipitated into methanol and dried under vacuo.

Yield 40%, M_n 36300 $gmol^{-1}$, M_w 50200 $gmol^{-1}$, PDI 1.38.

Further reactions were carried out using this procedure with the modifications to the reaction scheme described below:

Chlorinated macromonomer: M_n 20000 $gmol^{-1}$; HyperMac M_n 30600 $gmol^{-1}$, M_w 42900 $gmol^{-1}$, PDI 1.40. Yield 40%.

Chlorinated macromonomer: M_n 20000 $gmol^{-1}$; HyperMac M_n 100500 $gmol^{-1}$, M_w 230100 $gmol^{-1}$, PDI 2.29. Yield 23%.

Chlorinated macromonomer: M_n 20000 $gmol^{-1}$; HyperMac M_n 69080 $gmol^{-1}$, M_w 132700 $gmol^{-1}$, PDI 1.92. Yield 23%.

The following reaction combined the modification of the mechanical overhead stirrer with the change in solvent to NMP:

2.00g of M_n 20000 $gmol^{-1}$ chlorinated macromonomer (1.037 x 10^{-4} moles), 0.057g (4.148 x 10^{-4} moles) potassium carbonate and 0.109g (4.148 x 10^{-4} moles) 18-crown-6 ether were dissolved in 10ml (20% w/v solution) of NMP. The reaction temperature was raised to

reflux and the solution vigorously stirred with a teflon mechanical paddle at 900rpm. The progress of this reaction was monitored by removing small reaction samples and subjecting the sample to size-exclusion chromatography. The reaction was considered complete when no increase in molecular weight was observed. The mixture was then cooled and precipitated into methanol and dried under vacuo.
Yield 25%, M_n 91200 $gmol^{-1}$, M_w 180400 $gmol^{-1}$, PDI 1.97.

6.3.2 N,N-Dimethylacetamide (DMAc).

2.00g of M_n 20000 $gmol^{-1}$ chlorinated macromonomer (1.00×10^{-4} moles), 0.0573g (4.145×10^{-4} moles) potassium carbonate and 0.1096g (4.145×10^{-4} moles) 18-crown-6 ether were dissolved in 10ml (20% w/v solution) of DMAc. The reaction temperature was raised to reflux and the solution vigorously stirred with a teflon mechanical paddle at 900 rpm. The progress of this reaction was monitored by removing small reaction samples and subjecting the sample to size exclusion chromatography. The reaction was considered complete when no increase in molecular weight was observed. The mixture was then cooled and precipitated into methanol and dried under vacuo.
Yield 79%, M_n 89500 $gmol^{-1}$, M_w 148200 $gmol^{-1}$, PDI 1.65.

Following reactions were performed for investigation of concentration on the extent of reaction in DMAc:
Macromonomer: M_n 27000 $gmol^{-1}$; HyperMac M_n 186200 $gmol^{-1}$, M_w 580000 $gmol^{-1}$, PDI 3.12. Yield 48%.

(50% w/v DMAc Solution.) 5.00g of M_n 27000 $gmol^{-1}$ chlorinated macromonomer (1.85×10^{-4} moles), 0.1024g (7.405×10^{-4} moles) potassium carbonate and 0.1957g (7.405×10^{-4} moles) 18-crown-6 ether were dissolved in 10ml (50% w/v solution) of DMAc. The reaction temperature was raised to reflux and the solution vigorously stirred with a teflon mechanical paddle at 900rpm. The progress of this reaction was monitored by removing small reaction samples and subjecting the sample to size exclusion chromatography. The reaction was considered complete when no increase in molecular weight was observed. The mixture was then cooled and precipitated into methanol and dried under vacuo.

Yield 90%, M_n 165900 $gmol^{-1}$, M_w 651400 $gmol^{-1}$, PDI 3.92.

(10% w/v DMAc Solution.) 1.00g of M_n 27000 $gmol^{-1}$ chlorinated macromonomer (3.703 x 10^{-5} moles), 0.0204g (1.48 x 10^{-4} moles) potassium carbonate and 0.039g (1.48 x 10^{-4} moles) 18-crown-6 ether were dissolved in 10ml (10% w/v solution) of DMAc. The reaction temperature was raised to reflux and the solution vigorously stirred with a teflon mechanical paddle at 900 rpm. The progress of this reaction was monitored by removing small reaction samples and subjecting the sample to size exclusion chromatography. The reaction was considered complete when no increase in molecular weight was observed. The mixture was then cooled and precipitated into methanol and dried under vacuo.
Yield 46%, M_n 68900 $gmol^{-1}$, M_w 144000 $gmol^{-1}$, PDI 2.08.

(5% w/v DMAc Solution.) 0.5g of M_n 27000 $gmol^{-1}$ chlorinated macromonomer (1.85 x 10^{-5} moles), 0.0124g (8.93 x 10^{-5} moles) potassium carbonate and 0.0195g (8.93 x 10^{-5} moles) 18-crown-6 ether were dissolved in 10ml (5% w/v solution) of DMAc. The reaction temperature was raised to reflux and the solution vigorously stirred with a teflon mechanical paddle at 900 rpm. The progress of this reaction was monitored by removing small reaction samples and subjecting the sample to size exclusion chromatography. The reaction was considered complete when no increase in molecular weight was observed. The mixture was then cooled and precipitated into methanol and dried under vacuo.
Yield 46%, M_n 41500 $gmol^{-1}$, M_w 64300 $gmol^{-1}$, PDI 1.54.

6.4 Increased Nitrogen Flow Through Reaction Vessel.

In an attempt to remove volatile impurities from the solution, gas was blown through the flask condenser and out through a separate flask bubbler, increasing nitrogen flow across the solution. Other reaction parameter remained the same, as described below:
2.00g of M_n 20000 $gmol^{-1}$ chlorinated macromonomer (1.037 x 10^{-4} moles), 0.057g (4.148 x 10^{-4} moles) potassium carbonate and 0.109g (4.148 x 10^{-4} moles) 18-crown-6 ether were dissolved in 10ml (20% w/v solution) of DMF. The reaction temperature was raised to reflux and the solution vigorously stirred with a teflon mechanical paddle at 900rpm. The progress of this reaction was monitored by removing small reaction samples and subjecting

the sample to size exclusion chromatography. The reaction was considered complete when no increase in molecular weight was observed. The mixture was then cooled and precipitated into methanol and dried under vacuo.

Yield 49%, M_n 296300 $gmol^{-1}$, M_w 567600 $gmol^{-1}$, PDI 1.92.

Chlorinated macromonomer: M_n 20000 $gmol^{-1}$; HyperMac M_n 136800 $gmol^{-1}$, M_w 325800 $gmol^{-1}$, PDI 2.38. Yield 76%.

6.5 Increase in Stirring Rate.

Standard reaction described in section 6.2.2. was modified with an increase in the stirring rate of the mechanical Teflon paddle from 900 to 1500 rpm.

(20% w/v DMF Solution.) 2.00g of M_n 27000 $gmol^{-1}$ chlorinated macromonomer (7.41 x 10^{-5} moles), 0.0409g (2.961 x 10^{-4} moles) potassium carbonate and 0.0782g (2.961 x 10^{-4} moles) 18-crown-6 ether were dissolved in 10ml (20% w/v solution) of DMF. The reaction temperature was raised to reflux and the solution vigorously stirred with a teflon mechanical paddle at 1500 rpm. The progress of this reaction was monitored by removing small reaction samples and subjecting the sample to size exclusion chromatography. The reaction was considered complete when no increase in molecular weight was observed. The mixture was then cooled and precipitated into methanol and dried under vacuo.

Yield 49%, M_n 93400 $gmol^{-1}$, M_w 246200 $gmol^{-1}$, PDI 2.63.

Further reactions were carried out using this procedure with the modifications to the reaction scheme described below:

Chlorinated macromonomer: M_n 20000 $gmol^{-1}$; HyperMac M_n 189800 $gmol^{-1}$, M_w 341100 $gmol^{-1}$, PDI 1.79. Yield 56%.

Chlorinated macromonomer: M_n 20000 $gmol^{-1}$; HyperMac M_n 161600 $gmol^{-1}$, M_w 330800 $gmol^{-1}$, PDI 2.04. Yield 50%.

6.6 Modification of Reaction Base.

Standard HyperMac coupling reaction described in section 6.2.2 is modified using Cs_2CO_3 instead of K_2CO_3 as the base, as well as variation in temperature for optimization of the coupling reaction.

(20% w/v DMF Solution.) 2.00g of M_n 27000 $gmol^{-1}$ chlorinated macromonomer (7.41 x 10^{-5} moles), 0.0409g (2.961 x 10^{-4} moles) cesium carbonate was dissolved in 10ml (20% w/v solution) of DMF. The solution was vigorously stirred with a teflon mechanical paddle at 900 rpm at room temperature (24.2°C). The progress of this reaction was monitored by removing small reaction samples and subjecting the sample to size-exclusion chromatography. The reaction was considered complete when no increase in molecular weight was observed. The mixture was then cooled and precipitated into methanol and dried under vacuo.
Yield 67%, M_n 29700 $gmol^{-1}$, M_w 33800 $gmol^{-1}$, PDI 1.14.

(20% w/v DMF solution at 100°C). Chlorinated macromonomer: M_n 27000 $gmol^{-1}$; HyperMac M_n 386800 $gmol^{-1}$, M_w 948200 $gmol^{-1}$, PDI 2.45. Yield 95%.

(20% w/v DMF solution at reflux). Chlorinated macromonomer: M_n 27000 $gmol^{-1}$; HyperMac M_n 185600 $gmol^{-1}$, M_w 671000 $gmol^{-1}$, PDI 3.61. Yield 95%.

(40% w/v DMF solution at reflux). Chlorinated macromonomer: M_n 27000 $gmol^{-1}$; HyperMac M_n 168500 $gmol^{-1}$, M_w 467300 $gmol^{-1}$, PDI 2.77. Yield 97%.

(20% w/v DMF solution at 100°C). Chlorinated macromonomer: M_n 28000 $gmol^{-1}$; HyperMac M_n 172200 $gmol^{-1}$, M_w 439000 $gmol^{-1}$, PDI 2.54. Yield 68%.

6.6.1 Modified Williamson Coupling –'Super' HyperMac Synthesis.

(20% w/v DMF Solution.) 2.00g of M_n 28000 $gmol^{-1}$ brominated macromonomer (7.143 x 10^{-5} moles), 0.0909g (2.857 x 10^{-4} moles) cesium carbonate was dissolved in 10ml (20% w/v solution) of DMF. The solution was vigorously stirred with a teflon mechanical paddle at 900 rpm at 100°C. The progress of this reaction was monitored by removing small reaction samples and subjecting the sample to size-exclusion chromatography. The reaction was considered complete when no increase in molecular weight was observed. The mixture was then cooled and precipitated into methanol and dried under vacuo.
Yield 85%, M_n 417900 $gmol^{-1}$, M_w 2166000 $gmol^{-1}$, PDI 5.18.

(20% w/v DMF solution at 100°C). Brominated macromonomer: M_n 28000 $gmol^{-1}$; HyperMac M_n 352400 $gmol^{-1}$, M_w 2254000 $gmol^{-1}$, PDI.6.40 Yield 95%.

(20% w/v DMF solution at 70°C). Brominated macromonomer: M_n 28000 $gmol^{-1}$; HyperMac M_n 489400 $gmol^{-1}$, M_w 1739000 $gmol^{-1}$, PDI.3.55 Yield 96%.

(20% w/v DMF solution at 40°C). Brominated macromonomer: M_n 28000 $gmol^{-1}$; HyperMac M_n 525100 $gmol^{-1}$, M_w 1790000 $gmol^{-1}$, PDI3.40. Yield 76%.

(20% w/v DMF solution room temperature (19.5°C)). Brominated macromonomer: M_n 28000 $gmol^{-1}$; HyperMac M_n 510500 $gmol^{-1}$, M_w 1527000 $gmol^{-1}$, PDI 2.99. Yield 68%.

6.7 HyperMac Synthesis in the Presence of a B_3 Core Molecule.

Coupling reactions were carried out using brominated macromonomers in the presence of 5 and 10 mol % (with respect to macromonomer) of 1,1,1-tris(4-hydroxyphenyl)ethane – a B_3 core molecule. The core molecule was added with the macromonomer at the start of the reaction.

6.7.1 5% Core B_3.

2.00g of M_n 28000 $gmol^{-1}$ brominated macromonomer (7.143×10^{-5} moles), 0.0909g (2.857×10^{-4} moles) cesium carbonate and 0.001094g (3.5714×10^{-6} moles, 5% molar) 1,1,1-tris(4-hydroxyphenyl)ethane were dissolved in 10ml (20% w/v solution) of DMF. The solution vigorously stirred with a teflon mechanical paddle at 900 rpm at room temperature (21.5°C). The progress of this reaction was monitored by removing small reaction samples and subjecting the sample to size exclusion chromatography. The reaction was considered complete when no increase in molecular weight was observed. The mixture was then cooled and precipitated into methanol and dried under vacuo.
M_n 342400 $gmol^{-1}$, M_w 1018000 $gmol^{-1}$, PDI 2.97. Yield 74%.

6.7.2 10% Core B_3.

2.00g of M_n 28000 $gmol^{-1}$ brominated macromonomer (7.143×10^{-5} moles), 0.0909g (2.857×10^{-4} moles) cesium carbonate and 0.00218g (7.143×10^{-6} moles, 10% molar) 1,1,1-tris(4-hydroxyphenyl)ethane were dissolved in 10ml (20% w/v solution) of DMF. The solution vigorously stirred with a teflon mechanical paddle at 900 rpm at room temperature (21.5°C). The progress of this reaction was monitored by removing small reaction samples and subjecting the sample to size exclusion chromatography. The reaction was considered complete when no increase in molecular weight was observed. The mixture was then cooled and precipitated into methanol and dried under vacuo.
M_n 127600 $gmol^{-1}$, M_w 601600 $gmol^{-1}$, PDI 4.71 Yield 70%.

6.8 Polybutadiene HyperMacs Synthesis.

Polybutadiene macromonomers were constructed using a method modified from polystyrene macromonomer synthesis[3] as reported by Hutchings and Kimani.[6]

6.8.1 Polybutadiene Macromonomer Synthesis.

A typical anionic polymerisation is as follows; n-hexane (500ml) and butadiene (50g, 0.924 mol) were distilled into a 1 litre reaction flask. The required amount of 3-tert-butyldiemthylsiloxy-1-propyllithium 0.7M in cyclohexane was injected at room temperature. For a target of 6500 $gmol^{-1}$, 10.98ml initiator was added and stirred for 48 hours. After this period, a 2 mol excess of tetramethylethylenediamine (TMEDA) was added with respect to the initiator and a 1.5 mol of functionalized DPE (1,1-bis(4-tert-butyldimethylsiloxyphenyl)ethylene) was added to the solution. The reaction was stirred at room temperature for 5 days before being terminated with nitrogen sparged methanol. M_n 6500 $gmol^{-1}$, M_w 7100 $gmol^{-1}$. PDI 1.09, Yield 70%. ^{1}H NMR (500 MHz, C_6D_6). δ 6.2-5.4 (Ar), δ 5.6-5.4 =C**H** vinyl, δ 5.0 =C**H**$_2$ vinyl, δ 3.9 C**H**$_2$OPh, δ 2.2-1.8 CC**H**$_2$, δ 0.89-0.83 CC**H**$_3$, δ 0.0 $CH_2OSi(CH_3)_2C(CH_3)_3$ δ 0.0.

M_n 13800 $gmol^{-1}$, M_w 14500 $gmol^{-1}$. PDI 1.05, Yield 75%. ^{1}H NMR (500 MHz, C_6D_6). δ 6.2-5.4 (Ar), δ 5.6-5.4 =C**H** vinyl, δ 5.0 =C**H**$_2$ vinyl, δ 3.9 C**H**$_2$OPh, δ 2.2-1.8 CC**H**$_2$, δ 0.89-0.83 CC**H**$_3$, δ 0.0 $CH_2OSi(CH_3)_2C(CH_3)_3$ δ 0.0.

6.8.2 Polybutadiene Macromonomer Deprotection.

Deprotection, removal of the tert-butyldimethylsilyl (TBDMS) from the protected macromonomer, was achieved using an acid hydrolysis reaction. The protected macromonomer (45.0g, 3.00 x 10^{-3} moles) was dissolved in THF (450ml, 10% w/v solution) and concentrated HCl (37 wt%) (0.009 moles, 9.56ml) was added dropwise to the solution in a 10:1 ratio. The solution was then left to reflux overnight. The deprotected polymer solution was precipitated into a 10 w/v excess solution of methanol (4.5L), redissolved into benzene (450ml) and reprecipitated and dried under vacuo. Yield > 95%. ^{1}H NMR(500MHz, C_6D_6): C**H**$_2$OH δ 3.15, **H**O-Ph δ 3.7-3.8.

All deprotection reactions were carried out as described, with variations in volumes according to the material quantity.

6.8.3 Polybutadiene Macromonomer Bromination.

Procedures adapted from the bromination reaction reported in section 6.2.1.4. A typical bromination reaction is as follows:

In a 1 litre round bottom flask, 5.83g (4.02×10^{-4} mol) of the 13700 $gmol^{-1}$ AB_2 polybutadiene macromonomer and a 2.2 molar excess of triphenylphosphine (0.2109g, 8.041×10^{-4}moles) was dissolved in 60ml of dried benzene. The deprotected macromonomer was azeotropically dried by distilling the benzene out of the solution and dry benzene into the flask. This procedure was performed twice to dry the materials, before 60ml (10%w/v solution) of dichloromethane (DCM) was distilled into the flask creating the reaction solution.

The macromonomer solution was cooled in an ice/water bath and carbon tetrabromide (0.2933g, 8.845×10^{-4} mol) added in a solution of dichloromethane. The mixture was stirred at room temperature and the progress of the reaction followed by ^{1}H-NMR (in C_6D_6) until (24 hours) the signal for the CH_2-OH (3.26 ppm) had been completely replaced by a new signal for CH_2-Br at 2.75 ppm. The polymer was recovered in quantitative yield by precipitation into methanol, redissolved and reprecipitated once more, collected by filtration and dried to constant mass in vacuo.

Macromonomer M_n 13700 $gmol^{-1}$, M_w 14500 $gmol^{-1}$ PDI 1.05. Yield 75% ^{1}H NMR (500 MHz, C_6D_6). δ 6.2-5.4 (Ar), δ 5.6-5.4 =C**H** vinyl, δ 5.0 =CH_2 vinyl, δ 3.9 CH_2OPh, δ 2.75 CH_2-Br, δ 2.2-1.8 CCH_2, δ 0.89-0.83 CCH_3,

Macromonomer: M_n 6500 $gmol^{-1}$, M_w 7100 $gmol^{-1}$ PDI 1.07. Yield 35%. Mass 7.11g. Triphenylphosphine (0.6312g, 2.406×10^{-3} moles) and carbon tetrabromide 0.7254g, 2.1876×10^{-3} moles).

6.8.4 Polybutadiene HyperMac Synthesis.

Coupling reactions to make polybutadiene HyperMacs were achieved using the improved synthesis (polystyrene HyperMacs, section 6.6.1) at a lower concentration (10% w/v) in a 50:50 solution of DMF/THF at 60°C.

1.00g of M_n 13700 $gmol^{-1}$ brominated polybutadiene macromonomer (7.299 x 10^{-5} moles), 0.0951g (2.919 x 10^{-4} moles) cesium carbonate was dissolved in 10ml (20% w/v solution) of a 50:50 volume DMAc\THF. The reaction temperature was raised to 60°C and the solution vigorously stirred with a teflon mechanical paddle at 900 rpm. The progress of this reaction was monitored by removing small reaction samples and subjecting the sample to size exclusion chromatography. The reaction was considered complete when no increase in molecular weight was observed. The mixture was then cooled and precipitated into methanol containing 2% wt. 3,5-di-tert-4-butylhydroxytoluene (BHT) and dried under vacuo.
M_n 188100 $gmol^{-1}$, M_w 776800 $gmol^{-1}$, PDI 4.13 Yield 78%.

Brominated macromonomer: M_n 6500 $gmol^{-1}$; HyperMac M_n 83900 $gmol^{-1}$, M_w 493700 $gmol^{-1}$, PDI 5.88. Yield 82%.

6.9 Synthesis of SIS (HyperBlock).

All polymerizations were carried out using standard high-vacuum techniques at room temperature with benzene as the solvent. A typical macromonomer polymerization was as follows.

6.9.1 Synthesis of SIS AB_2 Macromonomer.

Benzene (500 mL) and styrene (8.65 g, 0.08 mol) were distilled, under vacuum, into a 1-litre reaction flask. A lithium initiator, 3-*tert*-butyldimethylsiloxy-1-propyllithium, 0.4 M in cyclohexane, as the initiator was injected through a septum. For a target M_n of 10 000 g mol^{-1} (PS block 1), 1.78 mL of initiator (7 mmol) was used. Upon addition of the initiator to the reaction mixture, a pale yellow colour was observed which evolved over 4 h into the orange-red color of living polystyryllithium. The solution was stirred overnight to allow complete propagation before a small sample of polymer solution (for molecular weight/NMR analysis) was removed and terminated with nitrogen-sparged methanol.

To the living polymer solution, isoprene (29.20g, 0.43 mol) (target 40 000gmol^{-1}) was added at room temperature, forming a colourless solution, and left to stir for 3 days to ensure complete conversion.

Synthesis of the second polystyrene block, target of 10 000 gmol^{-1}: (0.11 ml, 7mmol) of TMEDA was injected via a septa into the living solution, before styrene (9.15g, 0.87 mol) was added to the solution regenerating the orange-red color of living polystyrllithium which was left to stir at room temperature for 3 h.

To the remaining living polymer solution was added 1,1-bis(4-*tert*-butyldimethylsiloxyphenyl)-ethylene (DPE) (1.5 molar equiv with respect to lithium) as a solution in benzene. The reaction was stirred at room temperature for 5 days before the reaction was terminated with nitrogen-sparged methanol. The polymer was recovered by precipitation in methanol, redissolved in benzene, reprecipitated once more into methanol, and dried in vacuo. Yield >95%.

PS block M_n 14 700 g mol^{-1}, M_w 22 000 g mol^{-1} PDI 1.50

PS PI block M_n 34 000 g mol^{-1}, M_w 41 700 g mol^{-1} PDI 1.22

PS PI PS block M_n 46 500 g mol^{-1}, M_w 55 400 g mol^{-1} PDI 1.20

^{1}H NMR (500 MHz, C_6D_6): C**H**$_2$OSi δ 3.36, **H**C(Ph)$_2$ δ 3.5, Si(CH$_3$)$_2$C(C**H**$_3$)$_3$ δ 1.0, ArOSi(C**H**$_3$)$_2$C(CH$_3$) δ 0.1, CH$_2$OSi(C**H**$_3$)$_2$C(CH$_3$)$_3$ δ 0.0.

6.9.2 Synthesis of SIS AB$_2$ Macromonomer Deprotected.

The SIS AB$_2$ macromonomer with all three alcohol groups protected by *tert*-butyldimethylsilyl (TBDMS) groups was dissolved in THF (10% w/v solution). To the solution was added dropwise concentrated HCl (37 wt %), mole ratio of acid/protected alcohol was 5:1. The solution was then warmed to reflux and stirred at reflux for 30 minutes. The solution was cooled and the polymer recovered by precipitation into methanol, redissolved in benzene, reprecipitated once more into methanol, and dried in vacuo at room temperature for 2 days. Yield >96%. ^{1}H NMR (C_6D_6): C**H**$_2$OH δ 3.15, **H**O-Ph δ 3.7-3.8.

6.9.3 Synthesis of SIS AB$_2$ Brominated Macromonomer.

The reaction was performed under high vacuum.

The SIS macromonomer macromonomer (45.09g, 6 x10^{-4} mol) and 2.2 molar (0.63g, 1.9 x10^{-3} mol) quantity of PPh$_3$ were dried twice with benzene, before DCM was added to form a 10% w/v solution. The same procedure was performed with CBr$_4$ (0.55g, 2.1 x10^{-3} mol) and the flask brought to atmospheric pressure with nitrogen. The macromonomer solution was cooled in an ice/water bath and the CBr$_4$ solution was injected into the macromonomer solution forming a pale yellow solution. The reaction was left to stir at room temperature for 24 hours. A small sample was then worked up into methanol and submitted for ^{1}H-NMR to determine that the reaction had reached completion, before the reaction was precipitated into excess methanol. Yield >99%;

^{1}H NMR (C_6D_6): Movement of C**H**$_2$OH δ 3.26 completely replaced by C**H**$_2$Br at δ 2.75.

6.9.4 HyperBlock Synthesis.

Coupling reactions were carried out under an inert atmosphere of nitrogen. A typical polycondensation coupling reaction was carried out thus: 1 g of SIS AB_2 macromonomer (Total M_n 62100 g mol^{-1}, 1.6 x 10^{-5} mol) and 0.052 g (1.6x 10^{-4} mol) cesium carbonate, were dissolved in 10 mL of THF/DMF 50:50 solution. The solution temperature was raised to 40.0°C using an oil bath, and the mixture was stirred vigorously using a mechanical overhead stirrer. The progress of the coupling reaction was followed by extracting small samples periodically and subjecting the sample to size exclusion chromatography analysis (after the addition of 2,6 di-tert-butyl-4-methylphenol (BHT) to the SEC samples). The reaction was deemed to be complete when no further increase in molecular weight was observed. In this case, the reaction was complete after 24 h. The mixture was then cooled and recovered by precipitation into methanol with 2% BHT antioxidant. The product was redissolved in benzene and reprecipitated once again into methanol (with BHT) before drying in vacuo Reported yield are relatively low due to removal of small samples during the reaction for characterization.
M_n 366400 g mol^{-1}, M_w 970000 g mol^{-1}, PDI 2.7, Yield 79%.

(20% w/v DMF solution at 20°C) HyperBlock M_n 65500 $gmol^{-1}$, M_w 137900 $gmol^{-1}$, PDI.2.1 Yield 65%.

(20% w/v 50:50 solution of DMF/THF solution at 40°C) HyperBlock M_n 125000 $gmol^{-1}$, M_w 280200 $gmol^{-1}$, PDI.2.3 Yield 94%.

(10% w/v 50:50 solution of DMF/THF solution at 40°C) HyperBlock M_n 245900 $gmol^{-1}$, M_w 619700 $gmol^{-1}$, PDI.2.5 Yield 72%.

(5% w/v 50:50 solution of DMF/THF solution at 40°C) HyperBlock M_n 242700 $gmol^{-1}$, M_w 654300 $gmol^{-1}$, PDI.2.7 Yield 24%.

(10% w/v 50:50 solution of DMAc/THF solution at 40°C) HyperBlock M_n 129400 $gmol^{-1}$, M_w 292000 $gmol^{-1}$, PDI.2.3 Yield 89%.

(20% w/v 50:50 solution of DMAc/THF solution at 40°C) HyperBlock M_n 186200 $gmol^{-1}$, M_w 503000 $gmol^{-1}$, PDI.2.7 Yield 95%.

(10% w/v 50:50 solution of DMF/THF solution at 60°C) HyperBlock M_n 286400 $gmol^{-1}$, M_w 1463000 $gmol^{-1}$, PDI.5.1 Yield 95%.

(5% w/v 50:50 solution of DMF/THF solution at 80°C) HyperBlock M_n 97300 $gmol^{-1}$, M_w 283100 $gmol^{-1}$, PDI.2.9 Yield 79%.

(10% w/v 50:50 solution of DMF/THF solution at 80°C) HyperBlock M_n 269900 $gmol^{-1}$, M_w 723700 $gmol^{-1}$, PDI.2.7 Yield 78%.

Large scale reactions used for characterization:
Brominated SIS Macromonomer, M_n 62100 $gmol^{-1}$, 19.12g (3.079×10^{-4} moles) of macromonomer and 0.4013g (1.232×10^{-3} moles) cesium carbonate in 200ml 50:50 DMAc/THF.
HyperBlock M_n 287700 $gmol^{-1}$, M_w 1363000 $gmol^{-1}$, PDI 4.7. Yield 96%.

6.10 HyperMac Fractionation.

Fractionated HyperMacs, shown in Table 4.2 were used to probe the effect of polydispersity and molecular weight on the rheological properties of the HyperMacs.

6.10.1 Solution Blending of HyperMacs for Rheological Studies.

Two HyperMacs, (M_n 88400gmol^{-1} M_w 240900 gmol^{-1} PDI 2.73) and (M_n 83100 gmol^{-1} M_w 217800 gmol^{-1} PDI 2.62), made from a M_n 16100gmol^{-1} macromonomer were solution blended to produce circa 20g of material.

Solution blending was achieved by dissolving the two HyperMacs in 1 litre of toluene to give a 2% by weight solution. 250ml of the solution was precipitated into an excess of methanol and the polymer dried to constant mass at 40°C in a vacuum oven. Blended HyperMac (M_n 91800gmol^{-1} M_w 226700 gmol^{-1} PDI 2.46). The remaining polymer solution was retained for fractionation.

6.10.2 Fractionation of Blended HyperMac.

19.93g (1.237 x 10^{-3} moles) of a polystyrene HyperMac M_n 91800gmol^{-1}, M_w 226700 gmol^{-1}, PDI 2.46 was added to 1L of toluene (2% w/v solution) in a 3 litre separating funnel and placed in a temperature controlled water bath. Methanol was added dropwise to the HyperMac solution until it became turbid. The solution temperature was increased by 3-4 °C to clarify the solution which was then cooled, without stirring, overnight to room temperature (20°C). The higher molecular weight (lower) fraction was collected and precipitated into excess methanol and dried under vacuo. Methanol was added to the remaining polymer solution and the procedure was repeated over 14 days to produce 12 fractions (Table 4.2) for rheological characterisation.

6.11 Characterisation.

6.11.1 Rheology.

Void free sample disks of 1mm thick and 25mm or 8mm diameter were prepared by the use of a heated press and stainless steel moulds. The processing temperature was 443K and an inert atmosphere of nitrogen was applied to minimize degradation. Rheology measurements were performed on Rheometrics SR5 and TA Instruments AR 2000 rheometers with parallel plate geometry, using an environmental test chamber (ETC). Linear rheology experiments were run over a temperature range of 383 – 463 K under an atmosphere of nitrogen and gap corrections made for plate expansion/contraction. Frequency sweeps in the range of $1 \times 10^{-2} - 5 \times 10^{2}$ rad/s were performed in the temperature range at 10 K intervals and the data sets combined to form master curves by the time-temperature superposition principle.

6.11.2 Size Exclusion Chromatograph (SEC).

Molecular weight analysis was carried out by size exclusion chromatography (SEC) on a Viscotek TDA 302 with triple detectors (refractive index, viscosity and light scattering). A value of 0.185 (obtained from Viscotek) was used for the dn/dc of polystyrene. PLgel 2 x 300 mm 5 μm mixed C columns (with a linear range of molecular weight from 200- 2000 000 $gmol^{-1}$) were employed; THF was used as the eluent with a flow rate of 1.0 ml/min at a temperature of 303 K.

6.11.3 Nuclear Magnetic Resonance (NMR).

^{1}H NMR analysis was carried out on a Varian VNMRS 700 MHz, Varian Inova-500 MHz or Mercury-400 MHz spectrometer using C_6D_6 as a solvent. Spectra were referenced to the trace of C_6H_6 (7.2 ppm) present in the C_6D_6.

6.11.4 Differential Scanning Calorimetry (DSC).

Differential scanning calorimetry was performed on a TA Instruments Q1000 Series with a heating cycle; room temperature to 453 K, 453 K to 183 K at 10 K/min, 183 K to 503 K at 10 K/min; with 5 minute isothermal periods between each temperature ramp under an inert atmosphere.

6.11.5 Thermal Gravimetric Analysis (TGA).

The thermal stability of the polystyrene HyperMacs was tested by thermogravimetric analysis (TGA) (Perkin Elmer Pyris 1 TGA) at the temperature of 463 K.

6.11.6 Dynamic Mechanical Analysis (DMA).

Plaques for DMA (18mm x 9mm x 1mm) (l x w x t) were prepared by heat pressing materials (c. 1g) using a heat press at 423 K for 15 minutes. Measurements were performed on a T.A Instruments Q800 using a 35mm dual cantilever clamp between 173K and 443K at a 3K /min. scan rate, 1Hz frequency.

6.11.7 Small Angle X-ray Scattering (SAXS).

SAXS samples were solution cast as per the procedure for TEM before staining where samples were cut (4mm x 4mm) and positioned into sample holders for the Bruker Nanostar SAXS using Cu K_α $\lambda = 1.54$ Å at 40KV and 45 mA and a path length of 106 cm.

6.11.8 Transition Electron Microscopy (TEM).

Samples for TEM were prepared via literature preparation of Mays et al.[6] Disks were cast from solutions (3% w/v) in toluene onto aluminum plates from the solvent at room temperature for 14 days, and then annealed at 393 K for 7 days to equilibrate the morphologies.

Samples for transmission electron microscopy (TEM) analysis were prepared by cryo-ultramicrotomy using a Leica EM UC6 Ultramicrotome and Leica EM FC6 cryochamber

(Milton Keynes,UK). Cryosections of 50–70 nm thickness were cut using a cryo 35° diamond knife (Diatome, Switzerland) at a temperature of -140°C and then manipulated from the knife edge onto the grid. Sections were stained for 2-4 h with osmium tetroxide vapour then viewed with a Hitachi H7600 transmission electron microscope (Hitachi High Technologies Europe) using an accelerating voltage of 100kV.

6.12 References:

1. Quirk R.P., Wang Y. *Polym. Int.* 1993, 31, 51.
2. Hsieh H.L., Quirk R.P. Anionic Polymerization, Marcel Dekker, 1996.
3. Hutchings L.R., Dodds J.M., Roberts-Bleming S.J. *Macromolecules* 2005, 38, 5970.
4. Appel R, Warning K., *Chem. Ber.* 1975, *108*, 606, and Appel R., Wihler H.D., *Chem. Ber.* 1976, *109*, 3446.
5. Baughman T.W., Sworen J.C., Wagener K.B. *Tetrahedron*, 2004, 60, 10943.
6. Kimani S.M, Hutchings, L.R. *Macromole. Rapid Commun.* 2008, 29, 8, 633.
7. Zhu, Y., Burgaz, E., Gido, S.P., Staudinger, U., Weidisch, R., Uhrig, D., Mays, J.W. *Macromolecules*, 2006, 39, 4428.

Conclusions.

In this thesis a new strategy for the synthetic route to synthesize polymers with highly branched architectures by the polycondensation of AB_2 macromonomers has been described. The synthesis of polystyrene HyperMacs can be dramatically improved by the use of bromine (instead of chlorine) as a leaving group on the macromonomer and by the use of cesium carbonate (instead of potassium carbonate) as the base in the Williamson coupling reaction. These two combined modifications result in increases in the extent of coupling reaction much further than expected; there appears to be a synergistic benefit in using Br/Cs_2CO_3 in combination. The increase in the rate of the coupling reactions has allowed a reduction of the reaction temperature from 160°C to room temperature although the optimum temperature would seem to be 40°C. At these lower temperatures, the degradation of DMF (previously reported) no longer appears to be a limiting factor.

HyperMacs constructed from well defined macromonomers offer some control of the molecular weight between branch points and allows the variation of the total molecular weight of the HyperMac. At 40°C it has been shown that the rate of reaction is such that theoretically the reaction could be stopped at a chosen conversion – offering some control over the final molecular weight.

Polystyrene HyperMacs were shown to be thermorheologically simple polymers, obeying time–temperature superposition and showing shear thinning behaviour, with zero shear viscosity values increasing with molecular weight. The linear rheology of HyperMacs in the melt are modelled reasonably well, at least qualitatively, by the Cayley tree theory of hierarchical relaxation in tube models in branched polymers. Power-law fittings at high frequency and in the terminal region showed gradients in excellent agreement with this model branched polymer. Although reptation is unlikely to be the dominant relaxation mechanism for these highly branched materials, we observed that the longest relaxation time, scales with molecular weight as $\tau_{long} \alpha M_w^{3.2}$; however, in contrast to the rheological behavior of linear polymers, the entangled Rouse time and the viscosity scale as $\tau_e \alpha M_w^{-0.9}$ and $\eta_0 \alpha M_w^{-1.7}$, respectively. Furthermore the molecular weight of the macromonomer was shown to have an effect on the rheological properties – namely that only when the molecular

weight of the linear segments is significantly above the entanglement molecular weight of polystyrene do we see any evidence of chain entanglement.

Improvements to HyperMac synthesis enabled the preparation of HyperMacs in the presence of a B_3 core. Coupling reactions of a 28000 $gmol^{-1}$ polystyrene AB_2 macromonomer were carried out in the presence of 0, 5 and 10 mol% B_3 core. Dp_w values decreased with increasing core but the polydispersity index and branching factor changed negligibly with this modification. Rheology of these materials showed polystyrene core coupled HyperMacs shear thin in the melt and a breakdown of time-temperature superposition was observed.

Polybutadiene HyperMacs were synthesized in a scheme adapted from the improved polystyrene HyperMac synthesis. Macromonomer building blocks (M_n 6500 and 15600 $gmol^{-1}$) were constructed from butadiene using a functionalised protected initiator. The living polymer was end capped with a protected modified diphenylethylene derivative and the polybutadiene macromonomers were coupled using the modified Williamson ether coupling reactions forming branched materials with Dp_w values around 50. These materials were comparable to the polystyrene HyperMacs synthesized using the improved coupling strategy.

The synthesis of block copolymeric HyperMacs or HyperBlocks from polystyrene polyisoprene triblock copolymeric macromonomer has been achieved by modifying the synthetic route to polystyrene and polybutadiene HyperMacs. Sequential monomer addition followed by end capping with a protected functionalized diphenylethylene produced a triblock macromonomer with 46% polystyrene and the use of hexane returned a high 1,4 polyisoprene microstructure. HyperBlock coupling reactions used the modified Williamson ether coupling with Cs_2CO_3 and modified solvent mixtures to produce branched materials with Dp_w values typically approaching 25.

Characterisation of HyperBlocks using thermal analysis (DSC), mechanical analysis (DMA), small angle x-ray scattering (SAXS) and transmission electron microscopy (TEM) showed these materials had phase separated solid state morphologies with two observable glass transition temperatures (T_gs) corresponding to the polystyrene and polyisoprene constituents. Coupling of macromonomers forming HyperBlocks was seen to disrupt any long-range order seen in the linear material as observed by both SAXS and TEM, showing that branching introduces disorder into these materials.

The macromonomer approach for the construction of HyperMacs provides a versatile route to randomly branched homo and block polymeric materials with known molecular parameters between branch points. Control over the extent of random Williamson coupling reactions can be achieved offering some control over the extent of the coupling reaction.

Future Work.

A few ideas for future developments to the HyperMac project are discussed below:

- The synthesis of polyisoprene HyperMacs. Anionic polymerisation and modified Williamson ether coupling reactions produced HyperMacs from polystyrene and polybutadiene. Polymerisation of isoprene using anionic polymerisation is very similar to butadiene and with minimal modifications to the chemistry synthesis of polyisoprene HyperMacs would likely be trivial. Similar architectures constructed from polyisoprene are produced by Frey et al.[1] using a one pot approach, rather than macromonomer approach.
- Sulphonated polystyrene HyperMacs – an alternative route to water soluble branched materials. This would require minimal modifications to the polystyrene HyperMac synthesis to produce HyperMacs constructed from poly(sodium-4-styrene sulfonate). The polystyrene macromonomer could be directly treated with sulfuric acid and phosphorus pentoxide to produced a sulfonated polymer[2] that could be coupled to form a HyperMac with minimal modifications to the reaction scheme.
- Extend the range of compositions of the block copolymeric macromonomers used to construct HyperBlocks. As a proof of concept exercise it has been demonstrated that HyperMacs can be constructed from triblock copolymers of polystyrene and polyisoprene forming HyperBlocks. It would be good to extend this further by varying the polymer composition in the triblock macromonomers, but also synthesise diblock or tetrablock macromonomers for a better understanding of how branching and composition affect the structure and properties of HyperBlocks.
- Synthesis of block copolymer HyperMacs consisting of different AB_2 homopolymer macromonomers in a one-pot reaction. HyperBlocks and HyperMacs of polystyrene and polybutadiene have been synthesized in separate one-pot reactions. It would be interesting to mix different polymer macromonomers in different volume fractions and see how they couple into a blockcopolymer HyperMacs. It would be interesting to produce a HyperBlock and blockcopolymer HyperMac constructed from the same volume fraction of two polymers (polyisoprene and polystyrene) and see how branching

influences the morphology in the two compositions compared to linear material of the same composition.

- A_2 + B_3 approach for constructing HyperMacs. Hyperbranched architectures can be constructed from systems other than AB_2 macromonomers using functional groups to introduce branching. Increasing the molecular weight of the A_2 or B_3 components would result in HyperMac type materials.[3] This may provide a synthetic route to HyperMac type materials avoiding the use of anionic polymerization. RAFT or ATRP could be used to construct an A_2 macromonomer (homo or block copolymer) with a molecular B_3 used to construct the branched materials.
- Polyethylene oxide (PEO) HyperMacs. The HyperMacs produced to date have only been soluble in organic solvents. PEO has been used in medicinal applications due to its biocompatibility and it would be interesting to look at the properties of long chain branched PEO. Synthetically the functionalized initiator used for polystyrene HyperMacs and HyperBlocks could not be used as lithium alkyls[4] generally do not initiate ring opening anionic polymerization of ethylene oxide. Initiation to produce an oligomer of polystyrene and then sequential addition of ethylene oxide to the reaction, in the same train of thought as the HyperBlock macromonomer synthesis, could be a route around this problem. Nevertheless water soluble HyperMacs could potentially be synthesized.
- Rheology of polybutadiene HyperMacs. Polybutadiene has a lower entanglement molecular weight (M_e)[5] than polystyrene. It would be interesting to look at the differences in HyperMacs constructed from macromonomers with an increased number of entanglements.
- Rheology of HyperBlocks for comparison between linear, branched and commercial materials.
- Investigate the kinetics and materials formed from the addition of an A functionalized macromonomer with an AB_2 macromonomer in the one-pot coupling reaction. It has been suggested by Read et al.[6] that adding A macromonomers will ensure complete reaction with all the B functionalities – this ensures a uniform molecular weight between branch points. The polymer

would still be randomly branched, but the architecture should in theory be more analogous to metallocene catalyzed polyolefin material.

- Syntheses of macromonomers using functionalised protected DPE derivatives[7] resulted in almost quantitative addition to polymer living chain ends. Instead of termination with methanol to produce the AB_2 macromonomer, it could be possible to initiate polymerisation from this group with further additional monomer[8]. The sequential addition of materials to functionalized DPEs could provide a robust method to produce well-defined comb or barbed-wire materials, as polymer chains could then be grafted from functionalized DPE. This method would result in control between the branch points of both polymer backbone and arms. The resulting materials world be particularly valuable in structure-property correlation studies.

References.

1. Lopez-Villanueva F., Wurm F., Kilbinger A.F.M., Frey H. *Macromol. Rapid Commun.* 2007, 28, 704.
2. Fernyhough C.M., Young R.N., Ryan A.J., Hutchings L.R. *Polymer*, 2006, 47, 10, 3455.
3. Jikei M., Chon S., Kakimoto M., Kawauchi S., Imase T., Watanebe J. *Macromolecules*, 1999, 32, 2061.
4. Hsiech, H.L., Quirk, R.P. Anionic Polymerisation: Principles and Pracical Applications. Marcel Dekker, New York, 1996.
5. Larson R.G. 'The Structure and Rheology of Complex Fluids', Oxford University Press, Oxford, 1999.
6. Read D.J. Department of Applied Mathematics, University of Leeds, personal correspondence, 2008.
7. Hutchings L.R., Dodds J.M., Roberts-Bleming S.J. *Macromolecules* 2005, 38, 5970.
8. Iatrou H., Hadjischristidis N. *Macromolecules*, 1992, 25, 4649.

Appendix

Conferences/Meetings

Contributed Oral Presentations:

- Frontiers of Research Meeting and Macro Group UK Young Researchers Meeting'08, University of Warwick, HyperMacs – An Update. 18th April 2008.
- IP'07 IUPAC Biennial Conference, Bayreuth, Germany. Rheology of HyperMacs: Long chain branched analogues of hyperbranched polymers. 6th September 2007.
- Oak Ridge National Laboratory (ORNL), Tennessee, U.S.A. Rheology of HyperMacs, 24th August 2007.
- University of Tennessee (UT), Knoxville, U.S.A HyperMacs: Synthesis and Rheology. 9th August 2007.

Small Angle Neutron Scattering Experiments (SANS) Experiments:

- ISIS, Rutherford Appleton Laboratory, Oxford. 13^{th}-14^{th} December 2008, LOQ. Architecture effects on polymer blend miscibility.
- ILL, Grenoble 1^{st}-3^{rd} October 2008, D22. Tube reptation in bimodal polymer melts
- ILL, Grenoble, 3^{rd}-4^{th} November 2007, D22. Second experiment in a series for investigation of chain deformation during extensional flow.
- ILL, Grenoble, 22^{nd}-26^{th} March 2007. D22. Investigation into chain deformation during extensional flow using a reticulating polymer extruder.

Poster Presentations:

- Polymer Showcase 2008, HyperMacs and HyperBlocks: An Update, 16^{th}-18^{th} September 2008, York.
- MUPP2 Autumn Meeting, Cambridge. HyperMacs: Synthesis and Rheology, 17th-19th September 2007.

- IOP Polymer Physics Group Biennial Meeting, Durham University. Rheology of HyperMacs. 10th-12th September 2007.
- MUPP2 Spring meeting, Sheffield, Synthesis of PS HyperMacs. 27-29th March 2007.
- MUPP2 Autumn meeting, Durham Rheology of HyperMacs 20-21st September 2006.
- Polymer Showcase 2006, Wakefield, HyperMacs – Synthesis and Rheology, 12-13 September 2006.
- EUPOC Branched polymer conference, Lake Garda, Italy, HyperMacs: Synthesis and Rheology. May 2006.
- MUPP2 Spring Meeting Oxford, HyperMacs: Synthesis, March 2006.

Courses/Visits:

- IOP A Random walk through Polymer Science. A celebration of the career and achievements of Randal w. Richards. Durham 19th December 2008.
- MUPP2 Media training course. University of Leeds, 30th/31st October 2008.
- IOP Advances in Polymer Science and Neutron Scattering. – In honour of Dame Julia Higgins. Imperial College, London. 14th/15th September 2008.
- Exchange visit to Prof. Don. Baird at Virginia Tech. University, Blacksburg, U.S.A. 11th August- 5th Septmeber 2008.
- Exchange visit to the Prof. Jimmy Mays Group at University of Tennessee, Knoxville, U.S.A., 5th-25th August 2007.
- Showcase Science 2007, Oundle School. 14th-15th March 2007. Part of the MUPP2 outreach program for 6th form students for encouragement to pursue a career in science.
- Institute of Physics Conference: Phase Transitions in Polymeric Systems, IOP, London. December 2005.
- IRC in Polymer Science and Technology 5 day training course, Sheffield/Bradford, November 2005.
- MUPP2 Autumn Meeting, Leeds, September 2005.

9.5 Departmental Seminars List:

2005/2006

- October 26, Degussa Lecture
  Professor Benjamin List, Max-Planck-Institut für Kohlenforschung, Mülheim an der Ruhr. Asymmetric organocatalysis with amines and amino acids.
- November 9. Professor Matthew J. Rosseinsky, Department of Chemistry, University of Liverpool. New chemistry of oxides and microporous materials
- November 23. Professor Richard Winpenny, School of Chemistry, The University of Manchester. Studies of metal rings and other polymetallic cages
- January 11. Professor A Vleck, Department of Chemistry at Queen Mary, University of London. Ultrafast excited-state processes of d_6-metal carbonyl-diimine complexes: from excitation to photochemistry
- January 25. Professor Donald Fitzmaurice, Department of Chemistry, University College Dublin. Using biomolecules to assemble nanoscale wires and switches
- February 8. Professor Howard M Colquhoun, School of Chemistry, University of Reading. The message in the molecule: probing polymer sequences with a molecular tweezers.
- February 14. Dr Nigel Clarke, Chemistry Department, Durham University
  PET calves: The polymer science of drumming.
- March 1. Professor Stephen Mann, School of Chemistry, University of Bristol
  Beyond nano - The chemistry of emergence.
- May 12. RSC Award mini-symposium
  Dr Jean-Luc Fillaut, University of Rennes. Ruthenium acetylides as candidates for molecular materials.
- May 12. RSC Centenary Lectureship Award Winner
  Professor V. W.-W. Yam, Hong-Kong Department of Chemistry, University of Hong Kong. From design to assembly of luminescent metal-based molecular functional materials.

2006/2007

- June 20. Prof. RH Grubbs, Caltech, California. The Durham Lectures -. Olefin Metathesis: Fundamental Science to Commercial Applications.
- June 22. Prof. RH Grubbs, Caltech. The Design and Synthesis of new Selective Olefin Metathesis Catalysts.
- October 25. Prof. Harry Anderson, Department of Chemistry, University of Oxford, Some Recent Experiments with Molecular Wires - Organic Synthesis to Photophysics.
- November 8. Prof. Zhan Chen, Department of Chemistry, University of Michigan, Understanding Molecular Structures of Polymers and Biomolecules at Interfaces.
- November 22. Prof. Mike Turner , School of Chemistry, The University of Manchester, Organic Materials for Electronics - ROMP as a route to polyphenylvinylenes.
- November 8. Prof. Zhan Chen, Department of Chemistry, University of Michigan, Understanding Molecular Structures of Polymers and Biomolecules at Interfaces.
- February 7. Prof. Donna Blackmond. Department of Chemical Engineering and Chemical Technology, Imperial College, Exploring the Origin of Biological Homochirality: How Catalysis May Have Played a Role.
- May 18. Prof. Manfred Scheer, University of Regensburg. The coordination chemistry of Pn ligand complexes - From oligomers to spherical nanoscaled molecules.
- May 30. Prof. Ian Manners, School of Chemistry, University of Bristol, Functional metallized supramolecular materials via block copolymer self-assembly and living supramolecular polymerisations.
- June 4. Dr Dmitrii F. Perepichka,, Department of Chemistry, McGill University, Montreal, Canada. Two-dimensional molecular networks: an approach to molecular electronics.
- June 18. Prof. CNR Rao. Bangalore. The Durham Lectures. - New Chemistry with Nanomaterials.
- June 22. Prof. CNR Rao. Bangalore The Durham Lectures, Science in India.

2007/2008

- October 24. Prof. David McMillin, Purdue University, USA, Acids, Bases and the Photochemistry of Platinum(II) Polypyridines.
- January 23. Prof. Alison Rodger, Warwick, Looking at Long Molecules in Solution: Polarised Spectroscopy of Fibrous and Membrane Proteins.
- February 20. Dr. Julie Macpherson, Warwick, Carbon Nanotube Networks for Chemical Sensing.
- March 5. Prof. Werner Goedel, Chemnitz University of Technology, Germany. Particle Assisted Wetting, Porous Membranes and the Smallest Wedding Rings in Town.
- April 23. Dr. David Hodgson, Department of Chemistry, Durham University. A Transaminase Ribozyme - RNA Catalysed Proton Transfer from Carbon.
- April 23. Prof. Andrew B. Holmes, RSC Merck Lecture, University of Melbourne, Australia. Probing Intracellular Signalling with Phosphoinositides.
- April 23. Prof. Roeland Nolte, Musgrave Lecture, University of Radboud, Holland Macromolecular Architectures Inspired by Nature.
- June 20. Prof. Christian Amatore. CNRS Paris. Oxidative Stress: the Good and the Bad Sides.

Publications

- Dodds J.M., De Luca E., Hutchings L.R., Clarke N. 'Rheological Properties of HyperMacs – Long Chain Branched Analogues of Hyperbranched Polymers.' *XVth International Congress on Rheology - The Society of Rheology 80th Annual Meeting, pts 1 and 2.* 2008, 1027, 351.
- Clarke N, De Luca E, Dodds J.M, Kimani S.M. Hutchings LR. 'HyperMacs – Long Chain Hyperbranched Polymers: A Dramatically Improved Synthesis and Qualitative Rheological Analysis.' *European Polymer Journal.* 2008, **44**, 665.
- Dodds J.M., De Luca E., Hutchings L.R, Clarke N. 'Rheological Properties of HyperMacs – Long Chain Branched Analogues of Hyperbranched Polymers.' *Journal of Polymer Science Part B: Polymer Physics,* 2007, **45**, 19, 2762.
- Hutchings LR, Dodds JM, Roberts-Bleming SJ. 'HyperMacs. Long Chain Branched Analogues of Hyperbranched Polymers Prepared by the Polycondensation of AB_2 Macromonomers.' Macromolecular Symposia, 2006, 240, 56.
- Hutchings LR, Dodds JM, Roberts-Bleming SJ. 'HyperMacs: Highly Branched Polymers Prepared by the Polycondensation of AB_2 Macromonomers, Synthesis and Characterisation.' Macromolecules, 2005, **38**, 14, 5970.